Exponential Convergence of hp-FEM for Elliptic Problems in Polyhedra: Mixed Boundary Conditions and Anisotropic Polynomial Degrees

Originally published in:
Foundations of Computational Mathematics 18(3), https://doi.org/10.1007/s10208-017-9349-9

Found Comput Math (2018) 18:595–660
https://doi.org/10.1007/s10208-017-9349-9

FOUNDATIONS OF COMPUTATIONAL MATHEMATICS
The Journal of the Society for the Foundations of Computational Mathematics

Exponential Convergence of *hp*-FEM for Elliptic Problems in Polyhedra: Mixed Boundary Conditions and Anisotropic Polynomial Degrees

Dominik Schötzau[1] · **Christoph Schwab**[2]

Received: 24 January 2016 / Revised: 5 November 2016 / Accepted: 28 January 2017 /
Published online: 13 March 2017

Abstract We prove exponential rates of convergence of *hp*-version finite element methods on geometric meshes consisting of hexahedral elements for linear, second-order elliptic boundary value problems in axiparallel polyhedral domains. We extend and generalize our earlier work for homogeneous Dirichlet boundary conditions and uniform isotropic polynomial degrees to mixed Dirichlet–Neumann boundary conditions and to anisotropic, which increase linearly over mesh layers away from edges and vertices. In particular, we construct H^1-conforming quasi-interpolation operators with N degrees of freedom and prove exponential consistency bounds $\exp(-b\sqrt[5]{N})$ for piecewise analytic functions with singularities at edges, vertices and interfaces of boundary conditions, based on countably normed classes of weighted Sobolev spaces with non-homogeneous weights in the vicinity of Neumann edges.

Dedicated to Monique Dauge on the occasion of her 60th birthday.

Communicated by Endre Süli.

This work was supported in part by the Natural Sciences and Engineering Research Council of Canada (NSERC) and the Swiss National Science Foundation (SNF).

✉ Christoph Schwab
schwab@math.ethz.ch

Dominik Schötzau
schoetzau@math.ubc.ca

[1] Mathematics Department, University of British Columbia, 1984 Mathematics Road, Vancouver, BC V6T 1Z2, Canada

[2] Seminar for Applied Mathematics, ETH Zürich, Rämistrasse 101, 8092 Zürich, Switzerland

Keywords hp-FEM · Second-order elliptic problems in polyhedra · Mixed boundary conditions · Anisotropic polynomial degrees · Exponential convergence

Mathematics Subject Classification 65N30

1 Introduction

We prove exponential convergence estimates for conforming hp-version finite element methods (FEMs) for the following elliptic boundary value problem in an open and bounded polyhedron $\Omega \subset \mathbb{R}^3$ with mixed boundary conditions:

$$-\nabla \cdot (\boldsymbol{A}\nabla)u = f \qquad \text{in } \Omega \subset \mathbb{R}^3, \tag{1.1}$$

$$\gamma_0(u) = 0 \qquad \text{on } \Gamma_\iota \subset \partial\Omega, \quad \iota \in \mathcal{J}_D, \tag{1.2}$$

$$\gamma_1(u) = 0 \qquad \text{on } \Gamma_\iota \subset \partial\Omega, \quad \iota \in \mathcal{J}_N. \tag{1.3}$$

The Lipschitz boundary $\Gamma = \partial\Omega$ is assumed to consist of a finite union of plane, *axiparallel* faces Γ_ι indexed by $\iota \in \mathcal{J}$. The faces Γ_ι are bounded, plane polygons whose sides form the (open) edges of Ω. The set $\{\Gamma_\iota\}_{\iota\in\mathcal{J}}$ is partitioned into a subset of Dirichlet faces $\{\Gamma_\iota\}_{\iota\in\mathcal{J}_D}$ and a subset of Neumann faces $\{\Gamma_\iota\}_{\iota\in\mathcal{J}_N}$, with corresponding (disjoint) index sets $\mathcal{J}_D$ and $\mathcal{J}_N$, respectively (i.e., $\mathcal{J} = \mathcal{J}_D \dot\cup \mathcal{J}_N$). The diffusion coefficient matrix $\boldsymbol{A}$ is assumed to be constant and symmetric positive definite. The function f is a given forcing term, and the operators γ_0 and γ_1 denote the trace and (co)normal derivative operators, respectively.

Upon introducing the Sobolev space $V := \{v \in H^1(\Omega) : v|_{\Gamma_\iota} = 0,\ \iota \in \mathcal{J}_D\}$, the weak formulation of problem (1.1)–(1.3) is to find $u \in V$ such that

$$a(u, v) := \int_\Omega \boldsymbol{A}\nabla u \cdot \nabla v \,\mathrm{d}\boldsymbol{x} = \int_\Omega f v \,\mathrm{d}\boldsymbol{x} \qquad \forall v \in V, \tag{1.4}$$

where we understand the integral on the right-hand side in (1.4) as the duality pairing in $V^\star \times V$, with $V^\star$ denoting the dual space of V. For every $f \in V^\star$, problem (1.4) admits a weak solution $u \in V$. The solution is unique if $\mathcal{J}_D \neq \emptyset$, and unique in the factor space $V/\mathbb{R}$ if $\mathcal{J}_D = \emptyset$ (in which case we also require the compatibility condition $\int_\Omega f \,\mathrm{d}\boldsymbol{x} = 0$).

The hp-version of the finite element method for elliptic problems was proposed by I. Babuška, B. Q. Guo and coworkers, inspired by earlier exponential convergence results in free-knot, variable-order spline interpolation (see [6,18]). One of its key features is that it achieves *exponential convergence rates for solutions with singularities* in terms of the total number of freedom N.

Specifically, for elliptic problems in polygonal domains Ω with piecewise analytic data, Babuška and Guo proved exponential convergence bounds of the form $C\exp(-b\sqrt[3]{N})$; see [1,2,13,14] and the references therein. Key ingredients in their proof were *geometric mesh refinement* toward the singular set $\mathcal{S}$ of the solution (being the finite set of vertices of Ω) and *nonuniform elemental polynomial degrees* which increase $\mathfrak{s}$-linearly with the elements' distance from $\mathcal{S}$. In addition to these

approximation results, their papers also provide *elliptic regularity results in countably normed weighted spaces of the solutions*. This constituted an essential advance with respect to the earlier works in [6,11,18], where only particular singular solutions had been considered. Steps to extend the analytic regularity and the two-dimensional hp-convergence analysis to three dimensions were undertaken in [3,12,15,16] and the references therein. In the recent work [5], M. Costabel, M. Dauge and S. Nicaise established a new analytic regularity shift in scales of anisotropically and non-homogeneously weighted Sobolev spaces for variational solutions for a class of second-order, linear elliptic boundary value problems with constant coefficients. Their analytic regularity result will be the basis of our exponential convergence proof. We also mention the work [8,9], where exponentially accurate non-conforming h-p spectral element methods to solve elliptic problems in three dimensions were proposed and analyzed.

The present paper builds on and extends our work [20] on exponential convergence for hp-FEMs in polyhedral domains. It also builds on our earlier work [23–25] on hp-version discontinuous Galerkin (DG) methods for second-order elliptic boundary value problems in polyhedra. More precisely, in [20], we considered the boundary value problem (1.1) with the homogeneous Dirichlet boundary conditions in (1.2) imposed on the entire boundary $\partial\Omega$. For axiparallel configurations, we then used the non-conforming hp-version interpolation operators constructed in [24] in conjunction with suitable polynomial jump liftings to prove exponential rates of convergence in terms of the number of degrees of freedom for conforming hp-FEM discretizations on appropriate combinations of geometrically and anisotropically refined meshes and for the *uniform and isotropic polynomial degree* $p \geq 1$.

The principal contribution of the present work is the construction of exponentially convergent conforming hp-FE quasi-interpolation operators on axiparallel, σ-geometric mesh patches with *variable and anisotropic polynomial degree distributions* for the *mixed* second-order problem (1.1)–(1.3) (and generalizations thereof). Our main result shows the H^1-norm convergence rate estimate $C\exp(-b\sqrt[5]{N})$, where $b, C > 0$ are independent of N. While asymptotically of the same form as the rate in [20], the univariate hp-approximation results [6,11,18] suggest that the use of variable and, in particular, of *anisotropic polynomial degree distributions* will significantly reduce the number of degrees of freedom required to reach a prescribed accuracy of approximation. This is further corroborated in preliminary numerical results in three space dimensions.

Loosely speaking, our construction and convergence proof combine the arguments in [25] to define *non-conforming base projectors with exponential convergence in broken norms* with the constructions of *polynomially stable polynomial trace jump liftings* in [20]. However, the lower regularity of the solutions and the more general hp-finite element spaces under consideration entail several significantly new technical difficulties which are addressed in this work.

First, the mixed boundary conditions in (1.2), (1.3) are considerably more involved than the pure Dirichlet conditions analyzed in [20]. Indeed, with the regularity theory from [5], solutions of problem (1.1)–(1.3) with piecewise analytic data belong to countably normed Sobolev spaces $N^m_{\boldsymbol{\beta}}(\Omega)$ with *non-homogeneous weights*. In [25],

the non-homogeneous structure of the weights was dealt with by using L^2-projections, by splitting the errors in edge-perpendicular and edge-parallel contributions and by bounding these two contributions separately. While this construction ensured stability with respect to element anisotropy (up to algebraic losses in the polynomial degrees) in the context of discontinuous Galerkin discretizations, it is not sufficient for conforming hp-FEMs. Indeed, finding stable liftings of the polynomial jumps introduced by the L^2-projections in edge-parallel direction over edge-perpendicular faces between *highly anisotropic* elements along the same edge seems to be an open problem.

The first principal contribution of the paper thus is to overcome this difficulty by a novel construction of non-conforming hp-version base projectors. Our construction employs L^2-projections in edge-perpendicular directions and nodally exact H^1-projections in edge-parallel direction along anisotropic elements appearing in edge and in corner–edge neighborhoods. The nodal exactness property in parallel direction then removes the need for liftings over the critical faces mentioned above, while still allowing to split the errors in edge-perpendicular and edge-parallel contributions as in [25]. The non-conforming hp-base projectors presented in the this paper are well defined on $H^1(\Omega)$ (in contrast to those in [20]) and converge exponentially in broken norms. The proof follows along the lines of that in [25], with a few relevant modifications. For the sake of completeness, we outline the proof in Appendix 8.

Second, we consider in this paper the $\mathfrak{s}$-linear polynomial degree distributions introduced in [23], which increase *linearly and anisotropically* away from edges and corners with a *slope parameter* $\mathfrak{s} > 0$. While such degree distributions can be relatively easily accommodated by the discontinuous Galerkin approaches in [23–25], enforcing conformity for variable polynomial degrees and irregular mesh refinement is not straightforward. To do so, we introduce suitable hp-version elemental basis functions with respect to nodal, edge, face and interior degrees of freedom in combination with a *minimum rule* approach for edge and face polynomial degrees in the spirit of [7]. The second principal contribution of this paper then is the construction of conforming approximations in the presence of $\mathfrak{s}$-linear polynomial degree distributions and irregular meshes. Starting from the hp-base projectors, we generalize the *averaging strategy* in [28] to anisotropic elements, in order to assign unique nodal, edge and face values while retaining exponential convergence estimates. This yields intermediate approximations which are continuous across all regularly matching faces and which satisfy the homogeneous Dirichlet boundary conditions. Finally, we introduce polynomial edge and face jump liftings along the lines of our previous work [20] to remove discontinuities over all irregular faces. Our liftings admit bounds which are independent of element aspect ratios, with algebraic growth in the elemental polynomial degree, thereby preserving the exponential convergence estimates of the hp-version base projectors. Here, we emphasize again that in our averaging and lifting approaches, the partial conformity of the base projectors is essential in the handling of anisotropic elements.

The present analysis is in particular applicable to the pure Dirichlet problem, i.e., when $\mathcal{J}_N = \emptyset$, and extends to results in [20] to $\mathfrak{s}$-linear and anisotropic polynomial degree distributions. However, the scope of the paper is beyond the elliptic model problem (1.1)–(1.3): Our exponential convergence proofs apply directly to hp-FEMs for more general and vector-valued second-order elliptic boundary value problems

which admit analytic regularity shifts in the function classes of [5]. Moreover, we also provide an exponential L^2-norm consistency bound for L^2-projections under the weak $N^1_{\boldsymbol{\beta}}(\Omega)$-regularity (see Theorem 4.3). This may be of independent interest for approximations of the pressure in mixed hp-FEMs for the (Navier–)Stokes equations in polyhedra as considered in [21,22,27].

The outline of the article is as follows: In Sect. 2, we recapitulate the countably normed weighted spaces from [5]. In Sect. 3, we introduce the hp-version finite element methods and state our main result (Theorem 3.4), with an outline of its proof provided in Sect. 3.4. The new base projectors with partial conformity are introduced in Sect. 4. Details of their convergence properties can be found in Appendix 8. Finally, in Sects. 5 and 6, we complete the constructions of conforming approximations with the help of averaging and lifting operators, respectively.

Our notation employed throughout the paper is kept consistent with [23–25]. We shall use the notations "$\lesssim$" or "$\simeq$" to denote an inequality or an equivalence containing generic positive multiplicative constants which are independent of the discretization and regularity parameters, as well as of the geometric refinement level, but which may depend on the parameters σ and $\mathfrak{s}$.

2 Regularity

We review the countably normed classes of weighted spaces from [5].

2.1 Subdomains and Weights

We denote by $\mathcal{C}$ the finite set of corners $\boldsymbol{c}$, and by $\mathcal{E}$ the finite set of (open) edges $\boldsymbol{e}$ of Ω. The singular set of Ω is then given by

$$\mathcal{S} := \mathcal{C} \,\dot\cup\, \mathcal{E} = \Big(\bigcup_{\boldsymbol{c}\in\mathcal{C}} \boldsymbol{c}\Big) \,\dot\cup\, \Big(\bigcup_{\boldsymbol{e}\in\mathcal{E}} \boldsymbol{e}\Big) \subset \Gamma\,. \tag{2.1}$$

For $\boldsymbol{c} \in \mathcal{C}$, $\boldsymbol{e} \in \mathcal{E}$, and $\boldsymbol{x} \in \Omega$, we define the following distance functions:

$$r_{\boldsymbol{c}}(\boldsymbol{x}) = |\boldsymbol{x} - \boldsymbol{c}|, \qquad r_{\boldsymbol{e}}(\boldsymbol{x}) = \inf_{\boldsymbol{y}\in\boldsymbol{e}} |\boldsymbol{x} - \boldsymbol{y}|, \qquad \rho_{\boldsymbol{c}\boldsymbol{e}}(\boldsymbol{x}) = r_{\boldsymbol{e}}(\boldsymbol{x})/r_{\boldsymbol{c}}(\boldsymbol{x}). \tag{2.2}$$

For each corner $\boldsymbol{c} \in \mathcal{C}$, we denote by $\mathcal{E}_{\boldsymbol{c}} := \{\, \boldsymbol{e} \in \mathcal{E} \,:\, \boldsymbol{c} \cap \overline{\boldsymbol{e}} \neq \emptyset \,\}$ the set of all edges of Ω which meet at $\boldsymbol{c}$. Similarly, for any $\boldsymbol{e} \in \mathcal{E}$, the set of corners of $\boldsymbol{e}$ is given by $\mathcal{C}_{\boldsymbol{e}} := \{\, \boldsymbol{c} \in \mathcal{C} \,:\, \boldsymbol{c} \cap \overline{\boldsymbol{e}} \neq \emptyset \,\}$. Then, for $\varepsilon > 0$, $\boldsymbol{c} \in \mathcal{C}$, $\boldsymbol{e} \in \mathcal{E}$, respectively, $\boldsymbol{e} \in \mathcal{E}_{\boldsymbol{c}}$, we define the neighborhoods

$$\begin{aligned}
\omega_{\boldsymbol{c}} &= \{\, \boldsymbol{x} \in \Omega \,:\, r_{\boldsymbol{c}}(\boldsymbol{x}) < \varepsilon \;\wedge\; \rho_{\boldsymbol{c}\boldsymbol{e}}(\boldsymbol{x}) > \varepsilon \quad \forall\, \boldsymbol{e} \in \mathcal{E}_{\boldsymbol{c}} \,\},\\
\omega_{\boldsymbol{e}} &= \{\, \boldsymbol{x} \in \Omega \,:\, r_{\boldsymbol{e}}(\boldsymbol{x}) < \varepsilon \;\wedge\; r_{\boldsymbol{c}}(\boldsymbol{x}) > \varepsilon \quad \forall\, \boldsymbol{c} \in \mathcal{C}_{\boldsymbol{e}} \,\},\\
\omega_{\boldsymbol{c}\boldsymbol{e}} &= \{\, \boldsymbol{x} \in \Omega \,:\, r_{\boldsymbol{c}}(\boldsymbol{x}) < \varepsilon \;\wedge\; \rho_{\boldsymbol{c}\boldsymbol{e}}(\boldsymbol{x}) < \varepsilon \,\}.
\end{aligned} \tag{2.3}$$

Without loss of generality as in [23], the domain Ω can be partitioned into four *disjoint* subdomains, $\overline{\Omega} = \overline{\Omega_{\mathcal{C}} \,\dot\cup\, \Omega_{\mathcal{E}} \,\dot\cup\, \Omega_{\mathcal{CE}} \,\dot\cup\, \Omega_0}$, referred to as *corner*, *edge*, *corner–edge* and *interior* neighborhoods of Ω, respectively, where $\Omega_0 := \Omega \backslash \overline{\Omega_{\mathcal{C}} \cup \Omega_{\mathcal{E}} \cup \Omega_{\mathcal{CE}}}$ and

$$\Omega_{\mathcal{C}} = \bigcup_{\boldsymbol{c}\in\mathcal{C}} \omega_{\boldsymbol{c}}, \qquad \Omega_{\mathcal{E}} = \bigcup_{\boldsymbol{e}\in\mathcal{E}} \omega_{\boldsymbol{e}}, \qquad \Omega_{\mathcal{CE}} = \bigcup_{\boldsymbol{c}\in\mathcal{C}} \bigcup_{\boldsymbol{e}\in\mathcal{E}_{\boldsymbol{c}}} \omega_{\boldsymbol{ce}}\,. \tag{2.4}$$

We distinguish between Dirichlet and Neumann edges by setting

$$\mathcal{E}_D := \left\{ \boldsymbol{e} \in \mathcal{E} \,:\, \exists \boldsymbol{\iota} \in \mathcal{J}_D \text{ with } \boldsymbol{e} \cap \overline{\Gamma}_{\boldsymbol{\iota}} \neq \emptyset \right\}, \qquad \mathcal{E}_N := \mathcal{E} \backslash \mathcal{E}_D. \tag{2.5}$$

Edges in $\mathcal{E}_D$ abut on at least one Dirichlet face $\Gamma_{\boldsymbol{\iota}}$ for $\boldsymbol{\iota} \in \mathcal{J}_D$. Note that we possibly have $\mathcal{E}_N = \emptyset$.

2.2 Weighted Sobolev Spaces

To each $\boldsymbol{c} \in \mathcal{C}$ and $\boldsymbol{e} \in \mathcal{E}$ we associate a corner and an edge exponent $\beta_{\boldsymbol{c}}, \beta_{\boldsymbol{e}} \in \mathbb{R}$, respectively. We collect these quantities in the weight exponent vector $\boldsymbol{\beta} = \{\beta_{\boldsymbol{c}} : \boldsymbol{c} \in \mathcal{C}\} \cup \{\beta_{\boldsymbol{e}} : \boldsymbol{e} \in \mathcal{E}\} \in \mathbb{R}^{|\mathcal{C}|+|\mathcal{E}|}$. Inequalities of the form $\boldsymbol{\beta} < 1$ and expressions like $\boldsymbol{\beta} \pm s$, where $s \in \mathbb{R}$, are to be understood componentwise.

We choose local coordinate systems in $\omega_{\boldsymbol{e}}$ and $\omega_{\boldsymbol{ce}}$, for $\boldsymbol{c} \in \mathcal{C}$ and $\boldsymbol{e} \in \mathcal{E}_{\boldsymbol{c}}$, such that the edge $\boldsymbol{e}$ corresponds to the direction $(0, 0, 1)$. Then, we indicate quantities transversal to $\boldsymbol{e}$ by $(\cdot)^\perp$, and quantities parallel to $\boldsymbol{e}$ by $(\cdot)^\parallel$. In particular, if $\boldsymbol{\alpha} = (\alpha_1, \alpha_2, \alpha_3) \in \mathbb{N}_0^3$ is a multi-index of order $|\boldsymbol{\alpha}| = \alpha_1 + \alpha_2 + \alpha_3$, then we write $\boldsymbol{\alpha} = (\boldsymbol{\alpha}^\perp, \alpha^\parallel)$ with $\boldsymbol{\alpha}^\perp = (\alpha_1, \alpha_2)$ and $\alpha^\parallel = \alpha_3$, and denote the partial derivative operator $\mathsf{D}^{\boldsymbol{\alpha}}$ by $\mathsf{D}^{\boldsymbol{\alpha}} = \mathsf{D}_\perp^{\boldsymbol{\alpha}^\perp} \mathsf{D}_\parallel^{\alpha^\parallel}$, where $\mathsf{D}_\perp^{\boldsymbol{\alpha}^\perp}$ and $\mathsf{D}_\parallel^{\alpha^\parallel}$ signify derivatives in edge-perpendicular and edge-parallel directions, respectively. We further denote by $\mathsf{D}_\perp$ the gradient operator in edge-perpendicular direction, and set $\mathsf{D}_\parallel = \mathsf{D}_\parallel^1$.

The solution u of problem (1.1)–(1.3) belongs to scales of countably normed weighted Sobolev spaces; cf. [5]. The present exponential convergence results will be based on the weighted spaces $N^k_{\boldsymbol{\beta}}(\Omega)$ with anisotropic and non-homogeneous weighting at all corners $\boldsymbol{c} \in \mathcal{C}$ and edges $\boldsymbol{e} \in \mathcal{E}$; they are an extremal case of the families of spaces considered in [5]. For an order $k \geq 0$ and weight exponent $\boldsymbol{\beta}$, we introduce the semi-norm $|u|_{N^k_{\boldsymbol{\beta}}(\Omega)}$ by:

$$\begin{aligned} |u|^2_{N^k_{\boldsymbol{\beta}}(\Omega)} := \sum_{|\boldsymbol{\alpha}|=k} \Bigg\{ & \|\mathsf{D}^{\boldsymbol{\alpha}} u\|^2_{L^2(\Omega_0)} + \sum_{\boldsymbol{c}\in\mathcal{C}} \left\| r_{\boldsymbol{c}}^{\max\{\beta_{\boldsymbol{c}}+|\boldsymbol{\alpha}|,0\}} \mathsf{D}^{\boldsymbol{\alpha}} u \right\|^2_{L^2(\omega_{\boldsymbol{c}})} \\ & + \sum_{\boldsymbol{e}\in\mathcal{E}} \left\| r_{\boldsymbol{e}}^{\max\{\beta_{\boldsymbol{e}}+|\boldsymbol{\alpha}^\perp|,0\}} \mathsf{D}^{\boldsymbol{\alpha}} u \right\|^2_{L^2(\omega_{\boldsymbol{e}})} \\ & + \sum_{\boldsymbol{c}\in\mathcal{C}} \sum_{\boldsymbol{e}\in\mathcal{E}_{\boldsymbol{c}}\cap\mathcal{E}} \left\| r_{\boldsymbol{c}}^{\max\{\beta_{\boldsymbol{c}}+|\boldsymbol{\alpha}|,0\}} \rho_{\boldsymbol{ce}}^{\max\{\beta_{\boldsymbol{e}}+|\boldsymbol{\alpha}^\perp|,0\}} \mathsf{D}^{\boldsymbol{\alpha}} u \right\|^2_{L^2(\omega_{\boldsymbol{ce}})} \Bigg\}\,. \end{aligned} \tag{2.6}$$

For $m > k_{\boldsymbol{\beta}}$, with

$$k_{\boldsymbol{\beta}} := -\min\{\min_{\boldsymbol{c}\in\mathcal{C}} \beta_{\boldsymbol{c}}, \min_{\boldsymbol{e}\in\mathcal{E}} \beta_{\boldsymbol{e}}\}, \tag{2.7}$$

we write $N^m_{\boldsymbol{\beta}}(\Omega)$ for the space of functions u such that $\|u\|_{N^m_{\boldsymbol{\beta}}(\Omega)} < \infty$, with the norm $\|u\|^2_{N^m_{\boldsymbol{\beta}}(\Omega)} := \sum_{k=0}^m |u|^2_{N^k_{\boldsymbol{\beta}}(\Omega)}$. For subdomains $\Omega' \subseteq \Omega$ we shall denote by $|\cdot|_{N^k_{\boldsymbol{\beta}}(\Omega')}$ and $\|\cdot\|_{N^m_{\boldsymbol{\beta}}(\Omega')}$ the semi-norm (2.6) and norm as above with all domains of integration replaced by their intersections. We note that $M^m_{\boldsymbol{\beta}}(\Omega) \subset N^m_{\boldsymbol{\beta}}(\Omega)$, where $M^m_{\boldsymbol{\beta}}(\Omega)$ is the weighted Sobolev space with homogeneous weights considered in [5,20] for the pure Dirichlet problem.

2.3 Analytic Regularity

We adopt the analytic function classes of [5].

Definition 2.1 For a domain $\Omega' \subseteq \Omega$, the class $B_{\boldsymbol{\beta}}(\Omega')$ consists of all functions u such that $u \in N^m_{\boldsymbol{\beta}}(\Omega')$ for $m > k_{\boldsymbol{\beta}}$, with $k_{\boldsymbol{\beta}}$ as in (2.7), and such that there exists a constant $C_u > 0$ with $|u|_{N^k_{\boldsymbol{\beta}}(\Omega')} \le C_u^{k+1}\Gamma(k+1)$ for all $k > k_{\boldsymbol{\beta}}$.

The analytic regularity shifts of [5, Corollary 7.1] in (for $\mathcal{E}_D = \mathcal{E}$), [5, Theorem 7.3] (for $0 \subset \mathcal{E}_D \subset \mathcal{E}$) and in [5, Theorem 7.4] (for $\mathcal{E}_D = \emptyset$) for variational solutions u of problem (1.1)–(1.3) (with constant coefficients) can be summarized as follows.

Proposition 2.2 *There are bounds $b_{\mathcal{E}}, b_{\mathcal{C}} > 0$ (depending on Ω, the coefficient matrix $\boldsymbol{A}$ and the set $\mathcal{E}_D$) such that for weight exponent vectors $\boldsymbol{b}$ with*

$$0 < b_{\boldsymbol{c}} < b_{\mathcal{C}}, \quad 0 < b_{\boldsymbol{e}} < b_{\mathcal{E}}, \qquad \boldsymbol{c} \in \mathcal{C},\ \boldsymbol{e} \in \mathcal{E}, \tag{2.8}$$

such that for piecewise analytic f as specified in [5], the weak solution $u \in V$ defined (1.4) of problem (1.1)–(1.3) belongs to $B_{-1-\boldsymbol{b}}(\Omega)$.

Remark 2.3 As in [25, Remark 2.5], we assume that in (2.8) there holds

$$0 < b_{\boldsymbol{c}} < 1, \quad 0 < b_{\boldsymbol{e}} < 1, \qquad \boldsymbol{c} \in \mathcal{C},\ \boldsymbol{e} \in \mathcal{E}. \tag{2.9}$$

Then, $\kappa_{\boldsymbol{\beta}} = \kappa_{-1-\boldsymbol{b}} \in (1,2)$ in (2.7). In addition, we shall assume that, for any polyhedron Ω and right-hand side f in the class of problems considered here, there exists *some* $\theta \in (0,1)$ such that the weak solution $u \in V$ belongs to $H^{1+\theta}(\Omega)$. For weight exponents $b_{\boldsymbol{c}} \in (1/2, 1)$, $b_{\boldsymbol{e}} \in (0,1)$, this follows from [5, Remark 6.2(ii)] and [15, Theorem 3.5]. We also refer to the discussion in [25, Remark 2.5].

3 Finite Element Discretization and Exponential Convergence

3.1 Geometric Meshes

We review geometric mesh constructions from [23,24].

3.1.1 Geometric Mesh Patches

We partition the domain Ω into a finite number $\mathfrak{P}$ of open, axiparallel and hexahedral *patches* $\{Q_\mathfrak{p}\}_{\mathfrak{p}=1}^{\mathfrak{P}}$ which constitute the patch mesh $\mathcal{M}^0$. In the axiparallel setting, each $Q_\mathfrak{p} \in \mathcal{M}^0$ is an affine orthogonal image $Q_\mathfrak{p} = G_\mathfrak{p}(\widetilde{Q})$ of the *reference patch* $\widetilde{Q} = (-1, 1)^3$. We assume $\mathcal{M}^0$ to be regular, i.e., the intersection $\overline{Q}_\mathfrak{p} \cap \overline{Q}_{\mathfrak{p}'}$ of any two patches $Q_\mathfrak{p}, Q_{\mathfrak{p}'} \in \mathcal{M}^0$, $\mathfrak{p} \neq \mathfrak{p}'$, is either empty, a vertex, an entire edge, or an entire face of both patches. Without loss of generality we assume that (the closure of) each patch intersects with at most one corner $\boldsymbol{c} \in \mathcal{C}$, and with either none, one or several edges $\boldsymbol{e} \in \mathcal{E}_{\boldsymbol{c}}$ meeting in $\boldsymbol{c}$. In addition, we shall always assume that boundary faces on the patch $Q_\mathfrak{p}$ belong to exactly one boundary plane Γ_ι.

With each patch $Q_\mathfrak{p} \in \mathcal{M}^0$, we associate a *geometric reference mesh patch* $\widetilde{\mathcal{M}}_\mathfrak{p}$ *on* $\widetilde{Q}$. We recall from [23, Section 3.3] that the geometric mesh patches are generated recursively by iterating *four basic geometric refinement operations*, the so-called *hp-extensions* (Ex1)–(Ex4) on $\widetilde{Q}$, resulting in *four geometric mesh patch types* $\mathfrak{t} \in \{\boldsymbol{c}, \boldsymbol{e}, \boldsymbol{ce}, \text{int}\}$. That is, we take

$$\widetilde{\mathcal{M}}_\mathfrak{p} \in \widetilde{\mathcal{RP}} := \{\widetilde{\mathcal{M}}_\sigma^{\ell,\boldsymbol{c}}, \widetilde{\mathcal{M}}_\sigma^{\ell,\boldsymbol{e}}, \widetilde{\mathcal{M}}_\sigma^{\ell,\boldsymbol{ce}}, \widetilde{\mathcal{M}}_\sigma^{\ell,\text{int}}\} = \{\widetilde{\mathcal{M}}_\sigma^{\ell,\mathfrak{t}}\}_{\mathfrak{t}\in\{\boldsymbol{c},\boldsymbol{e},\boldsymbol{ce},\text{int}\}}. \tag{3.1}$$

Whenever $Q_\mathfrak{p}$ abuts at the singular set $\mathcal{S}$, we assign to $\widetilde{\mathcal{M}}_\mathfrak{p}$ (a suitably rotated and oriented version) of the geometrically refined reference mesh patches shown in Fig. 1 and denoted by $\widetilde{\mathcal{M}}_\sigma^{\ell,\boldsymbol{c}}$ (corner patch), $\widetilde{\mathcal{M}}_\sigma^{\ell,\boldsymbol{e}}$ (edge patch), and $\widetilde{\mathcal{M}}_\sigma^{\ell,\boldsymbol{ce}}$ (corner–edge patch), respectively. We implicitly allow for simultaneous geometric refinements toward several edges in the corner–edge patch $\widetilde{\mathcal{M}}_\sigma^{\ell,\boldsymbol{ce}}$, which corresponds to an overlap of at most three rotated versions of the basic corner–edge patch; see Fig. 3. The geometric refinements in these reference patches are characterized by (i) a fixed parameter $\sigma \in (0, 1)$ defining the subdivision ratio of the geometric refinements and (ii) the index ℓ defining the number of refinements. For interior patches $Q_\mathfrak{p} \in \mathcal{M}^0$, which have empty intersection with $\mathcal{S}$, we assign to $\widetilde{\mathcal{M}}_\mathfrak{p}$ a geometric reference mesh patch $\widetilde{\mathcal{M}}_\sigma^{\ell,\text{int}}$ on $\widetilde{Q}$, which comprises only *finitely many regular refinements* and does not introduce irregular faces in $\widetilde{Q}$. In the refinement process, the reference mesh $\widetilde{\mathcal{M}}_\sigma^{\ell,\text{int}}$ is kept unchanged and is independent of the refinement level ℓ. As different interior patches can be refined differently, without loss of generality the notation $\widetilde{\mathcal{M}}_\sigma^{\ell,\text{int}}$ is to be understood in a generic fashion.

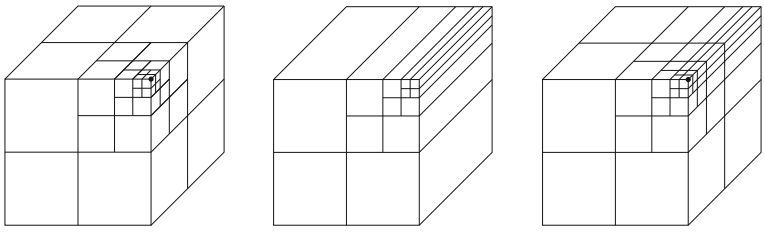

Fig. 1 Three geometric reference mesh patches on $\widetilde{Q}$ with $\sigma = 0.5$: corner patch $\widetilde{\mathcal{M}}_\sigma^{\ell,\boldsymbol{c}}$ (*left*), edge patch $\widetilde{\mathcal{M}}_\sigma^{\ell,\boldsymbol{e}}$ (*center*), and corner–edge patch $\widetilde{\mathcal{M}}_\sigma^{\ell,\boldsymbol{ce}}$ (*right*)

The geometric reference mesh patch $\widetilde{\mathcal{M}}_{\mathfrak{p}} \in \widetilde{\mathcal{RP}}$ introduces the corresponding patch partition $\mathcal{M}_{\mathfrak{p}} = G_{\mathfrak{p}}(\widetilde{\mathcal{M}}_{\mathfrak{p}}) := \{K : K = G_{\mathfrak{p}}(\widetilde{K}),\ \widetilde{K} \in \widetilde{\mathcal{M}}_{\mathfrak{p}}\}$ on $Q_{\mathfrak{p}}$. *Inter-patch continuity* of hp-approximations will be ensured by the following hypothesis; cf. [20, Assumption 3.1]. Here and in the sequel, we denote by $m_d(\cdot)$ the d-dimensional Lebesgue measure.

Assumption 3.1 For $\mathfrak{p} \neq \mathfrak{p}'$, let $Q_{\mathfrak{p}}, Q_{\mathfrak{p}'} \in \mathcal{M}^0$ be two distinct patches with $\Gamma_{\mathfrak{p}\mathfrak{p}'} := \overline{Q}_{\mathfrak{p}} \cap \overline{Q}_{\mathfrak{p}'} \neq \emptyset$ and either $m_2(\Gamma_{\mathfrak{p}\mathfrak{p}'}) > 0$ or $m_2(\Gamma_{\mathfrak{p}\mathfrak{p}'}) = 0, m_1(\Gamma_{\mathfrak{p}\mathfrak{p}'}) > 0$. Then the parametrizations induced by the patch maps on the patch interfaces $\Gamma_{\mathfrak{p}\mathfrak{p}'}$ are assumed to coincide "from either side": $G_{\mathfrak{p}} \circ \left(G_{\mathfrak{p}'}^{-1} \mid_{\Gamma_{\mathfrak{p}\mathfrak{p}'}}\right) = G_{\mathfrak{p}'} \circ \left(G_{\mathfrak{p}}^{-1} \mid_{\Gamma_{\mathfrak{p}\mathfrak{p}'}}\right)$. In addition, the mesh patches $\mathcal{M}_{\mathfrak{p}}, \mathcal{M}_{\mathfrak{p}'}$ are assumed to coincide on $\Gamma_{\mathfrak{p}\mathfrak{p}'}$.

3.1.2 Geometric Meshes

For fixed parameters $\sigma \in (0, 1)$ and $\ell \in \mathbb{N}$, a σ-geometric mesh on Ω is now given by the disjoint union

$$\mathcal{M} = \mathcal{M}_\sigma^\ell := \cup_{\mathfrak{p}=1}^{\mathfrak{P}} \mathcal{M}_{\mathfrak{p}}\,. \tag{3.2}$$

If we denote by $\widehat{K} := (-1, 1)^3$ the reference cube, then each $K \in \mathcal{M}$ is the image of $\widehat{K}$ under an element mapping $\Phi_K : \widehat{K} \to K$, given as *the composition of the corresponding patch map $G_{\mathfrak{p}}$ with an anisotropic dilation–translation*. To achieve a proper geometric refinement toward corners and edges of Ω without violating Assumption 3.1, the geometric refinements $\mathcal{M}_{\mathfrak{p}}$ in the patches $Q_{\mathfrak{p}}$ have to be suitably selected and oriented. For a fixed subdivision ratio $\sigma \in (0, 1)$, we call the sequence $\mathfrak{M}_\sigma = \{\mathcal{M}_\sigma^\ell\}_{\ell \geq 1}$ of geometric meshes a *σ-geometric mesh family*; see [23, Definition 3.4]. As before, we shall refer to the index ℓ as *refinement level*.

Without loss of generality as in [24, Section 5.1.4], every element $K \in \mathcal{M}$ can be assumed to be a Cartesian product of the form

$$K = K^\perp \times K^\parallel = (0, h_K^\perp)^2 \times (0, h_K^\parallel), \tag{3.3}$$

with $h_K^\perp \lesssim h_K^\parallel$. We call $K \in \mathcal{M}_\sigma^\ell$ *isotropic* if $h_K^\perp \simeq h_K^\parallel \simeq h_K$ uniformly in ℓ; otherwise, the element K is *anisotropic*. Elements in corner and interior patches are isotropic, whereas elements in edge and corner–edge patches may be anisotropic. We also note that the elemental diameters $h_K^\perp$ and $h_K^\parallel$ are related to the relative distances of element K to the edge $\boldsymbol{e}$ and corner $\boldsymbol{c}$ located nearest to K; cf. [24, Proposition 3.2].

3.1.3 Vertices, Edges and Faces

For an axiparallel hexahedral element K, we denote by $\mathcal{N}(K)$, $\mathcal{E}(K)$ and $\mathcal{F}(K)$ the sets of its elemental vertices, its elemental edges and its elemental faces, respectively. If $E \in \mathcal{E}(K)$ and $\mathcal{F} \in \mathcal{F}(K)$, we write $\mathcal{N}(E) \subset \mathcal{N}(K)$ and $\mathcal{N}(F) \subset \mathcal{N}(K)$ for the vertices of E and F, respectively, $\mathcal{E}(F) \subset \mathcal{F}(K)$ for the four elemental edges of F and $\mathcal{F}(E) \subset \mathcal{F}(K)$ for the two elemental faces sharing E.

Let $\mathcal{M} = \mathcal{M}_\sigma^\ell$ be a geometric mesh. The set of all vertex nodes of $\mathcal{M}$ is

$$\mathcal{N}(\mathcal{M}) := \bigcup_{K\in\mathcal{M}} \mathcal{N}(K)\,. \tag{3.4}$$

The subset $\mathcal{N}_D(\mathcal{M})$ of all Dirichlet nodes consists of all $\boldsymbol{N} \in \mathcal{N}(\mathcal{M})$ with $\boldsymbol{N} \in \overline{\Gamma}_{\boldsymbol{\iota}}$ for some index $\boldsymbol{\iota} \in \mathcal{J}_D$. The node $\boldsymbol{N}$ is called regular if $\boldsymbol{N} \in \mathcal{N}(K)$ for all $K \in \mathcal{M}$ with $\boldsymbol{N} \cap \overline{K} \neq \emptyset$; otherwise, it is called irregular.

The non-trivial two-dimensional intersection $F = F_{K,K'}$ of the elemental faces of two distinct neighboring elements $K, K' \in \mathcal{M}$ is called an *interior face of* $\mathcal{M}$. Note that $F_{K,K'} = F_{K,K'}$. For our class of geometric meshes and possibly after reordering the tuple (K, K'), we can always assume that $F = F_{K,K'}$ is an elemental face of K and a non-vanishing subset of an elemental face of K'. That is, we have

$$F \in \mathcal{F}(K) \quad \text{and} \quad F \subseteq F' \text{ for } F' \in \mathcal{F}(K') \text{ with } m_2(F \cap F') > 0, \tag{3.5}$$

where we recall that $m_2(\cdot)$ denotes the two-dimensional Lebesgue measure. The face F is called regular if $F \in \mathcal{F}(K)$ and $F \in \mathcal{F}(K')$; otherwise, it is said to be irregular. Furthermore, the non-empty and two-dimensional intersection $F = F_{K,\Gamma_{\boldsymbol{\iota}}}$ of an elemental face of $K \in \mathcal{M}$ with a Dirichlet plane $\Gamma_{\boldsymbol{\iota}}$ for $\boldsymbol{\iota} \in \mathcal{J}_D$ is a *Dirichlet boundary face of* $\mathcal{M}$. We always have $F_{K,\Gamma_{\boldsymbol{\iota}}} \in \mathcal{F}(K)$. *Neumann boundary faces* are defined correspondingly. However, as Neumann boundary conditions are enforced naturally, they will only play a minor role in our analysis. We write $\mathcal{F}_I(\mathcal{M})$, $\mathcal{F}_D(\mathcal{M})$ and $\mathcal{F}_N(\mathcal{M})$ for the sets of interior, Dirichlet and Neumann boundary faces of $\mathcal{M}$, respectively, and set $\mathcal{F}_{ID}(\mathcal{M}) := F_I(\mathcal{M}) \cup \mathcal{F}_D(\mathcal{M})$.

The non-trivial one-dimensional intersection $E = E_{F,F'}$ of two neighboring faces $F, F' \in \mathcal{F}(\mathcal{M})$ is called an *edge of* $\mathcal{M}$. The edge E is called *regular in* $\mathcal{M}$ if $E \in \mathcal{E}(K)$ whenever $E \cap \overline{K} \neq \emptyset$; otherwise, we call it irregular. Note that an edge E can be located in a Dirichlet or Neumann face $\Gamma_{\boldsymbol{\iota}}$, as well as on a Dirichlet or Neumann edge $\boldsymbol{e} \in \mathcal{E}_D \,\dot\cup\, \mathcal{E}_N$; in these cases, we call it a *Dirichlet or Neumann boundary edge of* $\mathcal{M}$. Moreover, the non-trivial one-dimensional intersection $E = E_{F,\boldsymbol{e}}$ of $F \in \mathcal{F}(\mathcal{M})$ with $\boldsymbol{e} \in \mathcal{E}_D \,\dot\cup\, \mathcal{E}_N$ is also called a Dirichlet or Neumann boundary edge. Edges of this form are always elemental edges of an element K. The set of all edges is denoted by $\mathcal{E}(\mathcal{M})$, and the sets of all Dirichlet and Neumann boundary edges by $\mathcal{E}_D(\mathcal{M})$ and $\mathcal{E}_N(\mathcal{M})$, respectively.

For a piecewise smooth function v, we define the jump of v over $F_{K,K'} \in \mathcal{F}_I(\mathcal{M})$, respectively over $F_{K,\Gamma_{\boldsymbol{\iota}}} \in \mathcal{F}_D(\mathcal{M})$ by

$$[\![v]\!]_{F_{K,K'}} := v|_K - v|_{K'} \quad \text{respectively by} \quad [\![v]\!]_{F_{K,\Gamma_{\boldsymbol{\iota}}}} := v|_K. \tag{3.6}$$

For $F \in \mathcal{F}(K)$, we denote by $h_{K,F}^\perp$ the height of K in direction perpendicular to F. We then introduce the *trace mesh size function* by

$$\mathtt{h}_F := \begin{cases} \min\left\{h_{K,F}^\perp, h_{K',F'}^\perp\right\}, & F = F_{K,K'} \in \mathcal{F}_I(\mathcal{M}), \\ h_{K,F}^\perp, & F = F_{K,\Gamma_{\boldsymbol{\iota}}} \in \mathcal{F}_D(\mathcal{M}), \end{cases} \tag{3.7}$$

with $F' \in \mathcal{F}(K')$ as in (3.5). The bounded variation property in [23, Section 3.3.2] implies $\mathtt{h}_F \simeq h^{\perp}_{K,F} \simeq h^{\perp}_{K',F'}$ for interior faces $F_{K,K'} \in \mathcal{F}_I(\mathcal{M})$.

3.2 Finite Element Spaces

We next introduce discontinuous and continuous finite element spaces with anisotropic and $\mathfrak{s}$-linear degree distributions.

3.2.1 Local Finite Element Spaces

Let $\mathcal{M} = \mathcal{M}^{\ell}_{\sigma}$ be a geometric mesh. With each $K \in \mathcal{M}$ and in accordance with (3.3), we assign an *anisotropic* polynomial degree vector $\boldsymbol{p}_K := (p^{\perp}_K, p^{\parallel}_K)$, with degrees $p^{\perp}_K \geq 1$ and $p^{\parallel}_K \geq 1$ in edge-perpendicular and edge-parallel directions, respectively. We may and will always assume that $p^{\perp}_K \leq p^{\parallel}_K$; cf. [24, Section 3]. For $K \in \mathcal{M}$, the elemental tensor-product polynomial space is

$$\mathbb{Q}_{\boldsymbol{p}_K}(K) := \{\, v \in L^2(K) \,:\, v|_K \circ \Phi_K \in \mathbb{Q}_{\boldsymbol{p}_K}(\widehat{K}) \,\}, \tag{3.8}$$

where $\Phi_K : \widehat{K} \to K$ is the element mapping and $\mathbb{Q}_{\boldsymbol{p}_K}(\widehat{K})$ the anisotropic tensor-product polynomial space on $\widehat{K} = \widehat{I}^3$ with $\widehat{I} = (-1, 1)$:

$$\mathbb{Q}_{\boldsymbol{p}_K}(\widehat{K}) := \mathbb{Q}_{p^{\perp}_K}(\widehat{I}^2) \otimes \mathbb{P}_{p^{\parallel}_K}(\widehat{I}) = \mathbb{P}_{p^{\perp}_K}(\widehat{I}) \otimes \mathbb{P}_{p^{\perp}_K}(\widehat{I}) \otimes \mathbb{P}_{p^{\parallel}_K}(\widehat{I}), \tag{3.9}$$

with $\mathbb{P}_p(I)$ denoting the univariate polynomials of degree less than or equal to p on an interval I. The polynomial degree vector $\boldsymbol{p}_K$ is called *isotropic* if $p^{\perp}_K = p^{\parallel}_K = p_K$. In this case, we write $\mathbb{Q}_{p_K}(K)$ in place of $\mathbb{Q}_{\boldsymbol{p}_K}(K)$.

The elemental polynomial degree vectors $\boldsymbol{p}_K$ are combined into the *polynomial degree distribution* $\boldsymbol{p} := \{\, \boldsymbol{p}_K : K \in \mathcal{M} \,\}$ on $\mathcal{M}$. We set $|\boldsymbol{p}| := \max_{K\in\mathcal{M}} |\boldsymbol{p}_K|$, with $|\boldsymbol{p}_K| := \max\{p^{\perp}_K, p^{\parallel}_K\}$. We then introduce the generic discontinuous space

$$V^0(\mathcal{M}, \boldsymbol{p}) := \left\{ v \in L^2(\Omega) \,:\, v|_K \in \mathbb{Q}_{\boldsymbol{p}_K}(K),\ K \in \mathcal{M} \right\}. \tag{3.10}$$

The *hp*-extensions (Ex1)–(Ex4) introduced in [23] provide $\mathfrak{s}$-*linear polynomial degree distributions* $\boldsymbol{p}_{\mathfrak{s}}(\widetilde{\mathcal{M}}^{\ell,\mathtt{t}}_{\sigma})$ on the geometric reference mesh patches $\widetilde{\mathcal{M}}^{\ell,\mathtt{t}}_{\sigma}$ for $\mathtt{t} \in \{\boldsymbol{c}, \boldsymbol{e}, \boldsymbol{ce}, \mathrm{int}\}$, which increase $\mathfrak{s}$-linearly and possibly anisotropically away from singularities for a *slope parameter* $\mathfrak{s} > 0$; see [23, Section 3] for more details. By construction, the patchwise distributions $\boldsymbol{p}_{\mathfrak{s}}(\widetilde{\mathcal{M}}^{\ell,\mathtt{t}}_{\sigma})$ induce a $\mathfrak{s}$-linear polynomial degree distribution on a geometric mesh $\mathcal{M}^{\ell}_{\sigma}$, which we denote by $\boldsymbol{p}_{\mathfrak{s}}(\mathcal{M}^{\ell}_{\sigma})$.

3.2.2 Face and Edge Polynomial Degrees

Let $\mathcal{M} = \mathcal{M}^{\ell}_{\sigma}$ be a geometric mesh and $\boldsymbol{p}$ a polynomial degree distribution on $\mathcal{M}$. To define conforming spaces, we introduce edge and face polynomial degrees in conjunction with a suitable *minimum rule* over neighboring edges and faces; cf. [7].

Let $K \in \mathcal{M}$ and let $p_K = (p_K^{\perp}, p_K^{\parallel})$ denote the elemental degree vector. For $E \in \mathcal{E}(K)$ and $F \in \mathcal{F}(K)$, we denote by $p_{K,E} \in \mathbb{N}$ and $\boldsymbol{p}_{K,F} = (p^1_{K,F}, p^2_{K,F}) \in \mathbb{N}^2$ the polynomial degrees induced by $\boldsymbol{p}_K$ on E and F in local coordinates, respectively. In agreement with (3.5), we further introduce the set

$$\delta_{K,F} := \{\, K' \in \mathcal{M} \,:\, \exists F' \in \mathcal{F}(K') \text{ with } m_2(F \cap F') > 0 \,\}. \tag{3.11}$$

Notice that $K \in \delta_{K,F}$ and that the cardinality of $\delta_{K,F}$ is bounded uniformly in ℓ.

For $F \in \mathcal{F}(K)$, the *minimum face degree* is

$$\overline{\boldsymbol{p}}_{K,F} := \min_{K' \in \delta_{K,F}} \boldsymbol{p}_{K',F'} \in \mathbb{N}^2, \tag{3.12}$$

where the set $F' \in \mathcal{F}(K')$ is as in (3.11) and where the minimum in (3.12) is understood componentwise and with consistent orientation of the elemental degrees with respect to F. If $E \in \mathcal{E}(K)$, we define the *minimum edge degree* as

$$\overline{p}_{K,E} := \min_{F \in \mathcal{F}(E)} \overline{p}_{K,F,E}, \tag{3.13}$$

where $\overline{p}_{K,F,E}$ is the degree induced by $\overline{\boldsymbol{p}}_{K,F}$ along E. This definition ensures that the minimum edge degrees are always equal to or smaller than the corresponding minimum face degrees.

Remark 3.2 In the axiparallel setting considered here and under Assumption 3.1, for any distinct axiparallel elements $K, K' \in \mathcal{M}$ which share a common edge E or an interior face $F_{K,K'}$, the traces of the elemental polynomial spaces on E and $F_{K,K'}$ in local coordinates induced by the corresponding elemental maps coincide. Therefore, for $E \in \mathcal{E}(K)$ and $F \in \mathcal{F}(K)$, the edge and face polynomial spaces $\mathbb{P}_{\overline{p}_{K,E}}(E)$ and $\mathbb{Q}_{\overline{\boldsymbol{p}}_{K,F}}(F)$ are well defined.

3.2.3 Finite Element Spaces

On an axiparallel element $K \in \mathcal{M}$, we consider polynomial functions $v|_K \in \mathbb{Q}_{\boldsymbol{p}_K}(K)$ which can be expanded into basis functions as

$$v|_K := v|_K^{\text{nod}} + v|_K^{\text{edge}} + v|_K^{\text{face}} + v|_K^{\text{int}}, \tag{3.14}$$

where, with the minimum degrees $\overline{\boldsymbol{p}}_{K,F}$ in (3.12) and $\overline{p}_{K,E}$ in (3.13),

$$\begin{aligned} v|_K^{\mathrm{nod}} &= \sum_{\boldsymbol{N}\in\mathcal{N}(K)} c_K^{\boldsymbol{N}} \Phi_K^{\boldsymbol{N}}, \\ v|_K^{\mathrm{edge}} &= \sum_{E\in\mathcal{E}(K)} \sum_{i=1}^{\overline{p}_{K,E}-1} c_K^{E,i} \Phi_K^{E,i}, \\ v|_K^{\mathrm{face}} &= \sum_{F\in\mathcal{F}(K)} \sum_{i=1}^{\overline{p}^1_{K,F}-1} \sum_{j=1}^{\overline{p}^2_{K,F}-1} c_K^{F,i,j} \Phi_K^{F,i,j}, \end{aligned} \tag{3.15}$$

with coefficients $c_K^{\boldsymbol{N}}$, $c_K^{E,i}$ and $c_K^{F,i,j}$. Here, the function $\Phi_K^{\boldsymbol{N}} \in \mathbb{Q}_1(K)$ denotes the trilinear nodal shape function on K with the property that $\Phi_K^{\boldsymbol{N}}(\boldsymbol{N}') = \delta_{\boldsymbol{N},\boldsymbol{N}'}$ for $\boldsymbol{N}' \in \mathcal{N}(K)$. For $E \in \mathcal{E}(K)$, the edge shape functions $\{\Phi_K^{E,i}\}_{i=1}^{\overline{p}_{K,E}-1}$ on K are polynomials of degree $\overline{p}_{K,E}$ along the edge E tensorized with linear blending functions in the two directions perpendicular to E. They vanish at the end points $\boldsymbol{N} \in \mathcal{N}(E)$, on the other elemental edges $E' \neq E$, as well as on faces $F \in \mathcal{F}(K)$ with $F \notin \mathcal{F}(E)$. Restricted to E, they span the space $\mathbb{P}_{\overline{p}_{K,E}}(E) \cap H_0^1(E)$. Similarly, for $F \in \mathcal{F}(K)$, the face shape functions $\{\Phi_K^{F,i,j}\}_{i,j}$ are anisotropic polynomials of vector degree $\overline{\boldsymbol{p}}_{K,F}$ on the face F, tensorized with linear blending functions in the direction perpendicular to F. They vanish at the nodes $\boldsymbol{N} \in \mathcal{N}(F)$, on the edges $E \in \mathcal{E}(F)$ and on the remaining elemental faces $F' \neq F$. Restricted to F, they span the space $\mathbb{Q}_{\overline{\boldsymbol{p}}_{K,F}}(F) \cap H_0^1(F)$. Finally, the interior part $v|_K^{\mathrm{int}}$ in (3.14) is a polynomial bubble function in $\mathbb{Q}_{\boldsymbol{p}_K}(K) \cap H_0^1(K)$; as it will be left unchanged in the subsequent analysis, we will not further specify it. For empty ranges of the indices in (3.15), the corresponding sums are understood as zero. We refer the reader to [7, Section 2.3] for an explicit construction of shape functions as in (3.14), (3.15). Shape functions are pushed forward from the reference element $\widehat{K}$ to K with the element map Φ_K.

For $K \in \mathcal{M}$, we collect the face and edge degrees in (3.12), (3.13) in the vector $\overline{\boldsymbol{p}}_K$, and define the elemental polynomial space

$$\mathbb{S}_{\overline{\boldsymbol{p}}_K}(K) := \left\{ v|_K \in \mathbb{Q}_{\boldsymbol{p}_K}(K) \,:\, v|_K \text{ is of the form (3.14), (3.15)} \right\}. \tag{3.16}$$

Thus, a polynomial $v \in \mathbb{S}_{\overline{\boldsymbol{p}}_K}(K)$ satisfies

$$v|_E \in \mathbb{P}_{\overline{p}_{K,E}}(E),\ E \in \mathcal{E}(K) \quad \text{and} \quad v|_F \in \mathbb{Q}_{\overline{\boldsymbol{p}}_{K,F}}(F),\ F \in \mathcal{F}(K). \tag{3.17}$$

We then introduce the *minimum rule hp-finite element spaces*

$$\overline{V}^0(\mathcal{M}, \boldsymbol{p}) := \left\{ v \in L^2(\Omega) \,:\, v|_K \in \mathbb{S}_{\overline{\boldsymbol{p}}_K}(K),\ K \in \mathcal{M} \right\}, \tag{3.18}$$

$$V^1(\mathcal{M}, \boldsymbol{p}) := \left\{ v \in V \,:\, v|_K \in \mathbb{S}_{\overline{\boldsymbol{p}}_K}(K),\ K \in \mathcal{M} \right\}; \tag{3.19}$$

cf. [7]. By construction, $\overline{V}^0(\mathcal{M}, \boldsymbol{p}) \subseteq V^0(\mathcal{M}, \boldsymbol{p})$.

3.3 Conforming *hp*-FEM and Exponential Convergence

For parameters $\sigma \in (0,1)$ and $\mathfrak{s} > 0$, let $\mathfrak{M}_\sigma = \{\mathcal{M}_\sigma^\ell\}_{\ell\geq 1}$ be a σ-geometric mesh family on Ω and $\{\boldsymbol{p}_\mathfrak{s}(\mathcal{M}_\sigma^\ell)\}_{\ell\geq 1}$ the corresponding $\mathfrak{s}$-linear polynomial degree distributions. We consider the sequence of conforming hp-version finite element spaces

$$V_{\sigma,\mathfrak{s}}^{\ell,1} := V^1(\mathcal{M}_\sigma^\ell, \boldsymbol{p}_\mathfrak{s}(\mathcal{M}_\sigma^\ell)), \qquad \ell \geq 1, \tag{3.20}$$

and introduce its non-conforming counterparts by setting

$$V_{\sigma,\mathfrak{s}}^{\ell,0} := V^0(\mathcal{M}_\sigma^\ell, \boldsymbol{p}_\mathfrak{s}(\mathcal{M}_\sigma^\ell)), \qquad \overline{V}_{\sigma,\mathfrak{s}}^{\ell,0} := \overline{V}^0(\mathcal{M}_\sigma^\ell, \boldsymbol{p}_\mathfrak{s}(\mathcal{M}_\sigma^\ell)), \qquad \ell \geq 1. \tag{3.21}$$

Remark 3.3 The fact that the conforming spaces $V_{\sigma,\mathfrak{s}}^{\ell,1}$ define proper linear spaces will follow from our construction of conforming approximations in Sects. 5 and 6 ahead. In the pure Neumann case (where $\mathcal{J}_D = \emptyset$), we note that the constant function belongs to $V_{\sigma,\mathfrak{s}}^{\ell,1}$, which will lead to well-defined factor spaces $V_{\sigma,\mathfrak{s}}^{\ell,1}/\mathbb{R}$.

The hp-version Galerkin discretization of the variational formulation (1.4) reads as usual: Find $u^\ell \in V_{\sigma,\mathfrak{s}}^{\ell,1}$ such that

$$a(u^\ell, v) = \int_\Omega f v dx \qquad \forall v \in V_{\sigma,\mathfrak{s}}^{\ell,1}\ , \tag{3.22}$$

where we implicitly use the corresponding factor spaces $V_{\sigma,\mathfrak{s}}^{\ell,1}/\mathbb{R}$ in the pure Neumann case. For every $\ell \geq 1$, the discrete variational problem (3.22) admits a unique solution $u^\ell \in V_{\sigma,\mathfrak{s}}^{\ell,1}$ which is quasi-optimal: There exists a constant $C > 0$ (only depending on Ω, the coefficient matrix $\boldsymbol{A}$ and the set $\mathcal{E}_D$) such that

$$\|u - u^\ell\|_{H^1(\Omega)} \leq C \inf_{v\in V_{\sigma,\mathfrak{s}}^{\ell,1}} \|u - v\|_{H^1(\Omega)}\ . \tag{3.23}$$

The main result of this paper is the H^1-norm exponential convergence of hp-FE approximations (3.22) for problem (1.1)–(1.3) with weak solutions $u \in B_{-1-\boldsymbol{b}}(\Omega)$. This follows from the quasi-optimality (3.23) and the following *approximation property* of the hp-version finite element spaces $V_{\sigma,\mathfrak{s}}^{\ell,1}$.

Theorem 3.4 *Let $\boldsymbol{b}$ be a weight exponent vector satisfying (2.9). For parameters $\sigma \in (0,1)$, $\mathfrak{s} > 0$, consider the sequence $V_{\sigma,\mathfrak{s}}^{\ell,1}$ of H^1-conforming hp-version finite element spaces in (3.20). Then there exist quasi-interpolants $\Pi_{\sigma,\mathfrak{s}}^{\ell,1} : V \to V_{\sigma,\mathfrak{s}}^{\ell,1}$ such that for functions $u \in V$ with $u \in B_{-1-\boldsymbol{b}}(\Omega) \cap H^{1+\theta}(\Omega)$ for some $\theta \in (0,1)$ there holds*

$$\|u - \Pi_{\sigma,\mathfrak{s}}^{\ell,1} u\|_{H^1(\Omega)} \leq C \exp(-b\ell)\ , \qquad \ell \geq 2\ , \tag{3.24}$$

with constants $b, C > 0$ independent of ℓ, but depending on the parameters σ, $\mathfrak{s}$, the macro-mesh $\mathcal{M}^0$ with its associated patch maps, the minimum weight exponent

in (2.9)*, the exponent* θ*, and on* u *through the analytic regularity constant* C_u *in Definition* 2.1.

In particular, if the variational solution $u \in V$ *of problem* (1.1)–(1.3) *belongs to* $B_{-1-\boldsymbol{b}}(\Omega) \cap H^{1+\theta}(\Omega)$ *for some* $\theta \in (0,1)$*, cf. Sect.* 2.3*, then the conforming finite element approximations* $u^\ell \in V^{\ell,1}_{\sigma,\mathfrak{s}}$ *in* (3.22) *converge exponentially:*

$$\|u - u^\ell\|_{H^1(\Omega)} \leq C \exp\left(-b\sqrt[5]{N}\right) , \tag{3.25}$$

where the constants $b, C > 0$ *are independent of* $N = \dim(V^{\ell,1}_{\sigma,\mathfrak{s}})$*, the number of degrees of freedom of the hp-FE discretization.*

Remark 3.5 The quasi-interpolation operators $\Pi^{\ell,1}_{\sigma,\mathfrak{s}}$ in (3.24) constructed ahead are well defined on the space $V \subseteq H^1(\Omega)$. This is in contrast to the interpolants used in [20] for homogeneous Dirichlet boundary conditions. They require H^2-regularity in each coordinate direction in the interior of Ω, and are set to zero on elements abutting at corners and edges of Ω.

Remark 3.6 The global *hp*-version quasi-interpolants $\Pi^{\ell,1}_{\sigma,\mathfrak{s}}$ in (3.24) are assembled from *hp-patch quasi-interpolants* $\Pi^{\ell,1,\mathfrak{p}}_{\sigma,\mathfrak{s}}$. We write formally

$$\Pi^{\ell,1}_{\sigma,\mathfrak{s}} = \sum\nolimits_{\mathfrak{p}=1}^{\mathfrak{P}} \Pi^{\ell,1,\mathfrak{p}}_{\sigma,\mathfrak{s}} , \tag{3.26}$$

with restrictions to patches $\mathfrak{p} \in [1, ..., \mathfrak{P}]$ implied in $\Pi^{\ell,1,\mathfrak{p}}_{\sigma,\mathfrak{s}}$ and where inter-patch continuity follows from Assumption 3.1. The *hp*-patch quasi-interpolants $\Pi^{\ell,1,\mathfrak{p}}_{\sigma,\mathfrak{s}}$ in (3.26), in turn, are obtained from *four families* $\{\widetilde{\Pi}^{\ell,1,\mathfrak{t}}_{\sigma,\mathfrak{s}}\}_{\ell\geq 1}$ *of hp-reference patch quasi-interpolants* on the geometric reference mesh patches $\widetilde{\mathcal{M}}^{\ell,\mathfrak{t}}_{\sigma}$, $\mathfrak{t} \in \{\boldsymbol{c}, \boldsymbol{e}, \boldsymbol{ce}, \mathrm{int}\}$, which are transported to the patches $Q_\mathfrak{p} \subset \Omega$ via the patch maps $G_\mathfrak{p}$. While no liftings are necessary for interior patches (i.e., for $\mathfrak{t} = \mathrm{int}$), for patches of type $\mathfrak{t} \in \{\boldsymbol{c}, \boldsymbol{e}, \boldsymbol{ce}\}$, our construction yields jump liftings with stability bounds in the $H^1(Q_\mathfrak{p})$-norm which grow algebraically in $|\boldsymbol{p}|$.

Furthermore, the exponential consistency in $H^1(\widetilde{Q})$ of $\widetilde{\Pi}^{\ell,1,\mathfrak{t}}_{\sigma,\mathfrak{s}}$ on the reference patch $\widetilde{Q}$ can be readily verified for solutions $u \in V$ of (1.1)–(1.3) whose pullbacks from the mesh patch $Q_\mathfrak{p}$ to $\widetilde{Q}$ satisfy the *analytic patch regularity*

$$\widetilde{u}_\mathfrak{p} := u|_{Q_\mathfrak{p}} \circ G_\mathfrak{p} \in B_\mathfrak{t}(\widetilde{Q}), \quad 1 \leq \mathfrak{p} \leq \mathfrak{P}, \quad \mathfrak{t} \in \{\boldsymbol{c}, \boldsymbol{e}, \boldsymbol{ce}, \mathrm{int}\} , \tag{3.27}$$

where $B_\mathfrak{t}(\widetilde{Q})$ is an *analytic regularity reference class on* $\widetilde{Q}$ with weighting toward corners or edges of $\widetilde{Q}$ depending on the refinement type $\mathfrak{t} \in \{\boldsymbol{c}, \boldsymbol{e}, \boldsymbol{ce}, \mathrm{int}\}$; see also [20, Section 4.4] for analytic reference classes $A_\mathfrak{t}(\widetilde{O})$ in the pure Dirichlet case. For $\mathfrak{t} \in \{\boldsymbol{c}, \boldsymbol{ce}\}$, we additionally require in (3.27) that $\widetilde{u}_\mathfrak{p} \in H^{1+\theta}(\widetilde{Q})$; cf. Remark 2.3. *All exponential convergence rate estimates in the present paper apply verbatim to any solution* $u \in H^1(\Omega)$ *which, in local patch coordinates, exhibit the above analytic patch regularity* (3.27).

Remark 3.7 The results of Theorem 3.4 remain valid for

$$V^1(\mathcal{M}_\sigma^\ell, p_\ell) := \big\{ v \in V \,:\, v|_K \in \mathbb{Q}_{p_\ell}(K),\ K \in \mathcal{M}_\sigma^\ell \big\}, \qquad \ell \geq 1, \tag{3.28}$$

with uniform, isotropic polynomial degree $p_\ell \geq 1$. For these spaces, the minimum rules in Sect. 3.2.2 are trivially satisfied. The exponential convergence bounds (3.24) and (3.25) follow in this case as well, provided that $p_\ell = \max\{1, \lfloor \mathfrak{s}\ell \rfloor\}$, albeit with a generally smaller constant $b > 0$ (depending on $\mathfrak{s}$).

Remark 3.8 The bounds (3.24) and (3.25) hold true in the pure Neumann case. This follows readily from Remark 3.3 and since $\Pi^{\ell,1}_{\sigma,\mathfrak{s}}$ reproduces constant functions.

Remark 3.9 The exponential convergence results in this paper apply verbatim to conforming *hp*-FEMs for second-order and possibly vector-valued elliptic problems which allow for analytic regularity shifts in the function classes in Definition 2.1. In particular, they are valid for stress–strain formulations of the equations of linear elasticity (with constant material parameters); see [5, Section 7].

3.4 Outline of the Proof

The proof of Theorem 3.4 follows along the general lines of [20, Section 3.4], but is significantly more involved due to the appearance of the non-homogeneously weighted Sobolev spaces and the anisotropic and variable polynomial degree distributions. In this section, we outline the key steps. From now on we will frequently use the shorthand notation "$\lesssim_p$" for inequalities which hold up to *algebraic losses* in $|\boldsymbol{p}|$:

$$x \lesssim_p y \quad \Leftrightarrow \quad x \lesssim |\boldsymbol{p}|^a\, y \quad \text{for some } a \in \mathbb{N}. \tag{3.29}$$

3.4.1 Base Projectors with Partial Conformity

We first introduce (non-conforming) base projectors $\pi^\ell_{\sigma,\mathfrak{s}}$ with partial conformity and exponential convergence estimates in broken norms.

To discuss the partial conformity, let $\mathcal{M} = \mathcal{M}^\ell_\sigma$ be a geometric mesh. For a set $\mathcal{F}' \subset \mathcal{F}_{ID}(\mathcal{M}^\ell_\sigma)$ of faces, we define

$$\mathrm{jmp}_{\mathcal{F}'}[u]^2 := \sum_{F \in \mathcal{F}'} \mathrm{h}_F^{-1} \|[\![u]\!]\|^2_{L^2(F)}. \tag{3.30}$$

Then, to avoid the need for jump liftings over edge-perpendicular faces between highly anisotropic elements, we construct base projectors $\pi^\ell_{\sigma,\mathfrak{s}}$ which are conforming across certain sets $\mathcal{F}^\perp_{ID}(\mathcal{M}) \subset \mathcal{F}_{ID}(\mathcal{M})$ of edge-perpendicular faces, and generally non-conforming edge-parallel faces $F \in \mathcal{F}^\parallel_{ID}(\mathcal{M}) := \mathcal{F}_{ID}(\mathcal{M}) \backslash F^\perp_{ID}(\mathcal{M})$, which can be characterized by the property that

$$F \subseteq F' \in \mathcal{F}(K): \quad \mathrm{h}_F \simeq h^\perp_{K,F'} \simeq h^\perp_K \text{ uniformly in } \ell. \tag{3.31}$$

If we write K as in (3.3), then (possibly after mapping) a face F satisfying (3.31) can be assumed to be of the form

$$F = (0, h_K^{\perp}) \times (0, h_K^{\parallel}) \text{ uniformly in } \ell \,. \tag{3.32}$$

Note that faces with (3.31), (3.32) appear (i) between isotropic elements and (ii) in edge-parallel direction between anisotropic elements in edge or corner–edge patches.

To state exponential convergence estimates in broken norms, we set

$$\|u\|^2_{L^2(\mathcal{M}')} := \sum_{K\in\mathcal{M}'} \|u\|^2_{L^2(K)} \tag{3.33}$$

and introduce the broken H^1-norms

$$\Upsilon^{\perp}_{\mathcal{M}'}[u]^2 := \sum_{K\in\mathcal{M}'} N_K^{\perp}[u]^2, \qquad \Upsilon^{\parallel}_{\mathcal{M}'}[u]^2 := \sum_{K\in\mathcal{M}'} N_K^{\parallel}[u]^2, \tag{3.34}$$

for any set $\mathcal{M}' \subseteq \mathcal{M}$ of axiparallel elements, with elemental norms defined by

$$\begin{aligned} N_K^{\perp}[u]^2 &:= (h_K^{\perp})^{-2}\|u\|^2_{L^2(K)} + \|\nabla u\|^2_{L^2(K)}, \\ N_K^{\parallel}[u]^2 &:= (h_K^{\parallel})^{-2}\|u\|^2_{L^2(K)} + \|\nabla u\|^2_{L^2(K)}. \end{aligned} \tag{3.35}$$

Evidently, we have

$$N_K^{\parallel}[u]^2 \lesssim N_K^{\perp}[u]^2, \qquad K \in \mathcal{M}', \tag{3.36}$$

whereas $N_K^{\perp}[u] \simeq N_K^{\parallel}[u]$ for isotropic elements K.

Proposition 3.10 *For all parameters $\sigma \in (0,1)$, $\mathfrak{s} > 0$ there are tensor projectors*

$$\pi^{\ell}_{\sigma,\mathfrak{s}} = \pi^{\ell,\perp}_{\sigma,\mathfrak{s}} \otimes \pi^{\ell,\parallel}_{\sigma,\mathfrak{s}} : H^1(\Omega) \to V^{\ell,0}_{\sigma,\mathfrak{s}}, \tag{3.37}$$

and sets $\mathcal{F}^{\perp}_{ID}(\mathcal{M}^{\ell}_{\sigma}) \subset \mathcal{F}_{ID}(\mathcal{M}^{\ell}_{\sigma})$ of edge-perpendicular faces such that: (i) $\pi^{\ell}_{\sigma,\mathfrak{s}}$ is conforming over faces $F \in \mathcal{F}_{ID}(\mathcal{M}^{\ell}_{\sigma})$; (ii) $\pi^{\ell}_{\sigma,\mathfrak{s}}$ is generally non-conforming over faces $F \in \mathcal{F}^{\parallel}_{ID}(\mathcal{M}^{\ell}_{\sigma}) := \mathcal{F}_{ID}(\mathcal{M}^{\ell}_{\sigma})\backslash\mathcal{F}^{\perp}_{ID}(\mathcal{M}^{\ell}_{\sigma})$; (iii) the faces $F \in \mathcal{F}^{\parallel}_{ID}(\mathcal{M}^{\ell}_{\sigma})$ satisfy (3.31), (3.32).

Moreover, for functions u with $u \in B_{-1-\boldsymbol{b}}(\Omega) \cap H^{1+\theta}(\Omega)$ for some $\theta \in (0,1)$ as in Theorem 3.4 and for the error $\eta^{\ell}_{\sigma,\mathfrak{s}} := u - \pi^{\ell}_{\sigma,\mathfrak{s}}u$, we have the H^1-norm bound

$$\Upsilon^{\parallel}_{\mathcal{M}^{\ell}_{\sigma}}[\eta^{\ell}_{\sigma,\mathfrak{s}}]^2 \le C\exp(-2b\ell), \tag{3.38}$$

as well as the jump bound

$$\mathrm{jmp}_{\mathcal{F}^{\parallel}_{ID}(\mathcal{M}^{\ell}_{\sigma})}[\eta^{\ell}_{\sigma,\mathfrak{s}}]^2 \le C\exp(-2b\ell), \tag{3.39}$$

with constants $b, C > 0$ independent of $\ell \ge 2$, but depending σ and $\mathfrak{s}$.

We will show the estimate (3.38) for a more general class of tensor projectors on $H^1(\Omega)$ in Sect. 4, see Theorem 4.3, with most parts of the proof relegated to Appendix 8. The jump bound in (3.39) will be established for the specifically chosen projectors in (3.37) under smoothness requirements which are slightly stronger than $u \in H^1(\Omega)$; in particular, $u \in B_{-1-\boldsymbol{b}}(\Omega)$ is sufficient.

In the following, we shall also split the sets $\mathcal{F}^{\parallel}_{ID}(\mathcal{M}^{\ell}_{\sigma})$ into interior and Dirichlet boundary faces, i.e., $\mathcal{F}^{\parallel}_{ID}(\mathcal{M}^{\ell}_{\sigma}) = \mathcal{F}^{\parallel}_{I}(\mathcal{M}^{\ell}_{\sigma}) \dot\cup F^{\parallel}_{D}(\mathcal{M}^{\ell}_{\sigma})$.

3.4.2 Discontinuous hp-Version Base Spaces

To exploit the approximation properties for the non-conforming base projectors $\pi^{\ell}_{\sigma,\mathfrak{s}} u$ in Proposition 3.10 for the minimum rule finite element spaces $\overline{V}^{\ell,0}_{\sigma,\mathfrak{s}}$ in (3.21), we introduce *discontinuous hp-base spaces* as follows. For axiparallel $K \in \mathcal{M}^{\ell}_{\sigma}$ we introduce the subsets $\mathcal{F}^{\perp}(K)$ and $\mathcal{F}^{\parallel}(K)$ of elemental faces of $\mathcal{F}(K)$, which are perpendicular and parallel, respectively, to the nearest singular edge. For $K \in \mathcal{F}^{\parallel}(K)$, we write $\boldsymbol{p}_{K,F} = (p^{\perp}_K, p^{\parallel}_K)$ to distinguish the perpendicular and parallel components $\boldsymbol{p}_{K,F}$.

Lemma 3.11 *Let $\boldsymbol{p}_{\mathfrak{s}}(\mathcal{M}^{\ell}_{\sigma})$ be a $\mathfrak{s}$-linear degree distribution on $\mathcal{M}^{\ell}_{\sigma}$. For $K \in \mathcal{M}^{\ell}_{\sigma}$, let the face degrees $\overline{\boldsymbol{p}}_{K,F}$ be defined in (3.12). Then there exists $\mu \in (0, 1]$ depending only on $\mathfrak{s} > 0$ such that*

$$\forall K \in \mathcal{F}^{\perp}(K): \qquad \mu p^{\perp}_K \le \overline{p}^{1}_{K,F} \le p^{\perp}_K, \quad \mu p^{\perp}_K \le \overline{p}^{2}_{K,F} \le p^{\perp}_K, \tag{3.40}$$

$$\forall K \in \mathcal{F}^{\parallel}(K): \qquad \mu p^{\perp}_K \le \overline{p}^{\perp}_{K,F} \le p^{\perp}_K, \quad \mu p^{\parallel}_K \le \overline{p}^{\parallel}_{K,F} \le p^{\parallel}_K. \tag{3.41}$$

Proof These properties follow from the construction of the $\mathfrak{s}$-linear degree distributions and their properties of bounded variation; cf. [23, Section 3.2 and Remark 3.9]. □

On $K \in \mathcal{M}^{\ell}_{\sigma}$, we then introduce the *base degree vector* $\check{\boldsymbol{p}}_K = (\check{p}^{\perp}_K, \check{p}^{\parallel}_K) \in \mathbb{N}^2$ as

$$\check{p}^{\perp}_K := \min_{F \in \mathcal{F}^{\perp}(K)} \{\min\{p^{1}_{K,F}, p^{2}_{K,F}\}\}, \qquad \check{p}^{\parallel}_K := \min_{F \in \mathcal{F}^{\parallel}(K)} \overline{p}^{\parallel}_{K,F}. \tag{3.42}$$

Hence,

$$\mathbb{Q}_{\check{\boldsymbol{p}}_K}(K) \subseteq \mathbb{S}_{\overline{\boldsymbol{p}}_K}(K), \qquad K \in \mathcal{M}^{\ell}_{\sigma}. \tag{3.43}$$

From Lemma 3.11, we further have $\mu p^{\perp}_K \le \check{p}^{\perp}_K$ and $\mu p^{\parallel}_K \le \check{p}^{\parallel}_K$. As a consequence, the base degree vectors $\{\check{\boldsymbol{p}}_K\}_{K \in \mathcal{M}^{\ell}_{\sigma}}$ give rise to a $\check{\mathfrak{s}}$-linear polynomial degree distribution $\boldsymbol{p}_{\check{\mathfrak{s}}}(\mathcal{M}^{\ell}_{\sigma})$, for a *base slope parameter* $\check{\mathfrak{s}}$ with $0 < \check{\mathfrak{s}} \le \mathfrak{s}$ and *only depending on* $\mathfrak{s}$. Hence, the *discontinuous hp-base spaces* $V^{\ell,0}_{\sigma,\check{\mathfrak{s}}}$ thus constructed satisfy

$$V^{\ell,0}_{\sigma,\check{\mathfrak{s}}} \subseteq \overline{V}^{\ell,0}_{\sigma,\mathfrak{s}}. \tag{3.44}$$

We point out that for the uniform and isotropic spaces in (3.28), the construction of discontinuous *hp*-base spaces is not necessary and can be omitted.

3.4.3 Averaging Over Regular Vertices, Edges and Faces

We denote by $\overline{V}^{\ell,0,\perp}_{\sigma,\mathfrak{s}}$ the subspace of functions in $\overline{V}^{\ell,0}_{\sigma,\mathfrak{s}}$ which are conforming over $\mathcal{F}^{\perp}_{ID}(\mathcal{M}^{\ell}_{\sigma})$ and possibly non-conforming over $\mathcal{F}^{\parallel}_{ID}(\mathcal{M}^{\ell}_{\sigma})$. We then adopt the approach of [28] to assign to $v \in \overline{V}^{\ell,0,\perp}_{\sigma,\mathfrak{s}}$ vertex, edge and face values which are obtained by *averaging* over *regularly matching* vertices, edges and faces.

Theorem 3.12 *There are linear averaging operators $\mathcal{A}^{\ell}_{\sigma,\mathfrak{s}} : \overline{V}^{\ell,0,\perp}_{\sigma,\mathfrak{s}} \to \overline{V}^{\ell,0,\perp}_{\sigma,\mathfrak{s}}$ such that the following holds: (i) $\mathcal{A}^{\ell}_{\sigma,\mathfrak{s}}(v)$ is continuous over regular faces in the interior of each mesh patch; (ii) $\mathcal{A}^{\ell}_{\sigma,\mathfrak{s}}(v)$ vanishes on all Dirichlet boundary faces; (iii) $\mathcal{A}^{\ell}_{\sigma,\mathfrak{s}}(v)$ is continuous across adjacent mesh patches; (iv) $\mathcal{A}^{\ell}_{\sigma,\mathfrak{s}}(v) = v$ for $v \in V^{\ell,1}_{\sigma,\mathfrak{s}}$; (v) for all $v \in \overline{V}^{\ell,0,\perp}_{\sigma,\mathfrak{s}}$ and with* jmp *as in* (3.30)*, there holds the stability bound*

$$\Upsilon^{\perp}_{\mathcal{M}^{\ell}_{\sigma}}[v - \mathcal{A}^{\ell}_{\sigma,\mathfrak{s}}(v)]^2 + \mathrm{jmp}_{\mathcal{F}^{\parallel}_{I}(\mathcal{M}^{\ell}_{\sigma})}[\mathcal{A}^{\ell}_{\sigma,\mathfrak{s}}(v)]^2 \lesssim_p \mathrm{jmp}_{\mathcal{F}^{\parallel}_{ID}(\mathcal{M}^{\ell}_{\sigma})}[v]^2 . \tag{3.45}$$

Remark 3.13 The construction of $\mathcal{A}^{\ell}_{\sigma,\mathfrak{s}}(v)$ in Theorem 3.12 is carried out on each element $K \in \mathcal{M}^{\ell}_{\sigma}$ separately, by adding averaged values associated with elemental vertices $\boldsymbol{N} \in \mathcal{N}(K)$, elemental edges $E \in \mathcal{E}(K)$ and elemental faces $F \in \mathcal{F}(K)$. As a consequence, $\mathcal{A}^{\ell}_{\sigma,\mathfrak{s}}$ can (in principle) be obtained from corresponding reference averaging operators on $\widetilde{Q}$ as in Remark 3.6, with inter-patch continuity being ensured by Assumption 3.1.

Theorem 3.12 will be established in Sect. 5.

3.4.4 Polynomial Jump Liftings

The averaged approximations $\mathcal{A}^{\ell}_{\sigma,\mathfrak{s}}(v)$ in Theorem 3.12 are non-conforming over *irregular faces in the interior of mesh patches*. Our proof then proceeds as in [20] by introducing suitable polynomially stable jump liftings on $\mathcal{M}^{\ell}_{\sigma}$ which preserve stability bounds as in (3.45). This leads to the following result.

Theorem 3.14 *Let $\mathcal{A}^{\ell}_{\sigma,\mathfrak{s}}$ be the averaging operator from Theorem 3.12. Then there exist linear operators $\mathcal{L}^{\ell}_{\sigma,\mathfrak{s}} : \mathrm{range}(\mathcal{A}^{\ell}_{\sigma,\mathfrak{s}}) \to V^{\ell,1}_{\sigma,\mathfrak{s}}$ such that the following holds: (i) $\mathcal{L}^{\ell}_{\sigma,\mathfrak{s}}(v) = v$ for $v \in V^{\ell,1}_{\sigma,\mathfrak{s}}$; (ii) we have the stability bound*

$$\Upsilon^{\perp}_{\mathcal{M}^{\ell}_{\sigma}}[v - \mathcal{L}^{\ell}_{\sigma,\mathfrak{s}}(v)] \lesssim_p \mathrm{jmp}_{\mathcal{F}^{\parallel}_{I}(\mathcal{M}^{\ell}_{\sigma})}[v]^2, \tag{3.46}$$

for all $v \in \mathrm{range}(\mathcal{A}^{\ell}_{\sigma,\mathfrak{s}}) \subset \overline{V}^{\ell,0,\perp}_{\sigma,\mathfrak{s}}$.

Remark 3.15 Since functions in $v \in \mathrm{range}(\mathcal{A}^{\ell}_{\sigma,\mathfrak{s}})$ have non-vanishing jumps only over irregular faces in the interior of mesh patches, upon mapping it is sufficient to construct $\mathcal{L}^{\ell}_{\sigma,\mathfrak{s}}$ on the reference mesh patches $\widetilde{\mathcal{M}}^{\ell,\mathfrak{t}}_{\sigma}$ of type $\mathfrak{t} \in \{\boldsymbol{c}, \boldsymbol{e}, \boldsymbol{ce}, \mathrm{int}\}$; inter-patch continuity will again follow from Assumption 3.1; cf. [20]. This observation

along with Remark 3.15 allows us to assemble $\Pi^{\ell,1}_{\sigma,\mathfrak{s}}$ from reference patch quasi-interpolants as discussed in Remark 3.6.

The proof of Theorem 3.14 will be detailed in Sect. 6.

Remark 3.16 The bounds (3.45) and (3.46) involve relatively large algebraic losses in the polynomial order $|\boldsymbol{p}|$. As in [20], this is due to the use of polynomial trace liftings which are linear in one or more directions. The algebraic losses can be possibly improved by employing polynomial liftings of higher order, but are inconsequential in establishing the exponential convergence rate (3.25).

3.4.5 Proof of Theorem 3.4

To prove (3.24), consider $u \in V$. Let $\pi^{\ell}_{\sigma,\check{\mathfrak{s}}} u \in V^{\ell,0}_{\sigma,\check{\mathfrak{s}}}$ be the base projection of u defined in (3.37) into the hp-base space $V^{\ell,0}_{\sigma,\check{\mathfrak{s}}}$ constructed in Sect. 3.4.2, for the base slope parameter $\check{\mathfrak{s}} > 0$. By Proposition 3.10 and the inclusion (3.44), we have $\pi^{\ell}_{\sigma,\check{\mathfrak{s}}} u \in \overline{V}^{\ell,0,\perp}_{\sigma,\mathfrak{s}}$. In addition, the broken H^1-norms of the interpolation errors $\eta^{\ell}_{\sigma,\check{\mathfrak{s}}} = u - \pi^{\ell}_{\sigma,\check{\mathfrak{s}}} u$ converge exponentially by (3.38), albeit with respect to the base slope $\check{\mathfrak{s}}$. We then define

$$\Pi^{\ell,1}_{\sigma,\mathfrak{s}}(u) := \big(\mathcal{L}^{\ell}_{\sigma,\mathfrak{s}} \circ \mathcal{A}^{\ell}_{\sigma,\mathfrak{s}} \circ \pi^{\ell}_{\sigma,\check{\mathfrak{s}}}\big)(u) \in V^{\ell,1}_{\sigma,\mathfrak{s}}, \tag{3.47}$$

with the operators $\mathcal{A}^{\ell}_{\sigma,\mathfrak{s}}$ and $\mathcal{L}^{\ell}_{\sigma,\mathfrak{s}}$ from Theorems 3.12 and 3.14. Clearly, the quasi-interpolation operator $\Pi^{\ell,1}_{\sigma,\mathfrak{s}}$ is well defined. It is linear, reproduces constant functions and can readily be seen to be idempotent on a subspace of $V^{\ell,1}_{\sigma,\mathfrak{s}}$.

We now set $v = \pi^{\ell}_{\sigma,\check{\mathfrak{s}}} u$, $v^{\mathrm{f}} := \mathcal{A}^{\ell}_{\sigma,\mathfrak{s}}(v)$, and $v^{\mathrm{c}} := \mathcal{L}^{\ell}_{\sigma,\mathfrak{s}}(v^{\mathrm{f}})$. With the triangle inequality and property (3.36), we obtain

$$\|u - \Pi^{\ell,1}_{\sigma,\mathfrak{s}} u\|^2_{H^1(\Omega)} \lesssim \Upsilon^{\parallel}_{\mathcal{M}^{\ell}_{\sigma}}[u - v]^2 + \Upsilon^{\perp}_{\mathcal{M}^{\ell}_{\sigma}}[v - v^{\mathrm{f}}]^2 + \Upsilon^{\perp}_{\mathcal{M}^{\ell}_{\sigma}}[v^{\mathrm{f}} - v^{\mathrm{c}}]^2.$$

The bounds (3.45) and (3.46) imply

$$\Upsilon^{\perp}_{\mathcal{M}^{\ell}_{\sigma}}[v - v^{\mathrm{f}}]^2 + \Upsilon^{\perp}_{\mathcal{M}^{\ell}_{\sigma}}[v^{\mathrm{f}} - v^{\mathrm{c}}]^2 \lesssim_p \mathrm{jmp}^{\parallel}_{\mathcal{F}_{ID}(\mathcal{M}^{\ell}_{\sigma})}[v]^2.$$

Since $v = \pi^{\ell}_{\sigma,\check{\mathfrak{s}}} u$ and $[\![u]\!]_F = 0$ for $F \in \mathcal{F}_{ID}(\mathcal{M}^{\ell}_{\sigma})$, we conclude that

$$\|u - \Pi^{\ell,1}_{\sigma,\mathfrak{s}} u\|^2_{H^1(\Omega)} \lesssim_p \Upsilon^{\parallel}_{\mathcal{M}^{\ell}_{\sigma}}[\eta^{\ell}_{\sigma,\check{\mathfrak{s}}}]^2 + \mathrm{jmp}^{\parallel}_{\mathcal{F}_{ID}(\mathcal{M}^{\ell}_{\sigma})}[\eta^{\ell}_{\sigma,\check{\mathfrak{s}}}]^2.$$

Referring to (3.38), (3.39) in Proposition 3.10 yields (3.24) for u piecewise analytic as in Theorem 3.4. The error bound (3.25) follows from (3.23) and (3.24) by noting that $N \simeq \ell^5 + \mathcal{O}(\ell^4)$.

4 Non-conforming Base Projectors

We prove exponential convergence in broken norms for non-conforming and tensorized hp-base projectors, and establish Proposition 3.10.

4.1 Tensor Projectors

We introduce a class of anisotropic tensor projectors on the reference cube $\widehat{K}$.

To this end, let $\widehat{I} = (-1, 1)$ be the reference interval. For $p \geq 0$, we denote by $\widehat{\pi}_{p,0}$ the univariate L^2-projection onto $\mathbb{P}_p(\widehat{I})$. For $p \geq 1$, we further introduce the univariate H^1-projector $\widehat{\pi}_{p,1} : H^1(\widehat{I}) \to \mathbb{P}_p(\widehat{I})$ by

$$(\widehat{\pi}_{p,1}\widehat{u})(\xi) := \widehat{u}(-1) + \int_{-1}^{\xi} (\widehat{\pi}_{p-1,0}\widehat{u}')(\eta)d\eta; \tag{4.1}$$

cf. [26, Theorem 3.14]. The projector satisfies $(\widehat{\pi}_{p,1}\widehat{u})' = \widehat{\pi}_{p-1,0}(\widehat{u}')$ and

$$(\widehat{\pi}_{p,1}\widehat{u})(\pm 1) = \widehat{u}(\pm 1). \tag{4.2}$$

Some hp-version approximation properties of $\widehat{\pi}_{p,0}$ and $\widehat{\pi}_{p,1}$ are collected in Sect. 8.1.1.

We consider next the reference cube $\widehat{K} = \widehat{I}^3$ with $\widehat{I} = (-1, 1)$. In analogy to (3.3), we write $\widehat{K} = \widehat{K}^{\perp} \times \widehat{K}^{\parallel} = \widehat{I}^2 \times \widehat{I}$. Let $\boldsymbol{p} = (p^{\perp}, p^{\parallel})$ be an anisotropic polynomial degree vector, and $r \in \{0, 1\}$ a conformity index in edge-parallel direction. For a function $\widehat{u} : \widehat{K} \to \mathbb{R}$, we define the tensor projector $\widehat{\pi}_{\boldsymbol{p},r}\widehat{u}$ into $\mathbb{Q}_{\boldsymbol{p}}(\widehat{K}) = \mathbb{Q}_{p^{\perp}}(\widehat{K}^{\perp}) \otimes \mathbb{P}_{p^{\parallel}}(\widehat{K}^{\parallel})$ by

$$\widehat{\pi}_{\boldsymbol{p},r}\widehat{u} := \left(\widehat{\pi}^{(1)}_{p^{\perp},0} \otimes \widehat{\pi}^{(2)}_{p^{\perp},0} \otimes \widehat{\pi}^{(3)}_{p^{\parallel},r}\right)\widehat{u} = \left(\widehat{\pi}^{\perp}_{p^{\perp},0} \otimes \widehat{\pi}^{\parallel}_{p^{\parallel},r}\right)\widehat{u}, \tag{4.3}$$

where the univariate projector $\widehat{\pi}^{(i)}_{p,t}$ acts in direction $\widehat{x}_i$, and where we write $\widehat{\pi}^{\perp}_{p^{\perp},0}$ and $\widehat{\pi}^{\parallel}_{p^{\parallel},r}$ to denote the projectors in edge-perpendicular and in edge-parallel direction, respectively. The projector $\widehat{\pi}_{\boldsymbol{p},0}$ is the (tensor-product) L^2-projection which is well defined for $\widehat{u} \in L^2(\widehat{K})$, whereas $\widehat{\pi}_{\boldsymbol{p},1}$ is an anisotropic projector which is well defined for $\widehat{u} \in L^2(\widehat{K}^{\perp}) \otimes H^1(\widehat{K}^{\parallel})$ and nodally exact in edge-parallel direction; cf. property (4.2). Note that $H^1(\widehat{K}) \subset L^2(\widehat{K}^{\perp}) \otimes H^1(\widehat{K}^{\parallel})$. In Sect. 8.1.2 we derive approximation properties for $\widehat{\pi}_{\boldsymbol{p},r}$ in (4.3), with the aid of tensor-product arguments and consistency bounds for the univariate projectors $\widehat{\pi}_{p,0}$ and $\widehat{\pi}_{p,1}$.

4.2 Exponential Convergence in Broken Norms

We next establish exponential convergence bounds in broken norms for the families of tensor projectors obtained in (4.3).

4.2.1 Families of Projectors

Consider the discontinuous spaces $V^{\ell,0}_{\sigma,\mathfrak{s}}$ in (3.21) on a geometric mesh $\mathcal{M} = \mathcal{M}^{\ell}_{\sigma} \in \mathfrak{M}_{\sigma}$ and for a $\mathfrak{s}$-linear degree distribution $\boldsymbol{p}_{\mathfrak{s}}(\mathcal{M}) = \{\boldsymbol{p}_K\}_{K\in\mathcal{M}}$. To each $K \in \mathcal{M}$, we assign an *elemental conformity index* $r_K \in \{0, 1\}$. We then investigate the tensor

projectors $\pi : H^1(\Omega) \to V^{\ell,0}_{\sigma,\mathfrak{s}}$ given by

$$\pi u|_K := \pi_{\boldsymbol{p}_K, r_K}(u|_K), \qquad K \in \mathcal{M}, \tag{4.4}$$

where the elemental projectors $\pi_{\boldsymbol{p}_K, r_K} : H^1(K) \to \mathbb{Q}_{\boldsymbol{p}_K}(K)$ are

$$\pi_{\boldsymbol{p}_K, r_K}(u|_K) := \big(\widehat{\pi}_{\boldsymbol{p}_K, r_K}(u|_K \circ \Phi_K)\big) \circ \Phi_K^{-1}, \tag{4.5}$$

with $\widehat{\pi}_{\boldsymbol{p}_K, r_K}$ defined in (4.3) and $\Phi_K : \widehat{K} \to K$ the element mapping. As the projectors $\pi_{\boldsymbol{p}_K, r_K}$ tensorize into $\pi_{\boldsymbol{p}_K, r_K} = \pi^{\perp}_{p^{\perp}_K, 0} \otimes \pi^{\parallel}_{p^{\parallel}_K, r_K}$ on $K = K^{\perp} \times K^{\parallel}$ and L^2-projections are used in perpendicular direction, we simply write

$$\pi u|_K = \pi^{\perp}_0 \otimes \pi^{\parallel} u|_K. \tag{4.6}$$

For $u \in H^1(\Omega)$, we consider the error terms

$$\eta = u - \pi u, \qquad \eta^{\perp}_0 = u - \pi^{\perp}_0 u, \qquad \eta^{\parallel} = u - \pi^{\parallel} u, \tag{4.7}$$

and note that

$$\eta = (u - \pi^{\perp}_0 u) + \pi^{\perp}_0 (u - \pi^{\parallel} u) = \eta^{\perp}_0 + \pi^{\perp}_0 \eta^{\parallel}. \tag{4.8}$$

In the above notation, we generally omit the dependence on r_K in edge-parallel direction. However, if $r_K = r \in \{0, 1\}$ for all $K \in \mathcal{M}^{\ell}_{\sigma}$, we write $\pi_r = \pi^{\perp}_0 \otimes \pi^{\parallel}_r$ for the projectors resulting in (4.4), (4.6), as well as η_r, $\eta^{\parallel}_r$ for the errors in (4.7). In particular, $\pi_0 = \pi^{\perp}_0 \otimes \pi^{\parallel}_0 : L^2(\Omega) \to V^{\ell,0}_{\sigma,\mathfrak{s}}$ is the usual L^2-projection. A specific choice of conformity indices r_K leading to $\pi^{\ell}_{\sigma,\mathfrak{s}}$ in Proposition 3.10 will be introduced in Sect. 4.3 below.

4.2.2 Error Bounds

We show that the full errors η can be bounded in terms of the errors $\eta^{\perp}$ and $\eta^{\parallel}$ in edge-perpendicular and in edge-parallel directions, in appropriate norms and except for corner elements; cf. [25].

We first establish the following stability result.

Lemma 4.1 *Let $K = K^{\perp} \times K^{\parallel} \in \mathcal{M}^{\ell}_{\sigma}$ be of the form (3.3) and $p^{\perp}_K \geq 1$. Then*

$$\|\mathsf{D}_{\perp}(\pi^{\perp}_{p^{\perp}_K, 0} u)\|^2_{L^2(K^{\perp})} \lesssim (p^{\perp}_K)^4 \|\mathsf{D}_{\perp} u\|^2_{L^2(K^{\perp})}, \qquad u \in H^1(K^{\perp}). \tag{4.9}$$

Furthermore, for the element errors in (4.7) and any $r_K \in \{0, 1\}$, we have

$$\begin{aligned} \|\eta\|^2_{L^2(K)} &\lesssim \|\eta^{\perp}_0\|^2_{L^2(K)} + \|\eta^{\parallel}\|^2_{L^2(K)}, \\ \|\mathsf{D}_{\perp}\eta\|^2_{L^2(K)} &\lesssim \|\mathsf{D}_{\perp}\eta^{\perp}_0\|^2_{L^2(K)} + (p^{\perp}_K)^4 \|\mathsf{D}_{\perp}\eta^{\parallel}\|^2_{L^2(K)}, \\ \|\mathsf{D}_{\parallel}\eta\|^2_{L^2(K)} &\lesssim \|\mathsf{D}_{\parallel}\eta^{\perp}_0\|^2_{L^2(K)} + \|\mathsf{D}_{\parallel}\eta^{\parallel}\|^2_{L^2(K)}. \end{aligned} \tag{4.10}$$

Proof Since both sides of the inequalities in (4.9) and (4.10) scale in the same way, it is sufficient to prove them for the reference element $\widehat{K} = \widehat{K}^\perp \times \widehat{K}^\parallel$. To show (4.9) on $\widehat{K}^\perp$, note that

$$\widehat{\mathsf{D}}_\perp(\widehat{\pi}^\perp_{p^\perp_K,0}\widehat{u}) = \widehat{\mathsf{D}}_\perp(\widehat{\pi}^\perp_{p^\perp_K,0}\widehat{u} - \widehat{\pi}^\perp_{0,0}\widehat{u}) = \widehat{\mathsf{D}}_\perp(\widehat{\pi}^\perp_{p^\perp_K,0}(\widehat{u} - \widehat{\pi}^\perp_{0,0}\widehat{u})). \tag{4.11}$$

The inverse inequality in [26, Theorem 4.7.6, eq. (4.6.5)], the L^2-stability of $\widehat{\pi}^\perp_{p^\perp_K,0}$ and standard approximation properties for $\widehat{\pi}^\perp_{0,0}$ yield (4.9) due to

$$\begin{aligned}\|\widehat{\mathsf{D}}_\perp(\widehat{\pi}^\perp_{p^\perp_K,0}\widehat{u})\|^2_{L^2(\widehat{K}^\perp)} &\lesssim (p^\perp_K)^4\|\widehat{\pi}^\perp_{p^\perp_K,0}(\widehat{u} - \widehat{\pi}^\perp_{0,0}\widehat{u})\|^2_{L^2(\widehat{K}^\perp)}\\ &\lesssim (p^\perp_K)^4\|\widehat{u} - \widehat{\pi}^\perp_{0,0}\widehat{u}\|^2_{L^2(\widehat{K}^\perp)} \lesssim (p^\perp_K)^4\|\widehat{\mathsf{D}}_\perp\widehat{u}\|^2_{L^2(\widehat{K}^\perp)}.\end{aligned}$$

The L^2-norm bound in (4.10) follows from the splitting (4.8) with the aid of the triangle inequality and the L^2-stability of the L^2-projection $\widehat{\pi}^\perp_{p^\perp_K,0}$. The second estimate in (4.10) is a consequence of (4.8), the triangle inequality and the p-dependent stability bound (4.9) in perpendicular direction. The third estimate in (4.10) is again obtained from (4.8), by employing the commutativity of $\widehat{\mathsf{D}}_\parallel$ and $\widehat{\pi}^\perp_{p^\perp_K,0}$, as well as the L^2-stability of $\widehat{\pi}^\perp_{p^\perp_K,0}$. □

To exclude corner elements, for $\boldsymbol{c} \in \mathcal{C}$, we set $\mathfrak{T}^\ell_{\sigma,\boldsymbol{c}} := \{\, K \in \mathcal{M}^\ell_\sigma \,:\, \overline{K} \cap \boldsymbol{c} \neq \emptyset\,\}$ and define

$$\mathfrak{T}^\ell_{\sigma,\mathcal{C}} := \bigcup_{\boldsymbol{c}\in\mathcal{C}} \mathfrak{T}^\ell_{\sigma,\boldsymbol{c}}, \qquad \mathcal{M}^\ell_{\sigma,\mathcal{C}} := \mathcal{M}^\ell_\sigma \setminus \mathfrak{T}^\ell_{\sigma,\mathcal{C}}\,. \tag{4.12}$$

Here, we will always assume that the initial patch mesh $\mathcal{M}^0$ is sufficiently fine so that $\mathfrak{T}^\ell_{\sigma,\boldsymbol{c}}$ and $\mathfrak{T}^\ell_{\sigma,\boldsymbol{c}'}$ are disjoint for $\boldsymbol{c} \neq \boldsymbol{c}'$.

Lemma 4.2 *Let $u \in H^1(\Omega)$ and let $\pi u = \pi^\perp_0 \otimes \pi^\parallel u$ be the base projector in (4.4) for any conformity indices $r_K \in \{0, 1\}$. For the error terms in (4.7), we have*

$$\Upsilon^\parallel_{\mathcal{M}^\ell_\sigma}[\eta]^2 \lesssim_p \Upsilon^\perp_{\mathcal{M}^\ell_{\sigma,\mathcal{C}}}[\eta^\perp_0]^2 + \Upsilon^\parallel_{\mathcal{M}^\ell_{\sigma,\mathcal{C}}}[\eta^\parallel]^2 + \Upsilon^\parallel_{\mathfrak{T}^\ell_{\sigma,\mathcal{C}}}[\eta]^2. \tag{4.13}$$

Moreover, let $u \in L^2(\Omega)$ and let $\pi_0 u = \pi^\perp_0 \otimes \pi^\parallel_0 u$ be the L^2-projection obtained in (4.4) by taking $r_K = 0$ for all $K \in \mathcal{M}^\ell_\sigma$. Then we have

$$\|\eta_0\|^2_{L^2(\mathcal{M}^\ell_\sigma)} \lesssim \|\eta^\perp_0\|^2_{L^2(\mathcal{M}^\ell_{\sigma,\mathcal{C}})} + \|\eta^\parallel_0\|^2_{L^2(\mathcal{M}^\ell_{\sigma,\mathcal{C}})} + \|\eta_0\|^2_{L^2(\mathfrak{T}^\ell_{\sigma,\mathcal{C}})}. \tag{4.14}$$

Proof These bounds follow from Lemma 4.1 and the inequality (3.36). □

4.2.3 Exponential Convergence

With (4.13), (4.14), we now state the following exponential convergence rates in broken norms. Note that these bounds do not imply the jump estimate (3.39); this result will be shown in Sect. 4.3.6 ahead.

Theorem 4.3 *Let $\boldsymbol{b}$ be a weight exponent vector satisfying (2.9). For parameters $\sigma \in (0,1)$ and $\mathfrak{s} > 0$, consider the sequence $V^{\ell,0}_{\sigma,\mathfrak{s}}$ of discontinuous finite element spaces (3.21).*

Let $u \in B_{-1-\boldsymbol{b}}(\Omega) \cap H^{1+\theta}(\Omega)$ for some $\theta \in (0,1)$, cf. Sect. 2.3, and let $\pi u = \pi_0^{\perp} \otimes \pi^{\parallel} u : H^1(\Omega) \to V^{\ell,0}_{\sigma,\mathfrak{s}}$ be the non-conforming family of tensor projectors in (4.4), for any elemental conformity indices $r_K \in \{0,1\}$. Then, for the errors η, $\eta_0^{\perp}$ and $\eta^{\parallel}$ in (4.7), we have

$$\Upsilon^{\parallel}_{\mathcal{M}^{\ell}_{\sigma}}[\eta]^2 \lesssim_p \Upsilon^{\perp}_{\mathcal{M}^{\ell}_{\sigma,\mathcal{C}}}[\eta_0^{\perp}]^2 + \Upsilon^{\parallel}_{\mathcal{M}^{\ell}_{\sigma,\mathcal{C}}}[\eta^{\parallel}]^2 + \Upsilon^{\parallel}_{\mathfrak{T}^{\ell}_{\sigma,\mathcal{C}}}[\eta]^2 \le C\exp(-2b\ell), \quad (4.15)$$

with constants $b, C > 0$ independent of $\ell \ge 2$.

In addition, let $u \in B_{-\boldsymbol{b}}(\Omega) \cap H^{\theta}(\Omega)$ for some $\theta \in (0,1)$, and let $\pi_0 u = \pi_0^{\perp} \otimes \pi_0^{\parallel} u$ be the L^2-projection obtained in (4.4) by taking $r_K = 0$ for all $K \in \mathcal{M}^{\ell}_{\sigma}$. For the errors η_0, $\eta_0^{\perp}$ and $\eta_0^{\parallel}$, we have

$$\|\eta_0\|^2_{L^2(\mathcal{M}^{\ell}_{\sigma})} \lesssim \|\eta_0^{\perp}\|^2_{L^2(\mathcal{M}^{\ell}_{\sigma,\mathcal{C}})} + \|\eta_0^{\parallel}\|^2_{L^2(\mathcal{M}^{\ell}_{\sigma,\mathcal{C}})} + \|\eta_0\|^2_{L^2(\mathfrak{T}^{\ell}_{\sigma,\mathcal{C}})} \le C\exp(-2b\ell), \quad (4.16)$$

with constants $b, C > 0$ independent of $\ell \ge 2$.

Note that upon adjusting the constants b, C to absorb the algebraic loss in $|\boldsymbol{p}|$, the bound (4.15) implies

$$\Upsilon^{\parallel}_{\mathcal{M}^{\ell}_{\sigma}}[\eta]^2 \le C\exp(-2b\ell), \quad (4.17)$$

with $b, C > 0$ independent of $\ell \ge 2$.

Remark 4.4 For simplicity, our proof of Theorem 4.3 is based on univariate hp-approximation bounds for $\widehat{\pi}_{p,0}$ and $\widehat{\pi}_{p,1}$ in (4.1) which require $p \ge 1$; cf. (8.1) and (8.3). Alternatively, the proof of the L^2-bound (4.16) could be solely based on the L^2-norm estimates for the L^2-projection in [26, Theorem 3.11], thereby allowing elemental polynomial degrees $p_K^{\perp} \ge 0$, $p_K^{\parallel} \ge 0$ in (4.16).

Remark 4.5 If $u \in H^1(\Omega)/\mathbb{R}$, respectively $u \in L^2(\Omega)/\mathbb{R}$ in Theorem 4.3, the bounds (4.15), (4.17), respectively (4.16) remain true over the factor space $V^{\ell,0}_{\sigma,\mathfrak{s}}/\mathbb{R}$. This follows from the fact that the elemental interpolants $\pi_{\boldsymbol{p}_K, r_K}$ in (4.4) reproduce constant functions.

Remark 4.6 The L^2-norm bound (4.16) is of independent interest in the context of mixed hp-FEMs for the (Navier–)Stokes equations or for linear elasticity in mixed form under $B_{-\boldsymbol{b}}(\Omega)$-regularity assumptions on the multipliers (although corresponding regularity shifts do not seem to be available in the literature). We refer to [21,22,27] and the references therein.

As in [25, Section 7], by superposition and due to the structure of the patch mappings, it is sufficient to provide the proof of the exponential convergence bounds in Theorem 4.3 for a reference corner–edge configuration on $\widetilde{Q}$ as shown in Fig. 1, which involves a single corner $\boldsymbol{c} \in \mathcal{C}$ and a single edge $\boldsymbol{e} \in \mathcal{E}_{\boldsymbol{c}}$ emanating from it. In this setting, the proof of the bound (4.17) follows the lines of [24, Section 7.2], albeit with essential modifications. For completeness, we review it in Appendix 8, and detail the relevant changes as compared to [24, Section 7.2]. The proof of the L^2-norm bound (4.16) is similar and will be outlined simultaneously.

4.3 The Base Projectors $\pi^{\ell}_{\sigma,\mathfrak{s}}$ with Partial Conformity

We introduce and analyze particular tensor-product projectors of the form (4.4), which lead to the base projectors $\pi^{\ell}_{\sigma,\mathfrak{s}}$ and the sets $\mathcal{F}^{\perp}_{ID}(\mathcal{M}^{\ell}_{\sigma}), \mathcal{F}^{\parallel}_{ID}(\mathcal{M}^{\ell}_{\sigma})$ in Proposition 3.10.

4.3.1 Base Projectors for Corner, Edge and Interior Patches

We define reference base projectors $\widetilde{\pi}_{\mathfrak{t}}$ on each reference mesh $\widetilde{\mathcal{M}}^{\ell,\mathfrak{t}}_{\sigma}$ for $\mathfrak{t} \in \{\boldsymbol{c}, \boldsymbol{e}, \boldsymbol{ce}, \mathrm{int}\}$ with respect to the linear polynomial degree distribution $\boldsymbol{p}_{\mathfrak{s}}(\widetilde{\mathcal{M}}^{\ell,\mathfrak{t}}_{\sigma})$. Recall that the elemental polynomial degree vectors $\boldsymbol{p}_K$ are isotropic for $\mathfrak{t} \in \{\boldsymbol{c}, \mathrm{int}\}$ and generally anisotropic for $\mathfrak{t} \in \{\boldsymbol{e}, \boldsymbol{ce}\}$. For reference patches $\widetilde{\mathcal{M}}^{\ell,\mathfrak{t}}_{\sigma}$ of type $\mathfrak{t} \in \{\boldsymbol{c}, \boldsymbol{e}, \mathrm{int}\}$, we take the reference base projectors $\widetilde{\pi}_{\mathfrak{t}}$ as

$$\widetilde{\pi}_{\mathfrak{t}}(u|_K) := \begin{cases} \pi_{\boldsymbol{p}_K,0}(u|_K), & K \in \widetilde{\mathcal{M}}^{\ell,\mathfrak{t}}_{\sigma},\ \mathfrak{t} \in \{\boldsymbol{c}, \mathrm{int}\}, \\ \pi_{\boldsymbol{p}_K,1}(u|_K), & K \in \widetilde{\mathcal{M}}^{\ell,\boldsymbol{e}}_{\sigma}, \end{cases} \tag{4.18}$$

with the nodally exact projector in (4.1) applied in edge-parallel direction.

4.3.2 Base Projectors for Corner–Edge Patches with Refinement Along One Edge

We next consider the corner–edge reference mesh patch $\widetilde{\mathcal{M}}^{\ell,\boldsymbol{ce}}_{\sigma}$ with refinement along one edge $\boldsymbol{e} \in \mathcal{E}_{\boldsymbol{c}}$ for a corner $\boldsymbol{c}$. Following [20], we partition $\widetilde{\mathcal{M}}^{\ell,\boldsymbol{ce}}_{\sigma}$ as

$$\widetilde{\mathcal{M}}^{\ell,\boldsymbol{ce}}_{\sigma} := \widetilde{\mathcal{M}}^{\ell,\boldsymbol{ce},\perp}_{\sigma} \,\dot\cup\, \widetilde{\mathcal{M}}^{\ell,\boldsymbol{ce},\parallel}_{\sigma}, \qquad \ell \geq 2, \tag{4.19}$$

where the mesh $\widetilde{\mathcal{M}}^{\ell,\boldsymbol{ce},\perp}_{\sigma}$ is a corner-patch-type mesh of elements which are isotropically refined into the corner $\boldsymbol{c}$. The mesh $\widetilde{\mathcal{M}}^{\ell,\boldsymbol{ce},\parallel}_{\sigma}$ consists of a sequence of $\ell - 1$ geometrically scaled edge-patch meshes, translated along the edge $\boldsymbol{e}$:

$$\widetilde{\mathcal{M}}^{\ell,\boldsymbol{ce},\parallel}_{\sigma} = \bigcup_{\ell'=2}^{\ell} \widetilde{\Psi}^{\ell',\boldsymbol{ce}}(\widetilde{\mathcal{M}}^{\ell',\boldsymbol{e}}_{\sigma}), \qquad \ell \geq 2, \tag{4.20}$$

where $\widetilde{\Psi}^{\ell',\boldsymbol{ce}}$ is a translation with respect to the edge-parallel variable $x^{\parallel}$ combined with a dilation by a factor only depending on σ, ℓ, ℓ', and where the mesh $\widetilde{\mathcal{M}}^{\ell',\boldsymbol{e}}_{\sigma}$ is a

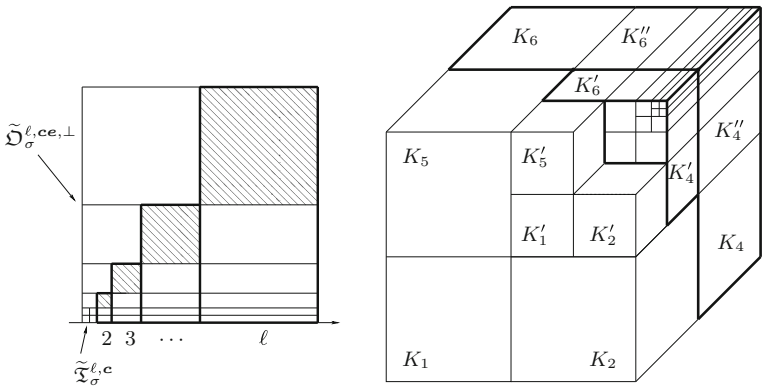

Fig. 2 *Left* patch decomposition (4.19)–(4.22) for $\sigma = 0.5$ and $\ell = 5$. The diagonal elements are *shaded*. *Right* the scaled edge-patch blocks $\widetilde{\Psi}^{\ell',\boldsymbol{ce}}(\widetilde{\mathcal{M}}_\sigma^{\ell',\boldsymbol{e}})$ and $\widetilde{\Psi}^{\ell'-1,\boldsymbol{ce}}(\widetilde{\mathcal{M}}_\sigma^{\ell'-1,\boldsymbol{e}})$ for $\sigma = 0.5$ and $\ell' = 5$. The diagonal elements K_4, K_6 and K_4', K_6' belong to $\widetilde{\mathcal{D}}_\sigma^{\ell',\boldsymbol{ce}}$ and $\widetilde{\mathcal{D}}_\sigma^{\ell'-1,\boldsymbol{ce}}$, respectively

reference edge mesh patch on $\widetilde{Q}$ with $\ell' + 1$ mesh layers. In Fig. 2 (left), a schematic illustration of the patch decomposition (4.19), (4.20) is provided in which the scaled edge-patch blocks are highlighted in boldface. In Fig. 2 (right), we show two adjacent edge-patch meshes as in (4.20) along the edge $\boldsymbol{e}$.

A particular role will be played by the subset $\widetilde{\mathcal{D}}_\sigma^{\ell,\boldsymbol{ce}} \subset \widetilde{\mathcal{M}}_\sigma^{\ell,\boldsymbol{ce},\parallel}$ of the elements in the outermost layer of each scaled mesh-patch block. It also consists of $\ell - 1$ layers:

$$\widetilde{\mathcal{D}}_\sigma^{\ell,\boldsymbol{ce}} := \bigcup_{\ell'=2}^{\ell} \widetilde{\mathcal{D}}_\sigma^{\ell',\boldsymbol{ce}}, \qquad \ell \geq 2. \tag{4.21}$$

Elements in $\widetilde{\mathcal{D}}_\sigma^{\ell,\boldsymbol{ce}}$ are referred to as *diagonal elements of* $\widetilde{\mathcal{M}}_\sigma^{\ell,\boldsymbol{ce},\parallel}$; cf. [20]. They are *isotropic* and are illustrated in Fig. 2. The isotropic mesh $\widetilde{\mathcal{M}}_\sigma^{\ell,\boldsymbol{ce},\perp}$ is decomposed into

$$\widetilde{\mathcal{M}}_\sigma^{\ell,\boldsymbol{ce},\perp} := \widetilde{\mathfrak{T}}_\sigma^{\ell,\boldsymbol{c}} \,\dot\cup\, \widetilde{\mathfrak{O}}_\sigma^{\ell,\boldsymbol{ce},\perp}, \tag{4.22}$$

where $\widetilde{\mathfrak{T}}_\sigma^{\ell,\boldsymbol{c}}$ is given by the eight elements nearest to $\boldsymbol{c}$, and where the remaining elements are collected in the mesh $\widetilde{\mathfrak{O}}_\sigma^{\ell,\boldsymbol{ce},\perp}$. We then choose the reference base projector on the reference corner–edge mesh as

$$\widetilde{\pi}_{\boldsymbol{ce}}(u|_K) := \begin{cases} \pi_{\boldsymbol{p}_K,0}(u|_K), & K \in \widetilde{\mathfrak{T}}_\sigma^{\ell,\boldsymbol{c}} \,\dot\cup\, \widetilde{\mathfrak{O}}_\sigma^{\ell,\boldsymbol{ce},\perp} \,\dot\cup\, \widetilde{\mathcal{D}}_\sigma^{\ell,\boldsymbol{ce}}, \\ \pi_{\boldsymbol{p}_K,1}(u|_K), & K \in \widetilde{\mathcal{M}}_\sigma^{\ell,\boldsymbol{ce},\parallel} \backslash \widetilde{\mathcal{D}}_\sigma^{\ell,\boldsymbol{ce}}, \end{cases} \tag{4.23}$$

where in $\pi_{\boldsymbol{p}_K,1}$ the nodally exact projectors in (4.1) are applied in direction of $\boldsymbol{e}$.

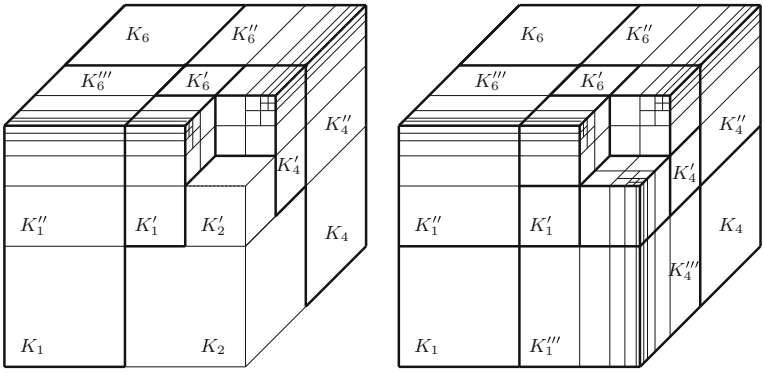

Fig. 3 Scaled edge-patch blocks for $\sigma = 0.5$ and $\ell' = 5$. *Left* refinement along two edges with diagonal elements K_1, K_4, K_6 and K_1', K_4', K_6'. *Right* refinement along three edges with diagonal elements K_1, K_4, K_6 and K_1', K_4', K_6'

4.3.3 Base Projectors for Corner–Edge Patches with Refinements Along Two or Three Edges

For a corner–edge patch $\widetilde{\mathcal{M}}_\sigma^{\ell,\boldsymbol{ce}}$ with refinement along two edges $\boldsymbol{e}_1, \boldsymbol{e}_2$ meeting at a common vertex $\boldsymbol{c}$ and isotropic refinement in perpendicular direction as illustrated in Fig. 3 (left), we write

$$\widetilde{\mathcal{M}}_\sigma^{\ell,\boldsymbol{ce}} := \widetilde{\mathcal{M}}_\sigma^{\ell,\boldsymbol{ce},\perp} \,\dot\cup\, \big(\widetilde{\mathcal{M}}_\sigma^{\ell,\boldsymbol{ce}_1,\parallel} \cup \widetilde{\mathcal{M}}_\sigma^{\ell,\boldsymbol{ce}_2,\parallel}\big), \qquad \ell \geq 2, \tag{4.24}$$

with two sequences of $\ell - 1$ scaled edge-patch meshes as in (4.20) and an isotropic corner-type mesh $\widetilde{\mathcal{M}}_\sigma^{\ell,\boldsymbol{ce},\perp}$ perpendicular to $\boldsymbol{e}_1, \boldsymbol{e}_2$. The latter mesh is again decomposed as

$$\widetilde{\mathcal{M}}_\sigma^{\ell,\boldsymbol{ce},\perp} := \widetilde{\mathfrak{T}}_\sigma^{\ell,\boldsymbol{c}} \,\dot\cup\, \widetilde{\mathfrak{O}}_\sigma^{\ell,\boldsymbol{ce},\perp}, \tag{4.25}$$

where $\widetilde{\mathfrak{T}}_\sigma^{\ell,\boldsymbol{c}}$ is the same set of corner elements as in (4.22) and $\widetilde{\mathfrak{O}}_\sigma^{\ell,\boldsymbol{ce},\perp}$ the set of all remaining elements. We denote by $\widetilde{\mathcal{D}}_\sigma^{\ell,\boldsymbol{ce}_i} \subset \widetilde{\mathcal{M}}_\sigma^{\ell,\boldsymbol{ce}_i,\parallel}$ the diagonal elements of $\widetilde{\mathcal{M}}_\sigma^{\ell,\boldsymbol{ce}_i,\parallel}$ defined as above; cf. Fig. 3 (left). We then set

$$\widetilde{\pi}_{\boldsymbol{ce}}(u|_K) := \begin{cases} \pi_{\boldsymbol{p}_K,0}(u|_K), & K \in \widetilde{\mathfrak{T}}_\sigma^{\ell,\boldsymbol{c}} \,\dot\cup\, \widetilde{\mathfrak{O}}_\sigma^{\ell,\boldsymbol{ce},\perp} \,\dot\cup\, \big(\widetilde{\mathcal{D}}_\sigma^{\ell,\boldsymbol{ce}_1} \cup \widetilde{\mathcal{D}}_\sigma^{\ell,\boldsymbol{ce}_2}\big), \\ \pi_{\boldsymbol{p}_K,1}(u|_K), & K \in \widetilde{\mathcal{M}}_\sigma^{\ell,\boldsymbol{ce}_i,\parallel} \backslash \widetilde{\mathcal{D}}_\sigma^{\ell,\boldsymbol{ce}_i},\ i = 1,2, \end{cases} \tag{4.26}$$

where again the univariate projectors (4.1) are employed along $\boldsymbol{e}_i$ for $i = 1, 2$.

Remark 4.7 The elements in $\widetilde{\mathcal{D}}_\sigma^{\ell,\boldsymbol{ce}_i}$ act as isotropic *buffer zones* and allow us to unambiguously assign different directions in $\widetilde{\mathcal{M}}_\sigma^{\ell,\boldsymbol{ce}_1,\parallel}$ and $\widetilde{\mathcal{M}}_\sigma^{\ell,\boldsymbol{ce}_2,\parallel}$.

Finally, if $\widetilde{\mathcal{M}}_\sigma^{\ell,\boldsymbol{ce}}$ is refined along three edges $\boldsymbol{e}_1, \boldsymbol{e}_2, \boldsymbol{e}_3$ meeting at a common vertex $\boldsymbol{c}$, as depicted in Fig. 3 (right), we analogously write

$$\widetilde{\mathcal{M}}_\sigma^{\ell,\boldsymbol{ce}} := \widetilde{\mathfrak{T}}_\sigma^{\ell,\boldsymbol{c}} \,\dot\cup\, \big(\widetilde{\mathcal{M}}_\sigma^{\ell,\boldsymbol{ce}_1,\parallel} \cup \widetilde{\mathcal{M}}_\sigma^{\ell,\boldsymbol{ce}_2,\parallel} \cup \widetilde{\mathcal{M}}_\sigma^{\ell,\boldsymbol{ce}_3,\parallel}\big), \tag{4.27}$$

now with three sequences of $\ell-1$ scaled edge-patch blocks. The set $\widetilde{\mathcal{D}}_\sigma^{\ell,\boldsymbol{ce}_i} \subset \widetilde{\mathcal{M}}_\sigma^{\ell,\boldsymbol{ce}_i,\|}$ denotes the diagonal elements of $\widetilde{\mathcal{M}}_\sigma^{\ell,\boldsymbol{ce}_i,\|}$. With (4.27), we define

$$\widetilde{\pi}_{\boldsymbol{ce}}(u|_K) := \begin{cases} \pi_{\boldsymbol{p}_K,0}(u|_K), & K \in \widetilde{\mathfrak{T}}_\sigma^{\ell,\boldsymbol{c}} \,\dot\cup\, \big(\cup_{i=1}^3 \widetilde{\mathcal{D}}_\sigma^{\ell,\boldsymbol{ce}_i}\big), \\ \pi_{\boldsymbol{p}_K,1}(u|_K), & K \in \widetilde{\mathcal{M}}_\sigma^{\ell,\boldsymbol{ce}_i,\|} \backslash \widetilde{\mathcal{D}}_\sigma^{\ell,\boldsymbol{ce}_i},\ 1 \le i \le 3, \end{cases} \tag{4.28}$$

once more with the nodally exact projectors applied in the direction $\boldsymbol{e}_i$.

4.3.4 The Base Projectors $\pi_{\sigma,\mathfrak{s}}^\ell$

The reference base projectors $\widetilde{\pi}_{\mathfrak{t}}$ in (4.18), (4.23), as well as the variants in (4.26) and (4.28), give rise to the (non-conforming) base tensor projectors $\pi_{\sigma,\mathfrak{s}}^\ell = \pi_{\sigma,\mathfrak{s}}^{\ell,\perp} \otimes \pi_{\sigma,\mathfrak{s}}^{\ell,\|} : H^1(\Omega) \to V_{\sigma,\mathfrak{s}}^{\ell,0}$ in (3.37) in Proposition 3.10. The bound (4.17) resulting from Theorem 4.3 then yields the broken norm error bound (3.38) there. Next, we define the sets $\mathcal{F}_{ID}^\perp(\mathcal{M}_\sigma^\ell)$, $\mathcal{F}_{ID}^\|(\mathcal{M}_\sigma^\ell)$ and prove the jump bound (3.39).

4.3.5 Partial Conformity

We first consider edge-perpendicular interfaces $\Gamma_{\mathfrak{p}\mathfrak{p}'}$ of two mesh patches $\mathcal{M}_\mathfrak{p}$, $\mathcal{M}_{\mathfrak{p}'}$ along the same edge $\boldsymbol{e}$. Recall that the interface $\Gamma_{\mathfrak{p}\mathfrak{p}'}$ consists of $\ell+1$ mesh layers, cf. [23, Section 3.2], and that the patches coincide on the interfaces due to Assumption 3.1. The definition of $\pi_{\sigma,\mathfrak{s}}^\ell$ and the nodal exactness property (4.2) imply the following results.

Lemma 4.8 *For $u \in V$, there holds: (i) if $\mathcal{M}_\mathfrak{p}$, $\mathcal{M}_{\mathfrak{p}'}$ are two adjacent edge mesh patches along the same edge, then $\pi_{\sigma,\mathfrak{s}}^\ell u$ is continuous across all layers of the interface $\Gamma_{\mathfrak{p}\mathfrak{p}'}$; (ii) if $\mathcal{M}_\mathfrak{p}$ is an edge mesh patch and $\mathcal{M}_{\mathfrak{p}'}$ an adjacent corner–edge patch along the same edge, then $\pi_{\sigma,\mathfrak{s}}^\ell u$ is continuous across the inner layers of the interface $\Gamma_{\mathfrak{p}\mathfrak{p}'}$, but is generally discontinuous across the outermost layer of $\Gamma_{\mathfrak{p}\mathfrak{p}'}$.*

Remark 4.9 Conformity properties analogous to those in Lemma 4.8 hold on edge-perpendicular boundaries of edge or corner–edge mesh patches which are situated on a Dirichlet boundary face Γ_ι for $\iota \in \mathcal{J}_D$. On the corresponding elemental boundaries, the projection $\pi_{\sigma,\mathfrak{s}}^\ell u$ vanishes if $u \in V$.

Next, we analyze the continuity within different edge-patch blocks $\widetilde{\Psi}^{\ell',\boldsymbol{ce}}(\widetilde{\mathcal{M}}_\sigma^{\ell',\boldsymbol{e}})$ in (4.20) and as appearing in the representations (4.19), (4.24) and (4.27).

Lemma 4.10 *For $u \in V$ and $3 \le \ell' \le \ell$, let $\widetilde{\Psi}^{\ell'-1,\boldsymbol{ce}}(\widetilde{\mathcal{M}}_\sigma^{\ell'-1,\boldsymbol{e}})$ and $\widetilde{\Psi}^{\ell',\boldsymbol{ce}}(\widetilde{\mathcal{M}}_\sigma^{\ell',\boldsymbol{e}})$ be two adjacent edge-patch blocks along the same edge. Then $\pi_{\sigma,\mathfrak{s}}^\ell u$ is continuous across perpendicular faces between $\widetilde{\Psi}^{\ell'-1,\boldsymbol{ce}}(\widetilde{\mathcal{M}}_\sigma^{\ell'-1,\boldsymbol{e}})$ and $\widetilde{\Psi}^{\ell',\boldsymbol{ce}}(\widetilde{\mathcal{M}}_\sigma^{\ell',\boldsymbol{e}})$, except for the faces between the diagonal elements in $\widetilde{\mathcal{D}}_\sigma^{\ell'-1,\boldsymbol{ce}}$ and the corresponding elements in $\widetilde{\Psi}^{\ell',\boldsymbol{ce}}(\widetilde{\mathcal{M}}_\sigma^{\ell',\boldsymbol{e}})$.*

To illustrate Lemma 4.10, we note that $\pi_{\sigma,\mathfrak{s}}^\ell u$ is generally non-conforming across the isotropic faces $F_{K_4',K_4''}$, $F_{K_6',K_6''}$ in Fig. 2 (right), and across the isotropic faces $F_{K_1',K_1''}$, $F_{K_4',K_4''}$, $F_{K_6',K_6''}$, $F_{K_6',K_6'''}$ in Fig. 3 (left).

The partial conformity in Lemma 4.8, Remark 4.9 and Lemma 4.10 allows us to identify sets $\mathcal{F}_{ID}^{\perp}(\mathcal{M}_\sigma^\ell)$ and $\mathcal{F}_{ID}^{\parallel}(\mathcal{M}_\sigma^\ell) = \mathcal{F}_{I}^{\parallel}(\mathcal{M}_\sigma^\ell) \cup \mathcal{F}_{D}^{\parallel}(\mathcal{M}_\sigma^\ell)$, over which $\pi_{\sigma,\mathfrak{s}}^\ell u$ is conforming and non-conforming, respectively. The faces $F \in \mathcal{F}_{ID}^{\parallel}(\mathcal{M}_\sigma^\ell)$ satisfy (3.31), (3.32), as claimed in Proposition 3.10.

4.3.6 Polynomial Face Jump Bounds

Next, we bound the face jumps of $\pi_{\sigma,\mathfrak{s}}^\ell u$ over the faces $F \in \mathcal{F}_{ID}^{\parallel}(\mathcal{M})$ for $\mathcal{M} = \mathcal{M}_\sigma^\ell$, and show the estimate (3.39).

To this end, we first recall the anisotropic trace inequality from [23, Lemma 4.2] (with $t = 2$).

Lemma 4.11 *For $F \in \mathcal{F}_{ID}^{\parallel}(\mathcal{M})$ with $F \subseteq F' \in \mathcal{F}(K)$ and $u \in H^1(K)$, there holds $\mathrm{h}_F^{-1}\|u\|_{L^2(F)}^2 \lesssim (h_K^\perp)^{-2}\|u\|_{L^2(K)}^2 + \|\mathsf{D}_\perp u\|_{L^2(K)}^2 \lesssim N_K^\perp[u]^2$.*

Next, we establish the following variant of the jump estimate of [25, Section 5.5], which is essential for controlling the jumps of $\pi_{\sigma,\mathfrak{s}}^\ell u$ over anisotropic faces of $\mathcal{M}$. Due to the appearance of H^1-projectors in edge-parallel direction, we require in this bound a local smoothness assumption which is slightly stronger than H^1-regularity.

Lemma 4.12 *Consider an* edge-parallel *face $F = F_{K_1,K_2} \in \mathcal{F}_I^{\parallel}(\mathcal{M})$ shared by two axiparallel elements $K_1 = K_1^\perp \times K^\parallel$ and $K_2 = K_2^\perp \times K^\parallel$ as in (3.3), with $K^\parallel = (0, h^\parallel)$ in parallel direction and with $K_1^\perp$ and $K_2^\perp$ two shape-regular and possibly non-matching rectangles of diameters $h_{K_1}^\perp \simeq h_{K_2}^\perp \simeq h^\perp$ in perpendicular direction, for parameters $h^\perp \lesssim h^\parallel$. Let the elemental polynomial degrees be given by $\boldsymbol{p}_{K_i} = (p_i^\perp, p^\parallel)$. Let $u \in H^1((\overline{K}_1^\perp \cup \overline{K}_2^\perp)^\circ) \otimes H^1(K^\parallel)$ and $\pi_1 u|_{K_i} = \pi_0^\perp \otimes \pi_1^\parallel u|_{K_i} = \pi_{\boldsymbol{p}_{K_i},1}(u|_{K_i})$ for $i = 1, 2$. For the error terms $\eta_1 = u - \pi_1 u$, $\eta_0^\perp = u - \pi_0^\perp u$ and $\eta_1^\parallel = u - \pi_1^\parallel u$ as in (4.7), we have the bound*

$$\mathrm{h}_F^{-1}\|[\![\pi_1 u]\!]_F\|_{L^2(F)}^2 \lesssim_p \sum_{i=1}^{2} \big(\|\mathsf{D}_\perp \eta_0^\perp\|_{L^2(K_i)}^2 + \|\mathsf{D}_\perp \eta_1^\parallel\|_{L^2(K_i)}^2\big). \tag{4.29}$$

Similarly, let $F = F_{K,\Gamma_\iota} \in \mathcal{F}_D^{\parallel}(\mathcal{M})$, $\iota \in \mathcal{J}_D$, be an edge-parallel *Dirichlet face of $K = K^\perp \times K^\parallel$, with $K^\parallel = (0, h^\parallel)$ and $K^\perp$ a shape-regular rectangle of diameter $h^\perp$, for $h^\perp \lesssim h^\parallel$. Let the elemental polynomial degrees be given by $\boldsymbol{p}_K = (p^\perp, p^\parallel)$. Let $u \in H^1(K^\perp) \otimes H^1(K^\parallel)$ with $u|_F = 0$ and $\pi_1 u|_K = \pi_0^\perp \otimes \pi_1^\parallel u|_K = \pi_{\boldsymbol{p}_K,1}(u|_K)$. Then we have the bound*

$$\mathrm{h}_F^{-1}\|[\![\pi_1 u]\!]_F\|_{L^2(F)}^2 \lesssim_p \|\mathsf{D}_\perp \eta_0^\perp\|_{L^2(K)}^2 + \|\mathsf{D}_\perp \eta_1^\parallel\|_{L^2(K)}^2. \tag{4.30}$$

Proof Note that the setting is such that property (3.31) is fulfilled with $\mathrm{h}_F \simeq h_{K_i}^\perp \simeq h^\perp$. On element K_i, $i = 1, 2$, we have

$$\eta_0^\perp - \pi_0^\perp \eta_0^\perp = (u - \pi_0^\perp u) - \pi_0^\perp(u - \pi_0^\perp u) = u - \pi_0^\perp u = \eta_0^\perp. \tag{4.31}$$

Then, we note that $\pi_1^{\|} u|_{K_i} \in H^1(K_i^{\perp}) \otimes \mathbb{P}_{p^{\|}}(K^{\|}) \subset H^1(K)$ for $i = 1, 2$. Hence, $\big(\pi_1^{\|} u|_{K_1}\big)|_F = \big(\pi_1^{\|} u|_{K_2}\big)|_F$ in $L^2(F)$. With this identity and since $\pi_0^{\perp}$ and $\pi_1^{\|}$ commute, we conclude that

$$\begin{aligned}\|[\![\pi_1 u]\!]_F\|_{L^2(F)}^2 &= \|\pi_1 u|_{K_1} - \pi_1 u|_{K_2}\|_{L^2(F)}^2 \\ &\lesssim \sum_{i=1}^{2} \|\pi_0^{\perp} \otimes \pi_1^{\|} u|_{K_i} - \pi_1^{\|} u|_{K_i}\|_{L^2(F)}^2 = \sum_{i=1}^{2} \|\pi_1^{\|} \eta_0^{\perp}|_{K_i}\|_{L^2(F)}^2.\end{aligned}$$

We then consider element K_i for $i = 1, 2$. With Lemma 4.11, we have

$$\mathrm{h}_F^{-1} \|\pi_1^{\|} \eta_0^{\perp}|_{K_i}\|_{L^2(F)}^2 \lesssim (h_{K_i}^{\perp})^{-2} \|\pi_1^{\|} \eta_0^{\perp}\|_{L^2(K_i)}^2 + \|\mathsf{D}_{\perp}(\pi_1^{\|} \eta_0^{\perp})\|_{L^2(K_i)}^2.$$

Property (4.31) and standard h-version approximation results for $\pi_0^{\perp}$ in perpendicular direction yield

$$\|\pi_1^{\|} \eta_0^{\perp}\|_{L^2(K_i)}^2 = \|(\pi_1^{\|} \eta_0^{\perp}) - \pi_0^{\perp}(\pi_1^{\|} \eta_0^{\perp})\|_{L^2(K_i)}^2 \lesssim (h_{K_i}^{\perp})^2 \|\mathsf{D}_{\perp}(\pi_1^{\|} \eta_0^{\perp})\|_{L^2(K_i)}^2.$$

Therefore,

$$\begin{aligned}\mathrm{h}_F^{-1} \|\pi_1^{\|} \eta_0^{\perp}|_{K_i}\|_{L^2(F)}^2 &\lesssim \|\mathsf{D}_{\perp}(\pi_1^{\|} \eta_0^{\perp})\|_{L^2(K_i)}^2 \\ &\lesssim \|\mathsf{D}_{\perp}((\pi_1^{\|} - \pi_0^{\|}) \eta_0^{\perp})\|_{L^2(K_i)}^2 + \|\mathsf{D}_{\perp}(\pi_0^{\|} \eta_0^{\perp})\|_{L^2(K_i)}^2.\end{aligned} \tag{4.32}$$

We next bound the two terms in the second line of (4.32). We write the first term as

$$\begin{aligned}(\pi_1^{\|} - \pi_0^{\|}) \eta_0^{\perp} &= (\pi_1^{\|} - \pi_0^{\|}) u - \pi_0^{\perp}(\pi_1^{\|} - \pi_0^{\|}) u \\ &= \pi_0^{\|}(\pi_1^{\|} u - u) - \pi_0^{\perp}\big(\pi_0^{\|}(\pi_1^{\|} u - u)\big).\end{aligned}$$

With the triangle inequality and the stability bound (4.9) for $\pi_0^{\perp}$, we find that

$$\|\mathsf{D}_{\perp}\big((\pi_1^{\|} - \pi_0^{\|}) \eta_0^{\perp}\big)\|_{L^2(K_i)}^2 \lesssim (p_i^{\perp})^4 \|\mathsf{D}_{\perp}\big(\pi_0^{\|}(\pi_1^{\|} u - u)\big)\|_{L^2(K_i)}^2.$$

Then, since $\mathsf{D}_{\perp}^{\boldsymbol{\alpha}^{\perp}}$ and $\pi_0^{\|}$ commute, the L^2-stability of the L^2-projection $\pi_0^{\|}$ implies

$$\|\mathsf{D}_{\perp}\big((\pi_1^{\|} - \pi_0^{\|}) \eta_0^{\perp}\big)\|_{L^2(K_i)}^2 \lesssim (p_i^{\perp})^4 \|\mathsf{D}_{\perp} \eta_1^{\|}\|_{L^2(K_i)}^2.$$

To estimate the second term in (4.32), we invoke the L^2-stability of $\pi_0^{\|}$ as before to obtain

$$\|\mathsf{D}_{\perp}(\pi_0^{\|} \eta_0^{\perp})\|_{L^2(K_1)}^2 \lesssim \|\mathsf{D}_{\perp} \eta_0^{\perp}\|_{L^2(K_1)}^2.$$

Combining these arguments yields (4.29).

The proof of (4.30) for a Dirichlet boundary face F is obtained analogously, by noting that $\big(\pi_1 u|_K\big)|_F = 0$ in $L^2(F)$. □

Lemma 4.13 *Let $u \in B_{-1-\boldsymbol{b}}(\Omega)$ and let $\pi^{\ell}_{\sigma,\mathfrak{s}} = \pi^{\ell,\perp}_{\sigma,\mathfrak{s}} \otimes \pi^{\ell,\|}_{\sigma,\mathfrak{s}}$ be the hp-base projectors introduced in Sect. 4.3.4. With the error terms defined as in (4.7), i.e., $\eta^{\ell}_{\sigma,\mathfrak{s}} = u - \pi^{\ell}_{\sigma,\mathfrak{s}} u$, $\eta^{\ell,\perp}_{\sigma,\mathfrak{s}} = u - \pi^{\ell,\perp}_{\sigma,\mathfrak{s}} u$ and $\eta^{\ell,\|}_{\sigma,\mathfrak{s}} = u - \pi^{\ell,\|}_{\sigma,\mathfrak{s}} u$, we have the bound*

$$\mathrm{jmp}_{\mathcal{F}^{\|}_{ID}(\mathcal{M}^{\ell}_{\sigma})}[\eta^{\ell}_{\sigma,\mathfrak{s}}]^2 \lesssim_p \Upsilon^{\perp}_{\mathcal{M}^{\ell}_{\sigma,\mathcal{C}}}[\eta^{\ell,\perp}_{\sigma,\mathfrak{s}}]^2 + \Upsilon^{\|}_{\mathcal{M}^{\ell}_{\sigma,\mathcal{C}}}[\eta^{\ell,\|}_{\sigma,\mathfrak{s}}]^2 + \Upsilon^{\|}_{\mathfrak{T}^{\ell}_{\sigma,\mathcal{C}}}[\eta^{\ell}_{\sigma,\mathfrak{s}}]^2. \tag{4.33}$$

Proof Anisotropic faces F in $\mathcal{F}^{\|}_{ID}(\mathcal{M}^{\ell}_{\sigma})$ arise in (mapped) edge patches $\widetilde{\mathcal{M}}^{\ell,\boldsymbol{e}}_{\sigma}$ and in the innermost ℓ' layers of edge-patch blocks $\Psi^{\ell',\boldsymbol{ce}}(\widetilde{\mathcal{M}}^{\ell',\boldsymbol{e}}_{\sigma})$ of (mapped) corner–edge patches $\widetilde{\mathcal{M}}^{\ell,\boldsymbol{ce}}_{\sigma}$ (with refinement along one, two or three edges); see Sects. 4.3.2 and 4.3.3. All these faces are edge-parallel and do not abut at corners. Hence, the jumps of $\pi^{\ell}_{\sigma,\mathfrak{s}} u$ over such faces can be bounded by the estimates in Lemma 4.12, upon noting that the same polynomial degrees are employed in edge-parallel direction and that, for $u \in B_{-1-\boldsymbol{b}}(\Omega)$, the smoothness assumptions in Lemma 4.12 are satisfied; see (2.6). The remaining faces in $\mathcal{F}^{\|}_{ID}(\mathcal{M}^{\ell}_{\sigma})$ are isotropic and the jumps over them can by bounded by isotropic versions of the trace inequality in Lemma 4.11, along with the stability bounds in Lemma 4.1. □

Lemma 4.13 along with estimate (4.15) for $\pi^{\ell}_{\sigma,\mathfrak{s}}$ then establishes the bound (3.39) for $\mathrm{jmp}_{\mathcal{F}^{\|}_{ID}(\mathcal{M}^{\ell}_{\sigma})}[\eta^{\ell}_{\sigma,\mathfrak{s}}]$, which completes the proof of Proposition 3.10.

5 Averaging Operators

We construct the averaging operators $\mathcal{A}^{\ell}_{\sigma,\mathfrak{s}} : \overline{V}^{\ell,0,\perp}_{\sigma,\mathfrak{s}} \to \overline{V}^{\ell,0,\perp}_{\sigma,\mathfrak{s}}$ in Theorem 3.12 over geometric meshes $\mathcal{M} = \mathcal{M}^{\ell}_{\sigma}$.

5.1 Sets of Adjacent Elements

Let $K \in \mathcal{M}$. For $\boldsymbol{N} \in \mathcal{N}(K)$, $E \in \mathcal{E}(K)$ and $F \in \mathcal{F}(K)$, we introduce the following sets of elements which *regularly* share $\boldsymbol{N}$, E and F, respectively:

$$\Delta_{K,\boldsymbol{N}} := \{\, K' \in \mathcal{M} \,:\, \boldsymbol{N} \in \mathcal{N}(K') \,\}, \tag{5.1}$$

$$\Delta_{K,E} := \{\, K' \in \mathcal{M} \,:\, E \in \mathcal{E}(K') \,\}, \tag{5.2}$$

$$\Delta_{K,F} := \{\, K' \in \mathcal{M} \,:\, F \in \mathcal{F}(K') \,\}. \tag{5.3}$$

Clearly, we have $K \in \Delta_{K,\boldsymbol{N}}$, $K \in \Delta_{K,E}$ and $K \in \Delta_{K,F} \subseteq \delta_{K,F}$, with $\delta_{K,F}$ introduced in (3.11), respectively. Then, $\mathrm{card}(\Delta_{K,\boldsymbol{N}}) \geq 1$, $\mathrm{card}(\Delta_{K,E}) \geq 1$, and $\mathrm{card}(\Delta_{K,F}) \in \{1, 2\}$. There holds

$$\boldsymbol{N} \in \mathcal{N}(E) :\ \Delta_{K,E} \subseteq \Delta_{K,\boldsymbol{N}} \qquad \text{and} \qquad E \in \mathcal{E}(F) :\ \Delta_{K,F} \subseteq \Delta_{K,E}. \tag{5.4}$$

Moreover, the sets defined in (5.1)–(5.3) have the property that

$$\Delta_{K,\boldsymbol{N}} = \Delta_{K',\boldsymbol{N}}, \qquad K' \in \Delta_{K,\boldsymbol{N}}, \tag{5.5}$$

$$\Delta_{K,E} = \Delta_{K',E}, \qquad K' \in \Delta_{K,E}, \tag{5.6}$$
$$\Delta_{K,F} = \Delta_{K',F}, \qquad K' \in \Delta_{K,F}. \tag{5.7}$$

In the following, we denote by $\mathcal{N}_D(K) \subset \mathcal{N}(K)$, $\mathcal{E}_D(K) \subset \mathcal{E}(K)$ and $\mathcal{F}_D(K) \subset \mathcal{F}(K)$, the sets of elemental nodes, edges and faces, respectively, which are situated on a Dirichlet boundary face $\overline{\Gamma}_{\boldsymbol{\iota}}$ for $\boldsymbol{\iota} \in \mathcal{J}_D$.

For $\boldsymbol{N} \in \mathcal{N}(K)\backslash\mathcal{N}_D(K)$, respectively $\boldsymbol{N} \in \mathcal{N}_D(K)$, we define

$$\begin{aligned} \mathcal{F}_I^{\shortparallel}(\Delta_{K,\boldsymbol{N}}) &:= \{\, F = F_{K,K'} \in \mathcal{F}_I^{\shortparallel}(\mathcal{M}) \,:\, K' \in \Delta_{K,\boldsymbol{N}}\backslash\{K\}\,\}, \\ \mathcal{F}_D^{\shortparallel}(\Delta_{K,\boldsymbol{N}}) &:= \{F = F_{K',\Gamma_{\boldsymbol{\iota}}} \in \mathcal{F}_D^{\shortparallel}(\mathcal{M}) \,:\, K' \in \Delta_{K,\boldsymbol{N}} \text{ and } \boldsymbol{\iota} \in \mathcal{J}_D\,\}. \end{aligned} \tag{5.8}$$

Similarly, for $E \in \mathcal{E}(K)\backslash\mathcal{E}_D(K)$, respectively $E \in \mathcal{E}_D(K)$, we set

$$\begin{aligned} \mathcal{F}_I^{\shortparallel}(\Delta_{K,E}) &:= \{\, F = F_{K,K'} \in \mathcal{F}_I^{\shortparallel}(\mathcal{M}) \,:\, K' \in \Delta_{K,E}\backslash\{K\}\,\}, \\ \mathcal{F}_D^{\shortparallel}(\Delta_{K,E}) &:= \{F = F_{K',\Gamma_{\boldsymbol{\iota}}} \in \mathcal{F}_D^{\shortparallel}(\mathcal{M}) \,:\, K' \in \Delta_{K,E} \text{ and } \boldsymbol{\iota} \in \mathcal{J}_D\}\,. \end{aligned} \tag{5.9}$$

Finally, if $F \in \mathcal{F}(K)\backslash\mathcal{F}_D(K)$, respectively $F \in \mathcal{F}_D(K)$, we introduce

$$\begin{aligned} \mathcal{F}_I^{\shortparallel}(\Delta_{K,F}) &:= \{\, F = F_{K,K'} \in \mathcal{F}_I^{\shortparallel}(\mathcal{M}) \,:\, K' \in \Delta_{K,F}\backslash\{K\}\,\}, \\ \mathcal{F}_D^{\shortparallel}(\Delta_{K,F}) &:= \{F = F_{K',\Gamma_{\boldsymbol{\iota}}} \in \mathcal{F}_D^{\shortparallel}(\mathcal{M}) \,:\, K' \in \Delta_{K,F} \text{ and } \boldsymbol{\iota} \in \mathcal{J}_D\}\,. \end{aligned} \tag{5.10}$$

We further define

$$\mathcal{F}_{ID}^{\shortparallel}(\Delta_{K,\boldsymbol{N}}) := \mathcal{F}_I^{\shortparallel}(\Delta_{K,\boldsymbol{N}}) \cup \mathcal{F}_D^{\shortparallel}(\Delta_{K,\boldsymbol{N}}), \tag{5.11}$$
$$\mathcal{F}_{ID}^{\shortparallel}(\Delta_{K,E}) := \mathcal{F}_I^{\shortparallel}(\Delta_{K,E}) \cup \mathcal{F}_D^{\shortparallel}(\Delta_{K,E}), \tag{5.12}$$
$$\mathcal{F}_{ID}^{\shortparallel}(\Delta_{K,F}) := \mathcal{F}_I^{\shortparallel}(\Delta_{K,F}) \cup \mathcal{F}_D^{\shortparallel}(\Delta_{K,F}). \tag{5.13}$$

Notice that any of the sets in (5.8)–(5.13) could be empty.

5.2 Averaging Over $\boldsymbol{\Delta_{K,N}}$

Let $v \in \overline{V}_{\sigma,\mathfrak{s}}^{\ell,0,\perp}$ be fixed. We first construct an approximation $v^{\mathrm{n}} \in \overline{V}_{\sigma,\mathfrak{s}}^{\ell,0,\perp}$ by modifying v at possibly all elemental vertices. For $K \in \mathcal{M}$ and $\boldsymbol{N} \in \mathcal{N}(K)$, we define the *averaged vertex value* $A_{K,\boldsymbol{N}}(v)$ by averaging v over all elements of $\Delta_{K,\boldsymbol{N}}$ in (5.1):

$$A_{K,\boldsymbol{N}}(v) := \begin{cases} \dfrac{1}{\operatorname{card}(\Delta_{K,\boldsymbol{N}})} \displaystyle\sum_{K' \in \Delta_{K,\boldsymbol{N}}} v|_{K'}(\boldsymbol{N}), & \boldsymbol{N} \in \mathcal{N}(K)\backslash\mathcal{N}_D(K), \\ 0, & \boldsymbol{N} \in \mathcal{N}_D(K). \end{cases} \tag{5.14}$$

The averaged value $A_{K,N}(v)$ in (5.14) is well defined irrespective of whether $\boldsymbol{N} \in \mathcal{N}(K)$ gives rise to a regular or irregular node in $\mathcal{N}(\mathcal{M})$. With (5.5), we have

$$A_{K,\boldsymbol{N}}(v) = A_{K',\boldsymbol{N}}(v), \qquad K' \in \Delta_{K,\boldsymbol{N}}. \tag{5.15}$$

Hence, the values $A_{K,N}$ assign a unique vertex value on the elements in $\Delta_{K,N}$ which match regularly at the vertex $\boldsymbol{N}$.

For $K \in \mathcal{M}$ and $\boldsymbol{N} \in \mathcal{N}(K)$, we denote by $\mathcal{L}_{K,\boldsymbol{N}}(v) \in \mathbb{Q}_1(K)$ the unique polynomial vertex lifting with the property that, for $\boldsymbol{N}' \in \mathcal{N}(K)$,

$$\mathcal{L}_{K,\boldsymbol{N}}(v)(\boldsymbol{N}') = \begin{cases} v|_K(\boldsymbol{N}) - A_{K,\boldsymbol{N}}(v) & \boldsymbol{N}' = \boldsymbol{N}, \\ 0 & \boldsymbol{N}' \neq \boldsymbol{N}. \end{cases} \tag{5.16}$$

Lemma 5.1 *For $K \in \mathcal{M}$ and $\boldsymbol{N} \in \mathcal{N}(K)$, let the vertex lifting $\mathcal{L}_{K,\boldsymbol{N}}(v)$ be defined by (5.16) with the averages $A_{K,\boldsymbol{N}}(v)$ in (5.14). Then there holds*

$$N_K^{\perp}[\mathcal{L}_{K,\boldsymbol{N}}(v)]^2 \lesssim |\boldsymbol{p}_K|^4 \mathrm{jmp}_{\mathcal{F}_{ID}^{\parallel}(\Delta_{K,\boldsymbol{N}})}[v]^2, \tag{5.17}$$

with $\mathcal{F}_{ID}^{\parallel}(\Delta_{K,\boldsymbol{N}})$ in (5.11) and $\mathrm{jmp}_{\mathcal{F}'}[v]$ defined in (3.30). If $\mathcal{F}_{ID}^{\parallel}(\Delta_{K,\boldsymbol{N}}) = \emptyset$, the sum on the right-hand side of (5.17) is understood as zero.

Proof From the definition (5.14) and anisotropic scaling, we readily find that

$$\|\mathcal{L}_{K,\boldsymbol{N}}(v)\|_{L^2(K)}^2 \lesssim (h_K^{\perp})^2 h_K^{\parallel} \big|v|_K(\boldsymbol{N}) - A_{K,\boldsymbol{N}}(v)\big|^2. \tag{5.18}$$

The univariate inverse estimate in [26, Theorem 3.91], applied in each direction and combined with anisotropic scaling (employing that $h_K^{\perp} \lesssim h_K^{\parallel}$, $p_K^{\perp} \leq p_K^{\parallel}$), yields the anisotropic inverse inequality

$$\|\nabla v\|_{L^2(K)}^2 \lesssim (p_K^{\parallel})^4 (h_K^{\perp})^{-2} \|v\|_{L^2(K)}^2, \qquad v \in \mathbb{Q}_{\boldsymbol{p}_K}(K)\,. \tag{5.19}$$

From (5.19) (recalling that $\mathcal{L}_{K,\boldsymbol{N}} \in \mathbb{Q}_1(K)$) and (5.18), we obtain

$$N_K^{\perp}[\mathcal{L}_{K,\boldsymbol{N}}(v)]^2 \lesssim (h_K^{\perp})^{-2} \|\mathcal{L}_{K,\boldsymbol{N}}(v)\|_{L^2(K)}^2 \lesssim h_K^{\parallel} \big|v|_K(\boldsymbol{N}) - A_{K,\boldsymbol{N}}(v)\big|^2. \tag{5.20}$$

We proceed by estimating $|v|_K(\boldsymbol{N}) - A_{K,\boldsymbol{N}}(v)|$ in (5.20). We consider first the case where $\boldsymbol{N} \in \mathcal{N}(K)$ is a node of $\mathcal{N}(K) \backslash \mathcal{N}_D(K)$. Then the triangle inequality, the fact that $\mathrm{card}(\Delta_{K,\boldsymbol{N}})^{-1}$ is bounded uniformly in ℓ, and the partial conformity of $v \in \overline{V}_{\sigma,\mathfrak{s}}^{\ell,0,\perp}$ imply

$$\begin{aligned}\left|v|_K(\boldsymbol{N}) - A_{K,N}(v)\right|^2 &\lesssim \frac{1}{\operatorname{card}(\Delta_{K,N})^2} \sum_{K'\in\Delta_{K,N}\backslash\{K\}} \left|v|_K(\boldsymbol{N}) - v|_{K'}(\boldsymbol{N})\right|^2 \\ &\lesssim \sum_{K'\in\Delta_{K,N}\backslash\{K\}} |[\![v]\!]_{F_{K,K'}}(\boldsymbol{N})|^2 \\ &\lesssim \sum_{K'\in\Delta_{K,N}\backslash\{K\}} \|[\![v]\!]_{F_{K,K'}}\|^2_{L^\infty(F_{K,K'})} \\ &\lesssim \sum_{F\in\mathcal{F}_I^{\shortparallel}(\Delta_{K,N})} \|[\![v]\!]_F\|^2_{L^\infty(F)}.\end{aligned} \tag{5.21}$$

If the sets $\Delta_{K,N}\backslash\{K\}$ or $\mathcal{F}_I^{\shortparallel}(\Delta_{K,N})$ are empty, then the right-hand side of (5.21) is understood as zero; then we have $v|_K(\boldsymbol{N}) = A_{K,N}(v)$.

Second, let $\boldsymbol{N} \in \mathcal{N}_D(K)$. Consider a Dirichlet boundary face $F = F_{K',\Gamma_\iota}$ with $\boldsymbol{N} \in \mathcal{N}(F)$, $F \in \mathcal{F}(K')$, for $K' \in \Delta_{K,N}$ and $\iota \in \mathcal{J}_D$. We may assume that $F \in \mathcal{F}_D^{\shortparallel}(\Delta_{K,N})$; otherwise, we have $v|_K(\boldsymbol{N}) = 0$, $A_{K,N}(v) = 0$ and $\mathcal{L}_{K,N}(v) = 0$ by the conformity properties of v and definitions (5.14), (5.16), respectively. Therefore,

$$\left|v|_K(\boldsymbol{N}) - A_{K,N}(v)\right|^2 \le \|[\![v]\!]_F\|^2_{L^\infty(F)} \le \sum_{F\in\mathcal{F}_D^{\shortparallel}(\Delta_{K,N})} \|[\![v]\!]_F\|^2_{L^\infty(F)}. \tag{5.22}$$

Combining (5.20), (5.21) and (5.22) gives

$$N_K^{\perp}[\mathcal{L}_{K,N}(v)]^2 \lesssim h_K^{\shortparallel} \sum_{F\in\mathcal{F}_{ID}^{\shortparallel}(\Delta_{K,N})} \|[\![v]\!]_F\|^2_{L^\infty(F)}. \tag{5.23}$$

To bound the L^∞-norms of the jumps of v in (5.23), we recall from [26, Theorems 3.92] the following univariate inverse inequality: let $I = (a, b)$ be an interval of size $h = b - a$. Then

$$|q(a)|^2 + |q(b)|^2 \le \|q\|^2_{L^\infty(I)} \lesssim p^2 h^{-1} \|q\|^2_{L^2(I)}, \qquad q \in \mathbb{P}_p(I), \tag{5.24}$$

for all polynomials $q \in \mathbb{P}_p(I)$. A face $F \in \mathcal{F}_{ID}^{\shortparallel}(\Delta_{K,N})$ can be written in the form (3.32). Applying (5.24) in the two directions on F (see also [23, Lemma 4.3(b)]) and the definition of the face polynomial degrees $\overline{\boldsymbol{p}}_{K,F}$ in (3.12) yield

$$\|[\![v]\!]_F\|^2_{L^\infty(F)} \lesssim |\boldsymbol{p}_K|^4 (h_K^{\perp})^{-1} (h_K^{\shortparallel})^{-1} \|[\![v]\!]_F\|^2_{L^2(F)}. \tag{5.25}$$

The bound (5.17) follows from (5.23) and (5.25) using that $\mathtt{h}_F \simeq h_K^{\perp}$ by (3.31). □

For $K \in \mathcal{M}$, we introduce the full vertex lifting

$$\mathcal{L}_K^{\mathrm{n}}(v) := \sum_{N\in\mathcal{N}(K)} \mathcal{L}_{K,N}(v) \in \mathbb{Q}_1(K). \tag{5.26}$$

We further define the approximation $v^{\mathrm{n}} \in \mathbb{S}_{\overline{\boldsymbol{p}}_K}(K)$ as

$$v^{\mathrm{n}}|_K := v|_K - \mathcal{L}^{\mathrm{n}}_K(v), \qquad K \in \mathcal{M}. \tag{5.27}$$

The function $v^{\mathrm{n}}|_K$ has assigned vertex values at all elemental vertex nodes:

$$v^{\mathrm{n}}|_K(\boldsymbol{N}) = A_{K,\boldsymbol{N}}(v), \qquad \boldsymbol{N} \in \mathcal{N}(K). \tag{5.28}$$

Note also that, in the expansion (3.14), (3.15), only the nodal parts of $v^{\mathrm{n}}|_K$ and $v|_K$ differ, while the edge, face and interior parts of $v^{\mathrm{n}}|_K$ and $v|_K$ coincide.

Proposition 5.2 *For $K \in \mathcal{M}$, let $v^{\mathrm{n}}|_K$ be defined in (5.27). Then, $v^{\mathrm{n}} \in \overline{V}^{\ell,0,\perp}_{\sigma,\mathfrak{s}}$ and there holds*

$$\Upsilon^{\perp}_{\mathcal{M}}[v - v^{\mathrm{n}}]^2 + \mathrm{jmp}_{\mathcal{F}^{\parallel}_{ID}(\mathcal{M})}[v^{\mathrm{n}}]^2 \lesssim |\boldsymbol{p}|^4 \, \mathrm{jmp}_{\mathcal{F}^{\parallel}_{ID}(\mathcal{M})}[v]^2. \tag{5.29}$$

Proof The function $v \in V^{\ell,0,\perp}_{\sigma,\mathfrak{s}}$ is continuous over all faces $F \in \mathcal{F}^{\perp}_{ID}(\mathcal{M})$. Property (5.15) and definition (5.16) then imply that the liftings $\mathcal{L}^{\mathrm{n}}_K(v)$ yield conforming approximations over the same faces. Since $v^{\mathrm{n}}|_K = v|_K - \mathcal{L}^{\mathrm{n}}_K(v)$, the approximation v^{n} is continuous over these faces as well, and thus, $v^{\mathrm{n}} \in \overline{V}^{\ell,0,\perp}_{\sigma,\mathfrak{s}}$. The bound for $\Upsilon^{\perp}_{\mathcal{M}}[v - v^{\mathrm{n}}]^2$ in (5.29) follows immediately by summing (5.17) over all elements $K \in \mathcal{M}$ and $\boldsymbol{N} \in \mathcal{N}(K)$. To bound the L^2-norms of the jumps of v^{n}, consider an interior face $F = F_{K,K'} \in \mathcal{F}^{\parallel}_{ID}(\mathcal{M})$. The definition (5.27), the triangle inequality and the trace inequality in Lemma 4.11 (noting that $\mathtt{h}_F \simeq h^{\perp}_K$) yield

$$\mathtt{h}_F^{-1} \|[\![v^{\mathrm{n}}]\!]_F\|^2_{L^2(F)} \lesssim \mathtt{h}_F^{-1} \|[\![v]\!]_F\|^2_{L^2(F)} + N^{\perp}_K[\mathcal{L}^{\mathrm{n}}_K(v)]^2 + N^{\perp}_{K'}[\mathcal{L}^{\mathrm{n}}_K(v)]^2.$$

A corresponding bound holds for Dirichlet faces $F \in \mathcal{F}^{\parallel}_{D}(\mathcal{M})$. Summing these estimates over all $F \in \mathcal{F}^{\parallel}_{ID}(\mathcal{M})$ and again applying (5.17) gives the desired bound for $\mathrm{jmp}_{\mathcal{F}^{\parallel}_{ID}(\mathcal{M})}[v^{\mathrm{n}}]^2$ in (5.29). □

5.3 Averaging Over $\Delta_{K,E}$

With (3.17) and since $\mathcal{L}^{\mathrm{n}}_K(v)$ in (5.26) is trilinear, the approximation $v^{\mathrm{n}} \in \overline{V}^{\ell,0,\perp}_{\sigma,\mathfrak{s}}$ from Sect. 5.2 satisfies

$$(v^{\mathrm{n}}|_K)|_E \in \mathbb{P}_{\overline{p}_{K,E}}(E), \qquad K \in \mathcal{M}, \ E \in \mathcal{E}(K), \tag{5.30}$$

with the minimum edge degree $\overline{p}_{K,E} \geq 1$ in (3.13). For $K \in \mathcal{M}$ and $E \in \mathcal{E}(K)$, we next average v^{n} over the set $\Delta_{K,E}$ in (5.2) and define:

$$A_{K,E}(v^{\mathrm{n}}) := \begin{cases} \dfrac{1}{\mathrm{card}(\Delta_{K,E})} \displaystyle\sum_{K' \in \Delta_{K,E}} \big(v^{\mathrm{n}}|_{K'}\big)|_E, & E \in \mathcal{E}(K) \backslash \mathcal{E}_D(K), \\ 0, & E \in \mathcal{E}_D(K). \end{cases} \tag{5.31}$$

By (5.30), the function $A_{K,E}(v^{\mathrm{n}})$ is a polynomial in $\mathbb{P}_{\overline{p}_{K,E}}(E)$.

Lemma 5.3 *Let $K \in \mathcal{M}$ and $E \in \mathcal{E}(K)$. Then, $A_{K,E}(v^{\mathrm{n}}) = A_{K',E}(v^{\mathrm{n}})$ for $K' \in \Delta_{K,E}$. Moreover, for $\boldsymbol{N} \in \mathcal{N}(E)$, we have $A_{K,E}(v^{\mathrm{n}})(\boldsymbol{N}) = v^{\mathrm{n}}|_K(\boldsymbol{N})$.*

Proof The first assertion follows from (5.6). Then, with (5.4), (5.15), there holds $A_{K',N}(v) = A_{K,N}(v)$ for $K' \in \Delta_{K,E}$. In combination with (5.31) and (5.28), this property yields

$$\begin{aligned} A_{K,E}(v^{\mathrm{n}})(\boldsymbol{N}) &= \frac{1}{\operatorname{card}(\Delta_{K,E})} \sum_{K' \in \Delta_{K,E}} A_{K',N}(v) \\ &= \frac{1}{\operatorname{card}(\Delta_{K,E})} \sum_{K' \in \Delta_{K,E}} A_{K,N}(v) = A_{K,N}(v) = v^{\mathrm{n}}|_K(\boldsymbol{N}). \end{aligned}$$

The second assertion follows. □

For $K \in \mathcal{M}$ and $E \in \mathcal{E}(K)$, we denote by $\mathcal{L}_{K,E}(v^{\mathrm{n}}) \in \mathbb{S}_{\overline{\boldsymbol{p}}_K}(K)$ the unique polynomial lifting which satisfies

$$\mathcal{L}_{K,E}(v^{\mathrm{n}})|_E = (v^{\mathrm{n}}|_K)|_E - A_{K,E}(v^{\mathrm{n}}) \in \mathbb{P}_{\overline{p}_{K,E}}(E) \quad \text{on } E, \tag{5.32}$$

and which is given by linear blending functions in the two directions orthogonal to E. With Lemma 5.3, there holds

$$\mathcal{L}_{K,E}(v^{\mathrm{n}})(\boldsymbol{N}) = 0, \qquad \boldsymbol{N} \in \mathcal{N}(E). \tag{5.33}$$

The lifting $\mathcal{L}_{K,E}(v)$ vanishes on the remaining elemental edges $E' \neq E$, as well as on faces $F \in \mathcal{F}(K)$ with $E \notin \mathcal{F}(E)$.

Lemma 5.4 *For $K \in \mathcal{M}$ and $E \in \mathcal{E}(K)$, let the edge lifting $\mathcal{L}_{K,E}(v^{\mathrm{n}})$ be defined by (5.32) with the averages $A_{K,E}(v^{\mathrm{n}})$ in (5.31). Then there holds*

$$N_K^{\perp}[\mathcal{L}_{K,E}(v^{\mathrm{n}})]^2 \lesssim |\boldsymbol{p}_K|^6 \mathrm{jmp}_{\mathcal{F}_{ID}^{\parallel}(\Delta_{K,E})}[v^{\mathrm{n}}]^2, \tag{5.34}$$

with $\mathcal{F}_{ID}^{\parallel}(\Delta_{K,E})$ in (5.12). If $\mathcal{F}_{ID}^{\parallel}(\Delta_{K,E}) = \emptyset$, the sum on the right-hand side is understood as zero.

Proof We denote by h_E the length of $E \in \mathcal{E}(K)$. Then, by (3.3), either $h_E \simeq h_K^{\perp}$ or $h_E \simeq h_K^{\parallel}$. From the definition of (5.32) and anisotropic scaling, we see that

$$\|\mathcal{L}_{K,E}(v^{\mathrm{n}})\|_{L^2(K)}^2 \lesssim \begin{cases} h_K^{\perp} h_K^{\parallel} \|v^{\mathrm{n}}|_K - A_{K,E}(v^{\mathrm{n}})\|_{L^2(E)}^2, & h_E \simeq h_K^{\perp}, \\ (h_K^{\perp})^2 \|v^{\mathrm{n}}|_K - A_{K,E}(v^{\mathrm{n}})\|_{L^2(E)}^2, & h_E \simeq h_K^{\parallel}. \end{cases} \tag{5.35}$$

Hence, the inverse inequality (5.19) implies

$$N_K^{\perp}[\mathcal{L}_{K,E}(v^{\mathrm{n}})]^2 \lesssim |\boldsymbol{p}_K|^4 \begin{cases} (h_K^{\perp})^{-1} h_K^{\parallel} \|v^{\mathrm{n}}|_K - A_{K,E}(v^{\mathrm{n}})\|_{L^2(E)}^2, & h_E \simeq h_K^{\perp}, \\ \|v^{\mathrm{n}}|_K - A_{K,E}(v^{\mathrm{n}})\|_{L^2(E)}^2, & h_E \simeq h_K^{\parallel}. \end{cases} \tag{5.36}$$

We continue by bounding $\|v^{\mathrm{n}}|_K - v^{\mathrm{e}}|_K\|_{L^2(E)}$. First, we consider the case $E \in \mathcal{E}(K)\backslash\mathcal{E}_D(K)$. From the definition (5.31), the triangle inequality, the uniform boundedness of $\mathrm{card}(\Delta_{K,E})^{-2}$, and the fact that $v^{\mathrm{n}} \in \overline{V}_{\sigma,\mathfrak{s}}^{\ell,0,\perp}$ (cf. Proposition 5.2), we obtain

$$\begin{aligned} \|v^{\mathrm{n}}|_K - A_{K,E}(v^{\mathrm{n}})\|_{L^2(E)}^2 &\lesssim \frac{1}{\mathrm{card}(\Delta_{K,E})^2} \sum_{K' \in \Delta_{K,E}\backslash\{K\}} \|v^{\mathrm{n}}|_K - v^{\mathrm{n}}|_{K'}\|_{L^2(E)}^2 \\ &\lesssim \sum_{K' \in \Delta_{K,E}\backslash\{K\}} \|[\![v^{\mathrm{n}}]\!]_{F_{K,K'}}\|_{L^2(E)}^2 \\ &\lesssim \sum_{F \in \mathcal{F}_I^{\parallel}(\Delta_{K,E})} \|[\![v^{\mathrm{n}}]\!]_F\|_{L^2(E)}^2. \end{aligned} \tag{5.37}$$

Again, if the sets $\Delta_{K,E}\backslash\{K\}$ or $F \in \mathcal{F}_I^{\parallel}(\Delta_{K,E})$ are empty, then the right-hand side of (5.37) is understood as zero, in which case we have $(v^{\mathrm{n}}|_K)|_E = A_{K,E}(v^{\mathrm{n}})$.

Second, let $E \in \mathcal{E}_D(K)$ be a Dirichlet edge. Then, consider a boundary face $F = F_{K',\Gamma_\iota}$ with $E \in \mathcal{E}(F)$, $F \in \mathcal{F}(K')$, for $K' \in \Delta_{K,E}$ and $\iota \in \mathcal{J}_D$. As before, we may assume $F \in \mathcal{F}_D^{\parallel}(\Delta_{K,E})$, otherwise, $\mathcal{L}_{K,E}(v^{\mathrm{n}}) = 0$ due to the partial conformity of v^{n} and (5.31), (5.32). We find that

$$\|v^{\mathrm{n}}|_K - A_{K,E}(v^{\mathrm{n}})\|_{L^2(E)}^2 \le \|[\![v^{\mathrm{n}}]\!]_F\|_{L^2(E)}^2 \lesssim \sum_{F \in \mathcal{F}_D^{\parallel}(\Delta_{K,E})} \|[\![v^{\mathrm{n}}]\!]_F\|_{L^2(E)}^2. \tag{5.38}$$

For $F \in \mathcal{F}_{ID}^{\parallel}(\Delta_{K,E})$ written in the form (3.32), the inequality (5.24) applied on $\overline{E} \subset \overline{F}$ in direction perpendicular to E implies

$$\|[\![v^{\mathrm{n}}]\!]_F\|_{L^2(E)}^2 \lesssim \begin{cases} |\boldsymbol{p}_K|^2 (h_K^{\parallel})^{-1} \|[\![v^{\mathrm{n}}]\!]_F\|_{L^2(F)}^2 & h_E \simeq h_K^{\perp}, \\ |\boldsymbol{p}_K|^2 (h_K^{\perp})^{-1} \|[\![v^{\mathrm{n}}]\!]_F\|_{L^2(F)}^2 & h_E \simeq h_K^{\parallel}. \end{cases} \tag{5.39}$$

Therefore, combining the inequalities in(5.36), (5.37), (5.38) and (5.39) gives the desired bound (5.34). □

We define the full edge lifting

$$\mathcal{L}_K^{\mathrm{e}}(v^{\mathrm{n}}) := \sum_{E \in \mathcal{E}(K)} \mathcal{L}_{K,E}(v^{\mathrm{n}}) \in \mathbb{S}_{\overline{\boldsymbol{p}}_K}(K), \qquad K \in \mathcal{M}, \tag{5.40}$$

and introduce the approximation $v^{\mathrm{e}} \in \mathbb{S}_{\overline{\boldsymbol{p}}_K}(K)$ by

$$v^{\mathrm{e}}|_K := v^{\mathrm{n}}|_K - \mathcal{L}^{\mathrm{e}}_K(v^{\mathrm{n}}), \qquad K \in \mathcal{M}. \tag{5.41}$$

The definition (5.41) only affects the edge parts of $v^{\mathrm{n}}|_K$ in (3.14), (3.15), while nodal, face and interior parts of $v^{\mathrm{n}}|_K$ are not modified. By construction and Lemma 5.3, there holds

$$\big(v^{\mathrm{e}}|_K\big)|_E = A_{K,E}(v^{\mathrm{n}}), \qquad E \in \mathcal{E}(K), \tag{5.42}$$
$$v^{\mathrm{e}}|_K(\boldsymbol{N}) = v^{\mathrm{n}}|_K(\boldsymbol{N}), \qquad \boldsymbol{N} \in \mathcal{N}(K). \tag{5.43}$$

The analog of Proposition 5.2 reads as follows.

Proposition 5.5 *For $K \in \mathcal{M}$, let $v^{\mathrm{e}}|_K$ be defined in (5.41). Then, $v^{\mathrm{e}} \in \overline{V}^{\ell,0,\perp}_{\sigma,\mathfrak{s}}$ and there holds*

$$\Upsilon^{\perp}_{\mathcal{M}}[v - v^{\mathrm{e}}]^2 + \mathrm{jmp}_{\mathcal{F}^{\parallel}_{ID}(\mathcal{M})}[v^{\mathrm{e}}]^2 \lesssim |\boldsymbol{p}|^{10}\, \mathrm{jmp}_{\mathcal{F}^{\parallel}_{ID}(\mathcal{M})}[v]^2. \tag{5.44}$$

Proof By construction, it follows that $v^{\mathrm{e}} \in \overline{V}^{\ell,0,\perp}_{\sigma,\mathfrak{s}}$. Then, by proceeding as in the proof of Proposition 5.2, the estimate (5.34) yields

$$\Upsilon^{\perp}_{\mathcal{M}}[v^{\mathrm{n}} - v^{\mathrm{e}}]^2 + \mathrm{jmp}_{\mathcal{F}^{\parallel}_{ID}(\mathcal{M})}[v^{\mathrm{e}}]^2 \lesssim |\boldsymbol{p}|^{6}\, \mathrm{jmp}_{\mathcal{F}^{\parallel}_{ID}(\mathcal{M})}[v^{\mathrm{n}}]^2.$$

The triangle inequality and the bound (5.29) now show (5.44). □

5.4 Averaging Over $\Delta_{K,F}$

With (3.17) and the definition of the minimum edge degrees in (3.13), the approximation $v^{\mathrm{e}} \in \overline{V}^{\ell,0,\perp}_{\sigma,\mathfrak{s}}$ satisfies:

$$(v^{\mathrm{e}}|_K)|_F \in \mathbb{Q}_{\overline{\boldsymbol{p}}_{K,F}}(F), \qquad K \in \mathcal{M},\ F \in \mathcal{F}(K), \tag{5.45}$$

with the minimum face degree $\overline{\boldsymbol{p}}_{K,F} \in \mathbb{N}^2$ in (3.12). We average v^{e} over $\Delta_{K,F}$ in (5.3):

$$A_{K,F}(v^{\mathrm{e}}) := \begin{cases} \dfrac{1}{\mathrm{card}(\Delta_{K,F})} \displaystyle\sum_{K' \in \Delta_{K,F}} (v^{\mathrm{e}}|_{K'})|_F, & F \in \mathcal{F}(K) \backslash \mathcal{F}_D(K), \\ 0, & F \in \mathcal{F}_D(K). \end{cases} \tag{5.46}$$

By (5.45), the function $A_{K,F}(v^{\mathrm{e}})$ is a polynomial in $\mathbb{Q}_{\overline{p}_{K,F}}(F)$.

Lemma 5.6 *Let $K \in \mathcal{M}$ and $F \in \mathcal{F}(K)$. Then, $A_{K,F}(v^{\mathrm{e}}) = A_{K',F}(v^{\mathrm{e}})$ for $K' \in \Delta_{K,F}$. Moreover, if $E \in \mathcal{E}(F)$ is an edge of F, we have $A_{K,F}(v^{\mathrm{e}})|_E = (v^{\mathrm{e}}|_K)|_E$.*

Proof The first property follows from (5.7). To show the second property, consider $\boldsymbol{x} \in E \in \mathcal{E}(K)$. With (5.4) and Lemma 5.3, $A_{K',E}(v^{\mathrm{n}}) = A_{K,E}(v^{\mathrm{n}})$ for $K' \in \Delta_{K,F}$. Employing (5.46) and (5.42) then yields

$$\begin{aligned} A_{K,F}(v^{\mathrm{e}})(\boldsymbol{x}) &= \frac{1}{\operatorname{card}(\Delta_{K,F})} \sum_{K' \in \Delta_{K,F}} A_{K',E}(v^{\mathrm{n}})(\boldsymbol{x}) \\ &= \frac{1}{\operatorname{card}(\Delta_{K,F})} \sum_{K' \in \Delta_{K,F}} A_{K,E}(v^{\mathrm{n}})(\boldsymbol{x}) = A_{K,E}(v^{\mathrm{n}})(\boldsymbol{x}) = v^{\mathrm{e}}|_K(\boldsymbol{x}), \end{aligned}$$

which completes the proof. □

For $K \in \mathcal{M}$ and $F \in \mathcal{F}(K)$, we denote by $\mathcal{L}_{K,F}(v^{\mathrm{e}}) \in \mathbb{S}_{\overline{\boldsymbol{p}}_K}(K)$ the unique polynomial lifting which is given by

$$\mathcal{L}_{K,F}(v^{\mathrm{e}})|_F := (v^{\mathrm{e}}|_K)|_F - A_{K,F}(v^{\mathrm{e}}) \in \mathbb{Q}_{\overline{\boldsymbol{p}}_{K,F}}(F) \quad \text{on } F, \tag{5.47}$$

and by a linear blending function in direction orthogonal to F. With Lemma 5.6, there holds

$$\mathcal{L}_{K,F}(v^{\mathrm{e}})|_E = 0, \qquad E \in \mathcal{E}(F). \tag{5.48}$$

Therefore, the lifting $\mathcal{L}_{K,F}(v^{\mathrm{e}})$ vanishes on all other elemental faces $F' \in \mathcal{F}(K)$ with $F' \neq F$.

Lemma 5.7 *For $K \in \mathcal{M}$ and $F \in \mathcal{F}(K)$, let the face lifting $\mathcal{L}_{K,F}(v^{\mathrm{e}})$ be defined by (5.47) with $A_{K,F}(v^{\mathrm{e}})$ in (5.46). Then there holds*

$$N_K^{\perp}[\mathcal{L}_{K,F}(v^{\mathrm{e}})]^2 \lesssim |\boldsymbol{p}_K|^4 \operatorname{jmp}_{\mathcal{F}_{ID}^{\parallel}(\Delta_{K,F})}[v^{\mathrm{e}}]^2, \tag{5.49}$$

with $\mathcal{F}_{ID}^{\parallel}(\Delta_{K,F})$ in (5.13). If $\mathcal{F}_{ID}^{\parallel}(\Delta_{K,F}) = \emptyset$, the sum on the right-hand side is understood as zero.

Proof Let first $F \in \mathcal{F}(K) \backslash \mathcal{F}_D(K)$. We have $\operatorname{card}(\Delta_{K,F}) \in \{1, 2\}$. If $\operatorname{card}(\Delta_{K,F}) = 1$, then F is irregular in $\mathcal{F}(\mathcal{M})$ or a Neumann boundary face in $\mathcal{F}_N(\mathcal{M})$. In this case, we find that $\mathcal{L}_{K,F}(v^{\mathrm{e}}) = 0$ and $\mathcal{F}_{ID}^{\parallel}(\Delta_{K,F}) = \emptyset$. Hence, (5.49) is satisfied. Next, let $\operatorname{card}(\Delta_{K,F}) = 2$. Then there is $K' \in \Delta_{K,F}$ such that $F = F_{K,K'} \in \mathcal{F}_I(\mathcal{M})$ is a regular face. We may assume that $F \in \mathcal{F}_I^{\parallel}(\mathcal{M})$; otherwise, we have $\mathcal{L}_{K,F}(v^{\mathrm{e}}) = 0$ since $v^{\mathrm{e}} \in \overline{V}_{\sigma,\mathfrak{s}}^{\ell,0,\perp}$. The properties (3.31), (3.32), anisotropic scaling and the inverse inequality (5.19) yield

$$\begin{aligned} N_K^{\perp}[\mathcal{L}_{K,F}(v^{\mathrm{e}})]^2 &\lesssim |\boldsymbol{p}_K|^4 \mathrm{h}_F^{-1} \|v^{\mathrm{e}}|_K - A_{K,F}(v^{\mathrm{e}})\|_{L^2(F)}^2 \\ &\lesssim |\boldsymbol{p}_K|^4 \mathrm{h}_F^{-1} \|[\![v^{\mathrm{e}}]\!]_F\|_{L^2(F)}^2. \end{aligned} \tag{5.50}$$

Second, consider $F \in \mathcal{F}_D(K)$. Then, $F = F_{K,\Gamma_\iota} \in \mathcal{F}_D(\mathcal{M})$ is a Dirichlet face for $\iota \in \mathcal{J}_D$. Again, we may assume $F \in \mathcal{F}_D^{\parallel}(\mathcal{M})$. Proceeding as before, we obtain

$$N_K^{\perp}[\mathcal{L}_{K,F}(v^{\mathrm{e}})]^2 \lesssim |\boldsymbol{p}_K|^4 \mathrm{h}_F^{-1} \|[\![v^{\mathrm{e}}]\!]_F\|_{L^2(F)}^2. \tag{5.51}$$

Referring to the bounds (5.50), (5.51) and the definition of the sets $\mathcal{F}_{ID}^{\parallel}(\Delta_{K,F})$ in (5.13) implies (5.49). □

For $K \in \mathcal{M}$, we define the full face lifting by

$$\mathcal{L}_K^{\mathrm{f}}(v^{\mathrm{e}}) := \sum_{F \in \mathcal{F}(K)} \mathcal{L}_{K,F}(v^{\mathrm{e}}) \in \mathbb{S}_{\overline{\boldsymbol{p}}_K}(K), \tag{5.52}$$

and introduce $v^{\mathrm{f}} \in \overline{V}_{\sigma,\mathfrak{s}}^{\ell,0,\perp}$ by setting

$$v^{\mathrm{f}}|_K := v^{\mathrm{e}}|_K - \mathcal{L}_K^{\mathrm{f}}(v^{\mathrm{e}}) \in \mathbb{S}_{\overline{\boldsymbol{p}}_K}(K), \qquad K \in \mathcal{M}. \tag{5.53}$$

The definition (5.53) only affects the face parts of $v^{\mathrm{e}}|_K$ in (3.14), (3.15), while the other parts of $v^{\mathrm{e}}|_K$ are left unchanged. In particular, the interior part of $v^{\mathrm{f}}|_K$ is equal to that of $v|_K$. By construction, the function v^{f} is conforming over all faces $F \in F_{ID}^{\perp}(\mathcal{M}) \cup \mathcal{F}_D^{\parallel}(\mathcal{M})$ and over all regularly matching interior faces $F \in \mathcal{F}_I^{\parallel}(\mathcal{M})$. With Lemmas 5.3 and 5.6, there holds

$$\big(v^{\mathrm{f}}|_K\big)|_F = A_{K,F}(v^{\mathrm{e}}), \qquad F \in \mathcal{F}(K), \tag{5.54}$$

$$\big(v^{\mathrm{f}}|_K\big)|_E = (v^{\mathrm{e}}|_K)|_E, \qquad E \in \mathcal{E}(K), \tag{5.55}$$

$$v^{\mathrm{f}}|_K(\boldsymbol{N}) = v^{\mathrm{n}}|_K(\boldsymbol{N}), \qquad \boldsymbol{N} \in \mathcal{N}(K). \tag{5.56}$$

We are now ready to establish Theorem 3.12 in Sect. 3.4.

Proof of Theorem 3.12 Given $v \in \overline{V}_{\sigma,\mathfrak{s}}^{\ell,0,\perp}$, we define $\mathcal{A}_{\sigma,\mathfrak{s}}^{\ell}(v) := v^{\mathrm{f}}$ with $v^{\mathrm{f}} \in \overline{V}_{\sigma,\mathfrak{s}}^{\ell,0,\perp}$ as introduced above. Clearly, $\mathcal{A}_{\sigma,\mathfrak{s}}^{\ell}$ is linear. By construction, the function v^{f} is conforming over all faces $F \in F_{ID}^{\perp}(\mathcal{M}_\sigma^\ell) \cup \mathcal{F}_D^{\parallel}(\mathcal{M}_\sigma^\ell)$ and over all regularly matching interior faces $F \in \mathcal{F}_I^{\parallel}(\mathcal{M}_\sigma^\ell)$. With Assumption 3.1, this implies items (i), (ii), (iii) in Theorem 3.12. In addition, if $v \in V_{\sigma,\mathfrak{s}}^{\ell,1}$, all liftings constructed in this section are zero, which implies item (iv). Similarly to the proofs of Propositions 5.2 and 5.5, it follows from (5.49) that

$$\Upsilon_{\mathcal{M}}^{\perp}[v^{\mathrm{e}} - v^{\mathrm{f}}]^2 + \mathrm{jmp}_{\mathcal{F}_I^{\parallel}(\mathcal{M})}[v^{\mathrm{f}}]^2 \lesssim |\boldsymbol{p}|^4 \,\mathrm{jmp}_{\mathcal{F}_{ID}^{\parallel}(\mathcal{M})}[v^{\mathrm{e}}]^2.$$

Hence, the triangle inequality and the bounds (5.29), (5.44) yield

$$\Upsilon_{\mathcal{M}}^{\perp}[v - v^{\mathrm{f}}]^2 + \mathrm{jmp}_{\mathcal{F}_I^{\parallel}(\mathcal{M})}[v^{\mathrm{f}}]^2 \lesssim |\boldsymbol{p}|^{14} \,\mathrm{jmp}_{\mathcal{F}_{ID}^{\parallel}(\mathcal{M})}[v]^2, \tag{5.57}$$

which is the bound (3.45) in Theorem 3.12. □

6 Polynomial Jump Lifting Operators

We construct the operators $\mathcal{L}^{\ell}_{\sigma,\mathfrak{s}}$ and prove Theorem 3.14. Throughout this section, we fix $v^{\mathrm{f}} = \mathcal{A}^{\ell}_{\sigma,\mathfrak{s}}(v)$ for $v \in \overline{V}^{\ell,0,\perp}_{\sigma,\mathfrak{s}}$. While conforming across regular faces and over different mesh patches, the approximations v^{f} are generally discontinuous over irregular faces between different mesh layers in the *interior of mesh patches*. By construction of our meshes, it is sufficient to consider *three* types of irregular mesh configurations in the context of the reference mesh patches.

6.1 Anisotropic Faces

Anisotropic irregular faces arise in the generic geometric situation illustrated in Fig. 4 along an edge $\boldsymbol{e}$ (i.e., in direction of $x^{\parallel}$).

The figure displays the elemental face $F \in \mathcal{F}(K)$ of the outer element K, which is subdivided into *two* irregular faces $F_1 := F_{K_1,K} \in \mathcal{F}(K_1)$ and $F_2 := F_{K_2,K} \in \mathcal{F}(K_2)$, for two refined elements K_1, K_2 in the inner layer. The corresponding irregular edge $E^{\parallel}$ on F is an elemental edge of K_1, K_2, but $E^{\parallel} \notin \mathcal{E}(K)$. All elements belong to the same mesh patch of the underlying geometric mesh. The elements $\{K, K_1, K_2\}$ and the faces $\{F, F_1, F_2\}$ are possibly *anisotropic*; their edge-parallel lengths are thus denoted by the generic parameter $h^{\parallel}$. The edge-perpendicular diameters of the elements involved are shape-regular and of size $h^{\perp}_K \simeq h^{\perp}_{K_i} \simeq h^{\perp}$ for $i = 1, 2$, with $h^{\perp} \lesssim h^{\parallel}$. The precise locations of the elements in edge-perpendicular direction are determined by the parameters $a^{\perp}_1, a^{\perp}_2, b^{\perp}_1, b^{\perp}_2$, whose values only depend on σ. The setting is such that the irregular faces F, F_j satisfy (3.31), (3.32). The configuration shown in Fig. 4 is prototypical as it appears along edges in reference edge mesh patches $\widetilde{\mathcal{M}}^{\ell,\boldsymbol{e}}_{\sigma}$ or in the scaled edge-patch blocks $\widetilde{\mathcal{M}}^{\ell,\boldsymbol{ce},\parallel}_{\sigma}$ introduced in (4.19), (4.20) for reference corner–edge mesh patches $\widetilde{\mathcal{M}}^{\ell,\boldsymbol{ce}}_{\sigma}$. We note that two rotated and superimposed configurations of this type can overlap over one of the smaller elements K_1 or K_2; cf. Fig. 1 and [20, Figure 2].

In Fig. 4, we have $E^{\parallel} = \{(a^{\perp}_1, 0, x^{\parallel}) : x^{\parallel} \in (0, h^{\parallel})\}$. We further introduce the parallel elemental edges $E^{\parallel}_1, E^{\parallel}_2 \in \mathcal{E}(K)$ given by $E^{\parallel}_1 = \{(0, 0, x^{\parallel}) : x^{\parallel} \in (0, h^{\parallel})\}$

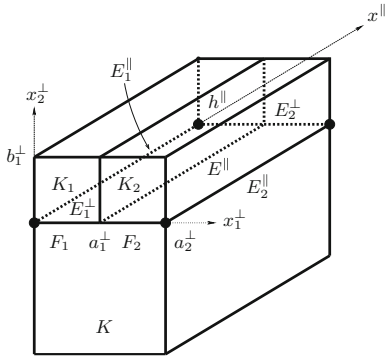

Fig. 4 Interface between K and K_1, K_2 for $\sigma = 0.5$ and length $h^{\parallel}$. The anisotropic irregular faces F_1, F_2, the irregular edge $E^{\parallel}$ and the elemental edges $E^{\perp}_1, E^{\parallel}_1, E^{\perp}_2, E^{\parallel}_2$ of K are illustrated. The highlighted nodes are regular vertex nodes

and $E_2^{\|} = \{(a_2^{\perp}, 0, x^{\|}) : x^{\|} \in (0, h^{\|})\}$. In the reference mesh patches these edges always appear as regular edges. With (5.4), the nodes highlighted in Fig. 4 are then regular vertex nodes. We further denote by $E_1^{\perp}, E_2^{\perp} \in \mathcal{E}(K)$ the perpendicular elemental edges of K given by $E_1^{\perp} = \{(x_1^{\perp}, 0, 0) : x_1^{\perp} \in (0, a_2^{\perp})\}$ and $E_2^{\perp} = \{(x_1^{\perp}, 0, h^{\|}) : x_1^{\perp} \in (0, a_2^{\perp})\}$. Accordingly, we have $\overline{E}_i^{\perp} = \overline{E}_{i1}^{\perp} \cup \overline{E}_{i2}^{\perp}$ for $i = 1, 2$, with $E_{ij}^{\perp} \in \mathcal{E}(K_j)$ irregular in $\mathcal{E}(\mathcal{M})$. Upon writing $\overline{\boldsymbol{p}}_{K,F} = (\overline{p}_{K,F}^{\perp}, \overline{p}_{K,F}^{\|})$ and $\overline{\boldsymbol{p}}_{K_j,F_j} = (\overline{p}_{K_j,F_j}^{\perp}, \overline{p}_{K_j,F_j}^{\|})$ and since $\Delta_{K,F} = \{K, K_1, K_2\}$, $\Delta_{K_j,F_j} = \{K_j, K\}$, the definitions (3.12) and (3.13) imply

$$\overline{p}_{K,F}^{\perp} \le \overline{p}_{K_j,F_j}^{\perp}, \qquad \overline{p}_{K,F}^{\|} \le \overline{p}_{K_j,F_j}^{\|}, \qquad \overline{p}_{K,E_i^{\perp}} \le \overline{p}_{K_j,E_{ij}^{\perp}}, \qquad 1 \le i, j \le 2. \tag{6.1}$$

With (6.1) and noting that $(v^{\mathrm{f}}|_K)|_{E_i^{\perp}} \in \mathbb{P}_{\overline{p}_{K,E_i^{\perp}}}(E_i^{\perp})$ and $(v^{\mathrm{f}}|_K)_F \in \mathbb{Q}_{\overline{\boldsymbol{p}}_{K,F}}(F)$, it follows that

$$(v^{\mathrm{f}}|_K)|_{E_{ij}^{\perp}} \in \mathbb{P}_{\overline{p}_{K_j,E_{ij}^{\perp}}}(E_{ij}^{\perp}), \qquad (v^{\mathrm{f}}|_K)|_{F_j} \in \mathbb{Q}_{\overline{\boldsymbol{p}}_{K_j,F_j}}(F_j), \qquad 1 \le i, j \le 2. \tag{6.2}$$

The face approximation v^{f} is generally discontinuous across the irregular face F_j; we then recall from (3.6) that $[\![v]\!]_{F_j} = v|_{K_j} - v|_K$. The properties in (6.2) imply

$$\big([\![v^{\mathrm{f}}]\!]_{F_j}\big)|_{E_{ij}^{\perp}} \in \mathbb{P}_{\overline{p}_{K_j,E_{ij}^{\perp}}}(E_{ij}^{\perp}), \qquad [\![v^{\mathrm{f}}]\!]_{F_j} \in \mathbb{Q}_{\overline{\boldsymbol{p}}_{K_j,F_j}}(F_j), \qquad j = 1, 2. \tag{6.3}$$

For a function v, we define the jump $[\![v]\!]_F$ over $\overline{F} = \overline{F}_1 \cup \overline{F}_2$ piecewise as

$$\big([\![v]\!]_F\big)|_{F_j} := [\![v]\!]_{F_j}, \qquad j = 1, 2. \tag{6.4}$$

Lemma 6.1 *In the configuration of Fig. 4, we have* $[\![v^{\mathrm{f}}]\!]_F \in C^0(\overline{F})$*, as well as* $[\![v^{\mathrm{f}}]\!]_F = 0$ *on* $\overline{E}_1^{\|}$ *and on* $\overline{E}_2^{\|}$.

Proof By Theorem 3.12, the approximation v^{f} is continuous across the regular face F_{K_1,K_2}, which implies $[\![v^{\mathrm{f}}]\!]_F \in C^0(\overline{F})$. Since $E_1^{\|}$ and $E_2^{\|}$ are regular edges, then $\{K, K_j\} \subset \Delta_{K,E_j^{\|}} = \Delta_{K_1,E_j^{\|}}$; see (5.6). The second assertion follows now from the construction of v^{f}; cf. (5.42) and (5.55). □

To remove non-vanishing jumps of v^{f} over the perpendicular elemental edge $E_1^{\perp}$ of K, we introduce the polynomial edge jump lifting $\mathcal{L}_{\boldsymbol{e}}^{F,E_1^{\perp}}(v^{\mathrm{f}})$ by

$$\mathcal{L}_{\boldsymbol{e}}^{F,E_1^{\perp}}(v^{\mathrm{f}}) := \begin{cases} [\![v^{\mathrm{f}}]\!]_F(x_1^{\perp}, 0, 0)(1 - x_2^{\perp}/b_1^{\perp})(1 - x^{\|}/h^{\|}), & \text{on } K_1, K_2, \\ 0, & \text{on } K. \end{cases} \tag{6.5}$$

Due to Lemma 6.1, $\mathcal{L}_{\boldsymbol{e}}^{F,E_1^{\perp}}(v^{\mathrm{f}}) \in C^0(\overline{K}_1 \cup \overline{K}_2)$. With (6.3) and since $\mathcal{L}_{\boldsymbol{e}}^{F,E_1^{\perp}}(v^{\mathrm{f}})$ is linear in directions of $x_2^{\perp}$ and $x^{\|}$, we have $\mathcal{L}_{\boldsymbol{e}}^{F,E_1^{\perp}}(v^{\mathrm{f}})|_{K_j} \in \mathbb{S}_{\overline{\boldsymbol{p}}_{K_j}}(K_j)$ for $j = 1, 2$. The

lifting reproduces $[\![v^{\mathrm{f}}]\!]_F$ on $E_1^\perp$ and vanishes on the planes $x_2^\perp = b_1^\perp, x^\parallel = h^\parallel$, as well as on the edges $E_1^\parallel, E_2^\parallel$. Moreover, it vanishes identically if $E_1^\perp$ is a Dirichlet boundary edge. A corresponding lifting $\mathcal{L}_{\boldsymbol{e}}^{F,E_2^\perp}(v^{\mathrm{f}})$ can be constructed for the edge $E_2^\perp$. In the geometry of Fig. 4, we then introduce the full edge lifting

$$\mathcal{L}_{\boldsymbol{e}}^{F,E}(v^{\mathrm{f}}) := \sum_{i=1}^{2} \mathcal{L}_{\boldsymbol{e}}^{F,E_i^\perp}(v^{\mathrm{f}}). \tag{6.6}$$

Lemma 6.2 *For $j = 1, 2$, there holds*

$$N_{K_j}^\perp[\mathcal{L}_{\boldsymbol{e}}^{F,E}(v^{\mathrm{f}})]^2 \lesssim |\boldsymbol{p}|^6 \mathfrak{h}_{F_j}^{-1} \|[\![v^{\mathrm{f}}]\!]_{F_j}\|_{L^2(F_j)}^2. \tag{6.7}$$

Proof The proof follows along the lines of Lemma 5.4: The definition (6.5) yields

$$\|\mathcal{L}_{\boldsymbol{e}}^{F,E_i^\perp}(v^{\mathrm{f}})\|_{L^2(K_j)}^2 \lesssim h^\perp h^\parallel \|[\![v^{\mathrm{f}}]\!]_{F_j}\|_{L^2(E_{ij}^\perp)}^2. \tag{6.8}$$

Then, the inequality (5.24) applied on $\overline{E}_{ij}^\perp \subset \overline{F}_j$ in edge-parallel direction implies

$$\|[\![v^{\mathrm{f}}]\!]_{F_j}\|_{L^2(E_{ij}^\perp)}^2 \lesssim |\boldsymbol{p}|^2 (h^\parallel)^{-1} \|[\![v^{\mathrm{f}}]\!]_{F_j}\|_{L^2(F_j)}^2. \tag{6.9}$$

The inverse estimate (5.19), the above bounds and employing that $h^\perp \simeq \mathfrak{h}_{F_j}$ give

$$N_{K_j}^\perp[\mathcal{L}_{\boldsymbol{e}}^{F,E_i^\perp}(v^{\mathrm{f}})]^2 \lesssim |\boldsymbol{p}|^4 (h^\perp)^{-2} \|\mathcal{L}_{\boldsymbol{e}}^{F,E_i^\perp}(v^{\mathrm{f}})\|_{L^2(K_j)}^2 \lesssim |\boldsymbol{p}|^6 \mathfrak{h}_{F_j}^{-1} \|[\![v^{\mathrm{f}}]\!]_{F_j}\|_{L^2(F_j)}^2. \tag{6.10}$$

This implies (6.7). □

Remark 6.3 The lifting $\mathcal{L}_{\boldsymbol{e}}^{F,E}(v^{\mathrm{f}})$ does not generally vanish on $x^\parallel = 0$ and $x^\parallel = h^\parallel$. However, with Assumption 3.1 the constructions of corresponding liftings in adjacent elements will lead to conformity of $v^{\mathrm{f},F,E}$ across $x^\parallel = 0$ and $x^\parallel = h^\parallel$ in edge-perpendicular direction. This will be detailed in Sect. 6.3.

Next, we introduce the auxiliary function

$$v^{\mathrm{f},F,E} := \begin{cases} v^{\mathrm{f}} - \mathcal{L}_{\boldsymbol{e}}^{F,E}(v^{\mathrm{f}}), & \text{on } K_1, K_2, \\ v^{\mathrm{f}}, & \text{on } K. \end{cases} \tag{6.11}$$

Then, $v^{\mathrm{f},F,E} \in C^0(\overline{K}_1 \cup \overline{K}_2)$ and $v^{\mathrm{f},F,E}|_{K_j} \in \mathbb{S}_{\overline{\boldsymbol{p}}_{K_j}}(K_j)$. With (6.1) and as in Lemma 6.1, we have $[\![v^{\mathrm{f},F,E}]\!]_{F_j} \in \mathbb{Q}_{\overline{\boldsymbol{p}}_{K_j,F_j}}(F_j)$ and $[\![v^{\mathrm{f},F,E}]\!]_F \in C^0(\overline{F})$. By construction,

$$[\![v^{\mathrm{f},F,E}]\!]_F = 0 \text{ on } E_i^\perp, \qquad [\![v^{\mathrm{f},F,E}]\!]_F = 0 \text{ on } E_i^\parallel, \qquad i = 1, 2. \tag{6.12}$$

Moreover, we have

$$(\llbracket v^{\mathrm{f},F,E}\rrbracket_{F_j})|_{E^\parallel} \in \mathbb{P}_{\overline{p}_{K_j,E^\parallel}}(E^\parallel), \qquad j=1,2, \tag{6.13}$$

since $\overline{p}_{K_j,E^\parallel} = \overline{p}^{\parallel}_{K_j,F_j}$ by (3.13), $(v^{\mathrm{f}}|_K)_{E^\parallel} \in \mathbb{P}_{\overline{p}^{\parallel}_{K,F}}(E^\parallel)$ and $\overline{p}^{\parallel}_{K,F} \le \overline{p}^{\parallel}_{K_j,F_j}$ by (6.1).

Following [20, Section 5.2.1], we introduce the lifting associated with F by

$$\mathcal{L}_{\boldsymbol{e}}^F(v^{\mathrm{f}}) := \begin{cases} \llbracket v^{\mathrm{f},F,E}\rrbracket_F(x_1^\perp,0,x^\parallel)(1-x_2^\perp/b_1^\perp), & \text{on } K_1,K_2,\\ 0, & \text{on } K, \end{cases} \tag{6.14}$$

with $v^{\mathrm{f},F,E}$ in (6.11). Clearly, $\mathcal{L}_{\boldsymbol{e}}^F(v^{\mathrm{f}}) \in C^0(\overline{K}_1\cup\overline{K}_2)$. Due to (6.12), (6.13), $\mathcal{L}_{\boldsymbol{e}}^F(v^{\mathrm{f}})|_{K_j} \in \mathbb{S}_{\overline{\boldsymbol{p}}_{K_j}}(K_j)$ for $j=1,2$, and $\mathcal{L}_{\boldsymbol{e}}^F(v^{\mathrm{f}})|_F = \llbracket v^{\mathrm{f},F,E}\rrbracket_F$. Moreover, the lifting $\mathcal{L}_{\boldsymbol{e}}^F(v^{\mathrm{f}})$ vanishes on the planes $x_2^\perp = b_1^\perp$, $x_1^\perp = 0$, $x_1^\perp = a_2^\perp$, and $x^\parallel = 0$, $x^\parallel = h^\parallel$.

Lemma 6.4 *For $j=1,2$, there holds*

$$N_{K_j}^\perp[\mathcal{L}_{\boldsymbol{e}}^F(v^{\mathrm{f}})]^2 \lesssim |\boldsymbol{p}|^{10}\mathrm{h}_{F_j}^{-1}\|\llbracket v^{\mathrm{f}}\rrbracket_{F_j}\|^2_{L^2(F_j)}. \tag{6.15}$$

Proof As in (5.49), we have

$$N_{K_j}^\perp[\mathcal{L}_{\boldsymbol{e}}^F(v^{\mathrm{f}})]^2 \lesssim |\boldsymbol{p}|^4\mathrm{h}_{F_j}^{-1}\|\llbracket v^{\mathrm{f},F,E}\rrbracket_{F_j}\|^2_{L^2(F_j)}. \tag{6.16}$$

Then, the trace inequality in Lemma 4.11 implies

$$\mathrm{h}_{F_j}^{-1}\|\llbracket v^{\mathrm{f},F,E}\rrbracket_{F_j}\|^2_{L^2(F_j)} \lesssim \mathrm{h}_{F_j}^{-1}\|\llbracket v^{\mathrm{f}}\rrbracket_{F_j}\|^2_{L^2(F_j)} + N_{K_j}^\perp[\mathcal{L}_{\boldsymbol{e}}^{F,E}(v^{\mathrm{f}})]^2.$$

Referring to (6.7) completes the proof. □

To analyze the lifting (6.14), we introduce the piecewise polynomial function

$$v^{\mathrm{f},F} := \begin{cases} v^{\mathrm{f}} - \mathcal{L}_{\boldsymbol{e}}^{F,E}(v^{\mathrm{f}}) - \mathcal{L}_{\boldsymbol{e}}^F(v^{\mathrm{f}}), & \text{on } K_1,K_2,\\ v^{\mathrm{f}}, & \text{on } K, \end{cases} \tag{6.17}$$

We have $v^{\mathrm{f},F} \in C^0(\overline{K}_1\cup\overline{K}_2)$ and $v^{\mathrm{f},F}|_{K_j} \in \mathbb{S}_{\overline{\boldsymbol{p}}_{K_j}}(K_j)$ for $j=1,2$.

Lemma 6.5 *The function $v^{\mathrm{f},F}$ in (6.17) is continuous across F.*

Proof Consider $\boldsymbol{x} \in F_j$ for $j=1,2$. Then, with the definitions in (6.6), (6.14),

$$\llbracket v^{\mathrm{f},F}\rrbracket_{F_j}(\boldsymbol{x}) = \llbracket v^{\mathrm{f}}\rrbracket_{F_j}(\boldsymbol{x}) - \mathcal{L}_{\boldsymbol{e}}^{F,E}(v^{\mathrm{f}})|_{K_j}(\boldsymbol{x}) - \llbracket v^{\mathrm{f},F,E}\rrbracket_{F_j}(\boldsymbol{x}),$$

with $v^{\mathrm{f},F,E}$ in (6.11). Since $\llbracket v^{\mathrm{f},F,E}\rrbracket_{F_j}(\boldsymbol{x}) = \llbracket v^{\mathrm{f}}\rrbracket_{F_j}(\boldsymbol{x}) - \mathcal{L}_{\boldsymbol{e}}^{F,E}(v^{\mathrm{f}})|_{K_j}(\boldsymbol{x})$, it follows that $\llbracket v^{\mathrm{f},F}\rrbracket_F(\boldsymbol{x}) = \llbracket v^{\mathrm{f},F}\rrbracket_{F_j}(\boldsymbol{x}) = 0$. □

6.2 Isotropic Faces

Isotropic irregular faces appear by subdivision of elemental faces into either *four* or *two* isotropic faces.

6.2.1 Refinement of One Elemental Face into Four Faces

First, we consider the generic configuration in Fig. 5 where the elemental face $F \in \mathcal{F}(K)$ of the outer element K is subdivided into *four* irregular faces $F_j = F_{K_j,K} \in \mathcal{F}(K_j)$, $1 \le j \le 4$, with four elements K_1, K_2, K_3, K_4 in the inner layer. All elements and faces involved are in the same mesh patch and are *isotropic* of mesh size h. As such, the faces F and F_j satisfy (3.31), (3.32). As before, the parameters a_1, a_2, b_1 and c_1, c_2 only depend on σ. We further denote by E_1, E_2, E_3, E_4 the elemental edges of K on $x_2 = 0$; cf. Fig. 5. The elemental vertices of K on $x_2 = 0$ always appear as regular vertex nodes in $\mathcal{N}(\mathcal{M})$. This configuration arises in reference corner mesh patches $\widetilde{\mathcal{M}}_\sigma^{\ell,\boldsymbol{c}}$ or in corner-type submeshes $\widetilde{\mathcal{M}}_\sigma^{\ell,\boldsymbol{ce},\perp}$ of reference corner–edge mesh patches $\widetilde{\mathcal{M}}_\sigma^{\ell,\boldsymbol{ce}}$ with refinement along one or two edges; cf. Fig. 1 and [20, Figures 4, 8 and 10]. Again, two rotated and superimposed configurations of this type can overlap over two of the elements in $\{K_1, K_2, K_3, K_4\}$; cf. Fig. 1 and [20, Figure 4].

From (3.12), we see that

$$\overline{p}^1_{K,F} \le \overline{p}^1_{K_j,F_j}, \qquad \overline{p}^2_{K,F} \le \overline{p}^2_{K_j,F_j}, \qquad 1 \le j \le 4. \tag{6.18}$$

Therefore, as in (6.1), we have

$$(v^{\mathrm{f}}|_K)|_{F_j} \in \mathbb{Q}_{\overline{\boldsymbol{p}}_{K_j,F_j}}(F_j), \qquad [\![v^{\mathrm{f}}]\!]_{F_j} \in \mathbb{Q}_{\overline{\boldsymbol{p}}_{K_j,F_j}}(F_j), \qquad 1 \le j \le 4. \tag{6.19}$$

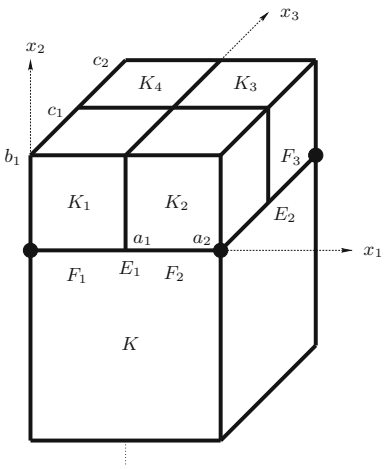

Fig. 5 Interface between K and K_1, K_2, K_3, K_4 for $\sigma = 0.5$. The isotropic irregular faces F_1, F_2, F_3 and the elemental edges E_1, E_2 of K are indicated. The highlighted nodes are regular vertex nodes

As in Sect. 6.1, we define the jump $[\![v^{\mathrm{f}}]\!]_F$ piecewise as

$$\big([\![v^{\mathrm{f}}]\!]_F\big)|_{F_j} := [\![v^{\mathrm{f}}]\!]_{F_j}, \qquad 1 \le j \le 4. \tag{6.20}$$

Lemma 6.6 *In the configuration of Fig. 5, there holds: (i)* $[\![v^{\mathrm{f}}]\!]_F \in C^0(\overline{F})$*; (ii)* $[\![v^{\mathrm{f}}]\!]_F(\boldsymbol{N}_i) = 0$ *at the four elemental vertices* $\boldsymbol{N}_1 = (0,0,0)$*,* $\boldsymbol{N}_2 = (a_2,0,0)$*,* $\boldsymbol{N}_3 = (a_2,0,c_2)$*, and* $\boldsymbol{N}_4 = (0,0,c_2)$*.*

Proof By Theorem 3.12, the approximation v^{f} in (5.53) is continuous over the regular faces F_{K_1,K_2}, F_{K_2,K_3}, F_{K_3,K_4} and F_{K_1,K_4}. As a consequence, we have $[\![v^{\mathrm{f}}]\!]_F \in C^0(\overline{F})$. Since $\{K, K_j\} \in \Delta_{K,\mathcal{N}} = \Delta_{K_j,\mathcal{N}}$ (see (5.5)), the second assertion follows again from the construction of v^{f} and property (5.56). □

We introduce edge liftings associated with the elemental edges E_1, E_2, E_3, E_4 of K. We focus in detail on edge $E_1 = \{(x_1,0,0) : x_1 \in (0,a_2)\} \in \mathcal{E}(K)$ intersecting with F_1, F_2 and K_1, K_2. By writing $\overline{E}_1 = \overline{E}_{11} \cup \overline{E}_{12}$ with $E_{1j} \in \mathcal{E}(K_j)$, $j = 1, 2$, it follows from (3.13), (6.18) that $\overline{p}_{K,E_1} \le \overline{p}_{K_j,E_{1j}}$, $j = 1, 2$. Therefore,

$$(v^{\mathrm{f}}|_K)|_{E_{1j}} \in \mathbb{P}_{\overline{p}_{K_j,E_{1j}}}(E_{1j}), \qquad \big([\![v^{\mathrm{f}}]\!]_{F_j}\big)|_{E_{1j}} \in \mathbb{P}_{\overline{p}_{K_j,E_{1j}}}(E_{1j}), \qquad j = 1, 2. \tag{6.21}$$

We then introduce the polynomial edge jump lifting associated with E_1 by

$$\mathcal{L}_{\boldsymbol{c}}^{F,E_1}(v^{\mathrm{f}}) := \begin{cases} [\![v^{\mathrm{f}}]\!]_F(x_1,0,0)(1-x_2/b_1)(1-x_3/c_1), & \text{on } K_1, K_2, \\ 0, & \text{on } K_3, K_4. \end{cases} \tag{6.22}$$

From Lemma 6.6, $\mathcal{L}_{\boldsymbol{c}}^{F,E_1}(v^{\mathrm{f}}) \in C^0(\cup_{j=1}^4 \overline{K}_j)$. Due to (6.19), (6.21) and since $\mathcal{L}_{\boldsymbol{c}}^{F,E_1}(v^{\mathrm{f}})$ is linear in directions of x_2, x_3, we have $\mathcal{L}_{\boldsymbol{c}}^{F,E_1}(v^{\mathrm{f}})|_{K_j} \in \mathbb{S}_{\overline{\boldsymbol{p}}_{K_j}}(K_j)$ for $1 \le j \le 4$. The lifting reproduces $[\![v^{\mathrm{f}}]\!]_F$ on E_1 and with Lemma 6.6 vanishes on the other edges E_2, E_3, E_4. It also vanishes on $x_2 = b_1$ and $x_3 = c_1$. It vanishes identically if E_1 is a Dirichlet boundary edge. Corresponding liftings $\{\mathcal{L}_{\boldsymbol{c}}^{F,E_i}(v^{\mathrm{f}})\}_{i=2}^4$ can again be constructed for the other edges E_2, E_3, E_4. The full edge lifting is thus defined as

$$\mathcal{L}_{\boldsymbol{c}}^{F,E}(v^{\mathrm{f}}) := \sum_{i=1}^4 \mathcal{L}_{\boldsymbol{c}}^{F,E_i}(v^{\mathrm{f}}). \tag{6.23}$$

Proceeding as in Lemma 6.2 (with isotropic scaling) immediately yields the stability bound

$$N_{K_j}^{\perp}[\mathcal{L}_{\boldsymbol{c}}^{F,E}(v^{\mathrm{f}})]^2 \lesssim |\boldsymbol{p}|^6 \mathfrak{h}_{F_j}^{-1} \|[\![v^{\mathrm{f}}]\!]_{F_j}\|_{L^2(F_j)}^2, \qquad 1 \le j \le 4. \tag{6.24}$$

Remark 6.7 As will be discussed in Sect. 6.3, the conformity of $\mathcal{L}_{\boldsymbol{c}}^{F,E}(v^{\mathrm{f}})$ across outer boundaries of $\{K_1, K_2, K_3, K_4\}$ will follow from the constructions of corresponding liftings in adjacent layers of elements; cf. Remark 6.3.

We next consider the piecewise polynomial function

$$v^{\mathrm{f},F,E} := \begin{cases} v^{\mathrm{f}} - \mathcal{L}_{\boldsymbol{c}}^{F,E}(v^{\mathrm{f}}), & \text{on } K_1, K_2, K_3, K_4, \\ v^{\mathrm{f}}, & \text{on } K. \end{cases} \tag{6.25}$$

Then, $v^{\mathrm{f},F,E} \in C^0(\cup_{j=1}^4 \overline{K}_j)$. and $v^{\mathrm{f},F,E}|_{K_j} \in \mathbb{S}_{\overline{\boldsymbol{p}}_{K_j}}(K_j)$. With (6.18), (6.19) and similarly to Lemma 6.6, we have $[\![v^{\mathrm{f},F,E}]\!]_F \in C^0(\overline{F})$ and $[\![v^{\mathrm{f},F,E}]\!]_{F_j} \in \mathbb{Q}_{\overline{\boldsymbol{p}}_{K_j,F_j}}(F_j)$. Moreover, the analog of property (6.12) holds:

$$[\![v^{\mathrm{f},F,E}]\!]_F = 0 \text{ on } E_i, \qquad 1 \le i \le 4. \tag{6.26}$$

If $E' \in \mathcal{E}(F_j)$ with $E' \cap E_i = \emptyset$ for all $1 \le i \le 4$ (i.e., $E' \in \mathcal{E}(K_j)$ is irregular between K, K_j and situated in the interior of F), we further have

$$([\![v^{\mathrm{f},F,E}]\!]|_{F_j})|_{E'} \in \mathbb{P}_{\overline{p}_{K_j,E'}}(E'), \tag{6.27}$$

since, as in (6.13), $\overline{p}_{K_j,E'} = \overline{p}^k_{K_j,F_j}$ for an index $k = 1, 2$, $(v^{\mathrm{f}}|_K)_{E'} \in \mathbb{P}_{\overline{p}^k_{K,F}}(E')$ and $\overline{p}^k_{K,F} \le \overline{p}^k_{K_j,F_j}$ due to (6.18).

Following [20, Section 5.3.1], we then introduce the lifting over the face F by

$$\mathcal{L}_{\boldsymbol{c}}^F(v^{\mathrm{f}}) := \begin{cases} [\![v^{\mathrm{f},F,E}]\!]_F(x_1, 0, x_3)(1 - x_2/b_1), & \text{on } K_1, K_2, K_3, K_4, \\ 0, & \text{on } K, \end{cases} \tag{6.28}$$

with $v^{\mathrm{f},F,E}$ in (6.25). Then, $\mathcal{L}_{\boldsymbol{c}}^F(v^{\mathrm{f}}) \in C^0(\cup_{j=1}^4 \overline{K}_j)$ and $\mathcal{L}_{\boldsymbol{c}}^F(v^{\mathrm{f}})|_{K_j} \in \mathbb{S}_{\overline{\boldsymbol{p}}_{K_j}}(K_j)$, $1 \le j \le 4$, in view of (6.26), (6.27). The lifting $\mathcal{L}_{\boldsymbol{c}}^F(v^{\mathrm{f}})$ vanishes on $x_2 = b_1$ and over the sets $E_i \times (0, c_1)$, $1 \le i \le 4$. Proceeding as in proof of (6.15) (with isotropic scaling) yields

$$N_{K_j}^{\perp}[\mathcal{L}_{\boldsymbol{c}}^F(v^{\mathrm{f}})]^2 \lesssim |\boldsymbol{p}|^{10} \mathfrak{h}_{F_j}^{-1} \|[\![v^{\mathrm{f}}]\!]_{F_j}\|^2_{L^2(F_j)}, \qquad 1 \le j \le 4. \tag{6.29}$$

Analogously to (6.17), we introduce

$$v^{\mathrm{f},F} := \begin{cases} v^{\mathrm{f}} - \mathcal{L}_{\boldsymbol{c}}^{F,E}(v^{\mathrm{f}}) - \mathcal{L}_{\boldsymbol{c}}^F(v^{\mathrm{f}}), & \text{on } K_1, K_2, K_3, K_4, \\ v^{\mathrm{f}}, & \text{on } K, \end{cases} \tag{6.30}$$

We have $v^{\mathrm{f},F} \in C^0(\cup_{j=1}^4 \overline{K}_j)$ and $v^{\mathrm{f},F}|_{K_j} \in \mathbb{S}_{\overline{\boldsymbol{p}}_{K_j}}(K_j)$ for $1 \le j \le 4$.

The following variant of Lemma 6.5 holds true.

Lemma 6.8 *The approximation $v^{\mathrm{f},F}$ in (6.30) is continuous across F.*

6.2.2 Refinement of Two Elemental Faces into Two Faces

Second, we consider the isotropic configuration depicted in Fig. 6. It involves an element K where *two adjacent elemental faces* $F, F' \in \mathcal{F}(K)$ are subdivided by using isotropic versions of the irregular refinement in Fig. 4, thereby yielding the elements K_1, K_2 and K_1', K_2'.

As in Sect. 6.1, we then introduce the irregular faces $F_j := F_{K_j,K} \in \mathcal{F}(K_j)$ and $F_j' := F_{K_j',K} \in \mathcal{F}(K_j')$ for $j = 1, 2$. Then, $\overline{F} = \overline{F}_1 \cup \overline{F}_2$ and $\overline{F}' = \overline{F}_1' \cup \overline{F}_2'$. In Fig. 6, we further illustrate the elements K_1^D, K_2^D on the diagonal. We consider the elemental edge $E \in \mathcal{E}(K)$ given by

$$E := \{ (x_1, 0, 0) \,:\, 0 < x_1 < a_1 \}. \tag{6.31}$$

All elements are situated in the same mesh patch. This geometry only arises in diagonal elements of corner–edge mesh patches *with simultaneous refinement along two or three edges* $\boldsymbol{e}_i$, with K, K_1^D and K_2^D corresponding to diagonal elements; cf. Fig. 3. With (6.4) and the continuity properties of v^{f}, we have $[\![v^{\mathrm{f}}]\!]_F = [\![v^{\mathrm{f}}]\!]_{F'}$ on $\overline{E}$. However, the edge liftings $\mathcal{L}_{\boldsymbol{e}}^{F,E}(v^{\mathrm{f}})$ over $\mathfrak{d}_{\boldsymbol{e}}^F := \{K, K_1, K_2\}$ associated with F as in (6.5) and $\mathcal{L}_{\boldsymbol{e}}^{F',E}(v^{\mathrm{f}})$ over $\mathfrak{d}_{\boldsymbol{e}}^{F'} =: \{K, K_1', K_2'\}$ associated with F' are *not necessarily* continuous across the regular faces F_{K_j,K_j^D} and F_{K_j',K_j^D} for $j = 1, 2$. To correct for this, we introduce on $\{K_1^D, K_2^D\}$ the additional *diagonal edge lifting*

$$\mathcal{L}_D(v^{\mathrm{f}}) := [\![v^{\mathrm{f}}]\!]_F(x_1, 0, 0)(1 - x_2/b_1)(1 - x_3/c_1), \qquad \text{on } K_1^D, K_2^D. \tag{6.32}$$

This lifting reproduces $[\![v^{\mathrm{f}}]\!]_F$ on $\overline{E}$. Since $[\![v^{\mathrm{f}}]\!]_F(\boldsymbol{N}) = 0$ for $\boldsymbol{N} = (0, 0, 0)$ and $\boldsymbol{N} = (a_1, 0, 0)$, see Lemma 6.1, it vanishes on $\partial K_1^D \cap \{x_1 = 0\}$ and $\partial K_2^D \cap \{x_1 = a_1\}$, implying that it does not affect the values of v^{f} outside the configuration depicted in Fig. 6. We also have $\mathcal{L}_D(v^{\mathrm{f}}) \in C^0(\overline{K}_1^D \cup \overline{K}_2^D)$ and $\mathcal{L}_D(v^{\mathrm{f}})|_{K_j^D} \in \mathbb{S}_{\overline{\boldsymbol{p}}_{K_j^D}}(K_j^D)$ for $j = 1, 2$. As in (6.24), the following (isotropic) stability bound holds:

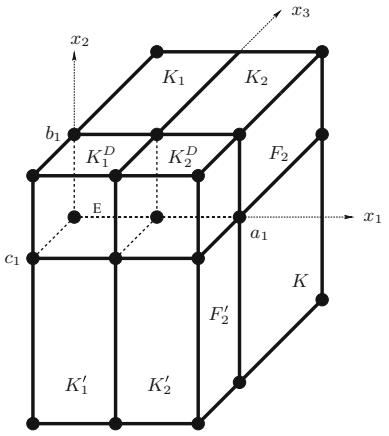

Fig. 6 Two elemental faces $F, F' \in \mathcal{F}(K)$ are irregularly subdivided as in Fig. 4. The elements $K_1, K_2, K_1', K_2', K_1^D, K_2^D$, the irregular faces F_2, F_2' and the elemental edge $E \in \mathcal{E}(K)$ are illustrated. The highlighted nodes are regular vertex nodes

$$N_{K_j^D}^{\perp}[\mathcal{L}_D(v^{\mathrm{f}})]^2 \lesssim |\boldsymbol{p}|^6 \mathfrak{h}_{F_j} \|[\![v^{\mathrm{f}}]\!]\|_{L^2(F_j)}^2, \qquad j = 1, 2. \tag{6.33}$$

Similarly to (6.11) and in the geometry of Fig. 6, we then introduce the auxiliary function

$$v^{\mathrm{f},D} := \begin{cases} v^{\mathrm{f}} - \mathcal{L}_{\boldsymbol{e}}^{F,E}(v^{\mathrm{f}}), & \text{on } K_1, K_2, \\ v^{\mathrm{f}} - \mathcal{L}_{\boldsymbol{e}}^{F',E}(v^{\mathrm{f}}), & \text{on } K_1', K_2', \\ v^{\mathrm{f}} - \mathcal{L}_D(v^{\mathrm{f}}), & \text{on } K_1^D, K_2^D, \\ v^{\mathrm{f}}, & \text{on } K. \end{cases} \tag{6.34}$$

We have $v^{\mathrm{f},D}|_K \in \mathbb{S}_{\overline{\boldsymbol{p}}_K}(K)$ for $K \in \{K_1, K_2, K_1', K_2', K_1^D, K_2^D\}$. Then, since the faces F_{K_i,K_i^D} and F_{K_i',K_i^D} are regularly matching for $i = 1, 2$, the function v^{f} is conforming over these two faces due to Theorem 3.12. From the definition of the liftings it then follows that

$$v^{\mathrm{f},D} \in C^0(\overline{K}_1 \cup \overline{K}_2 \cup \overline{K}_1' \cup \overline{K}_2' \cup \overline{K}_1^D \cup \overline{K}_2^D). \tag{6.35}$$

6.3 Superposition

We superimpose the constructions in Sects. 6.1 and 6.2. Upon employing the patch maps $G_{\mathfrak{p}}$, it is sufficient to consider the geometric reference mesh patches. For $\widetilde{\mathcal{M}} \in \{\widetilde{\mathcal{M}}_\sigma^{\ell,\mathrm{t}}\}_{\mathrm{t}\in\{\boldsymbol{c},\boldsymbol{e},\boldsymbol{ce},\mathrm{int}\}}$, we denote by $\mathfrak{F}_{\boldsymbol{e}}(\widetilde{\mathcal{M}})$ and $\mathfrak{F}_{\boldsymbol{c}}(\widetilde{\mathcal{M}})$ the sets of all *macro-faces* F appearing as in Figs. 4 and 5, respectively. We denote by $\mathfrak{d}_{\boldsymbol{e}}^F = \{K, K_1, K_2\}$, respectively $\mathfrak{d}_{\boldsymbol{c}}^F = \{K, K_1, \dots, K_4\}$, the sets of elements associated with these configurations. The geometry in Fig. 6 involves two isotropic versions of the configuration in Fig. 4. We then denote by $\mathfrak{D}(\widetilde{\mathcal{M}})$ the set of all pairs $D = \{K_1^D, K_2^D\}$ of elements appearing on the diagonal as in Fig. 6.

Let $\mathcal{M}_{\mathfrak{p}} = G_{\mathfrak{p}}(\widetilde{\mathcal{M}})$ be a mesh patch and let $\widetilde{\mathcal{M}} \in \{\widetilde{\mathcal{M}}_\sigma^{\ell,\mathrm{t}}\}_{\mathrm{t}\in\{\boldsymbol{c},\boldsymbol{e},\boldsymbol{ce},\mathrm{int}\}}$ be the corresponding geometric reference mesh patch. The averaged approximations $v^{\mathrm{f}}|_{\mathcal{M}_{\mathfrak{p}}}$ in Theorem 3.12 restricted to the mesh patch $\mathcal{M}_{\mathfrak{p}}$ can be pulled back to the reference patch $\widetilde{\mathcal{M}}$ and will be denoted by $\widetilde{v}^{\mathrm{f}}|_{\widetilde{\mathcal{M}}}$. We now define $\widetilde{v}^{\mathrm{c}}|_{\widetilde{\mathcal{M}}}$ as:

$$\begin{aligned} \widetilde{v}^{\mathrm{c}}|_{\widetilde{\mathcal{M}}} := \widetilde{v}^{\mathrm{f}}|_{\widetilde{\mathcal{M}}} &- \sum_{F\in\mathfrak{F}_{\boldsymbol{e}}(\widetilde{\mathcal{M}})} \big(\mathcal{L}_{\boldsymbol{e}}^{F,E}(\widetilde{v}^{\mathrm{f}}) + \mathcal{L}_{\boldsymbol{e}}^{F}(\widetilde{v}^{\mathrm{f}})\big) \\ &- \sum_{F\in\mathfrak{F}_{\boldsymbol{c}}(\widetilde{\mathcal{M}})} \big(\mathcal{L}_{\boldsymbol{c}}^{F,E}(\widetilde{v}^{\mathrm{f}}) + \mathcal{L}_{\boldsymbol{c}}^{F}(\widetilde{v}^{\mathrm{f}})\big) - \sum_{D\in\mathfrak{D}(\widetilde{\mathcal{M}})} \mathcal{L}_D(\widetilde{v}^{\mathrm{f}}). \end{aligned} \tag{6.36}$$

Here, $\mathcal{L}_{\boldsymbol{e}}^{F,E}(\widetilde{v}^{\mathrm{f}})$ and $\mathcal{L}_{\boldsymbol{e}}^{F}(\widetilde{v}^{\mathrm{f}})$ are the liftings in (6.5), (6.6) and (6.14) associated with the face F and the elements in $\mathfrak{d}_{\boldsymbol{e}}^F$. The liftings $\mathcal{L}_{\boldsymbol{c}}^{F,E}(\widetilde{v}^{\mathrm{f}})$ and $\mathcal{L}_{\boldsymbol{c}}^{F}(\widetilde{v}^{\mathrm{f}})$ are given in (6.22), (6.23) and (6.28) with respect to the set $\mathfrak{d}_{\boldsymbol{c}}^F$. Finally, $\mathcal{L}_D(\widetilde{v}^{\mathrm{f}})$ are liftings as in (6.32) over the element pairs $D = \{K_1^D, K_2^D\}$ depicted in Fig. 6.

Remark 6.9 The liftings $\mathcal{L}_{\boldsymbol{e}}^{F}(\widetilde{v}^{\mathrm{f}})$, $\mathcal{L}_{\boldsymbol{c}}^{F}(\widetilde{v}^{\mathrm{f}})$ and $\mathcal{L}_D(\widetilde{v}^{\mathrm{f}})$ in (6.36) are locally supported and vanish at the patch interfaces of $\widetilde{\mathcal{M}}$. Hence, they do not affect inter-patch continuity.

For $\mathcal{M}_\mathfrak{p} = G_\mathfrak{p}(\widetilde{\mathcal{M}})$, we then set $v^\mathrm{c}|_{\mathcal{M}_\mathfrak{p}} = \widetilde{v}^\mathrm{c}|_{\widetilde{\mathcal{M}}} \circ G_\mathfrak{p}^{-1}|_{Q_\mathfrak{p}}$. This gives rise to a finite element function $v^\mathrm{c} \in \overline{V}^{\ell,0}_{\sigma,\mathfrak{s}}$. The approximation v^c belongs in fact to the conforming space $V^{\ell,1}_{\sigma,\mathfrak{s}}$, as we show in two steps.

Lemma 6.10 *The approximation v^c vanishes on all Dirichlet boundary faces and is continuous across adjacent mesh patches.*

Proof Since $\widetilde{v}^\mathrm{f}$ and the liftings $\mathcal{L}_{\boldsymbol{e}}^{F,E}(\widetilde{v}^\mathrm{f})$, $\mathcal{L}_{\boldsymbol{c}}^{F,E}(\widetilde{v}^\mathrm{f})$ in (6.36) vanish on patch faces corresponding to Dirichlet boundary faces, it follows with Remark 6.9 that $\widetilde{v}^\mathrm{c}$ vanishes on Dirichlet boundary faces. The approximation v^f is conforming across adjacent mesh patches; see Theorem 3.12. Similarly, from Assumption 3.1 and the continuity properties of v^f, we conclude that mapped versions of the liftings $\mathcal{L}_{\boldsymbol{e}}^{F,E}(\widetilde{v}^\mathrm{f})$ and $\mathcal{L}_{\boldsymbol{c}}^{F,E}(\widetilde{v}^\mathrm{f})$ in (6.36) yield conforming approximations over the corresponding mesh layers across two matching irregular configurations of two adjacent mesh patches. With Remark 6.9, this implies inter-patch continuity. □

We next establish the inner-patch continuity of v^c.

Lemma 6.11 *On each mesh patch $\mathcal{M}_\mathfrak{p}$, the approximation $v^\mathrm{c}|_{\mathcal{M}_\mathfrak{p}}$ is continuous across all faces within $\mathcal{M}_\mathfrak{p}$.*

Proof Since $\mathcal{M}_\mathfrak{p} = G_\mathfrak{p}(\widetilde{\mathcal{M}})$ for $\widetilde{\mathcal{M}} \in \{\widetilde{\mathcal{M}}_\sigma^{\ell,\mathfrak{t}}\}_{\mathfrak{t}\in\{\boldsymbol{c},\boldsymbol{e},\boldsymbol{ce},\mathrm{int}\}}$, upon mapping it is sufficient to verify separately the continuity of $\widetilde{v}^\mathrm{c}$ in (6.36) for each reference mesh patch type. Note that $\widetilde{v}^\mathrm{f}$ is continuous over all regular faces where no additional jump liftings are necessary; cf. Theorem 3.12.

Interior patches: By construction, only regular faces arise in an interior patch $\widetilde{\mathcal{M}} = \widetilde{\mathcal{M}}_\sigma^{\ell,\mathrm{int}}$. That is, $\mathfrak{F}_{\boldsymbol{e}}(\widetilde{\mathcal{M}}) = \mathfrak{F}_{\boldsymbol{c}}(\widetilde{\mathcal{M}}) = \mathfrak{D}(\widetilde{\mathcal{M}}) = \emptyset$ in (6.36). Hence, $\widetilde{v}^\mathrm{c}|_{\widetilde{\mathcal{M}}} = \widetilde{v}^\mathrm{f}|_{\widetilde{\mathcal{M}}}$ and the inner-patch continuity follows.

Edge patches: For $\widetilde{\mathcal{M}} = \widetilde{\mathcal{M}}_\sigma^{\ell,\boldsymbol{e}}$, we have $\mathfrak{F}_{\boldsymbol{e}}(\widetilde{\mathcal{M}}) \neq \emptyset$ and $\mathfrak{F}_{\boldsymbol{c}}(\widetilde{\mathcal{M}}) = \mathfrak{D}(\widetilde{\mathcal{M}}) = \emptyset$. In each of the $\ell - 1$ outermost layers of the patch, the definition (6.36) involves two rotated and overlapping versions of the anisotropic irregular configurations in Fig. 4, along a common edge corresponding to $E_1^\parallel$ or $E_2^\parallel$ in Fig. 4; cf. Fig. 1 and [20, Figure 2]. Let then F be an irregular face in the patch. By the properties of the liftings $\mathcal{L}_{\boldsymbol{e}}^{F,E}(\widetilde{v}^\mathrm{f})$ and $\mathcal{L}_{\boldsymbol{e}}^{F}(\widetilde{v}^\mathrm{f})$, the jump $[\![\widetilde{v}^\mathrm{c}]\!]_F$ coincides with $[\![\widetilde{v}^{\mathrm{f},F}]\!]_F$, where $\widetilde{v}^{\mathrm{f},F}$ is defined in (6.17) over the elements $\mathfrak{d}_{\boldsymbol{e}}^F$ associated with F. Then Lemma 6.5 ensures the conformity across the irregular face F.

Corner patches: For $\widetilde{\mathcal{M}} = \widetilde{\mathcal{M}}_\sigma^{\ell,\boldsymbol{c}}$, there holds $\mathfrak{F}_{\boldsymbol{e}}(\widetilde{\mathcal{M}}) = \mathfrak{D}(\widetilde{\mathcal{M}}) = \emptyset$. As before, in each of the $\ell - 1$ outermost layers in the patch, the definition (6.36) yields three rotated and superimposed versions of the geometry in Fig. 5, along edges corresponding to E_i in Fig. 5; cf. Fig. 1 and [20, Figure 4]. If two geometries are superposed over such an edge E_i, the continuity properties of $\widetilde{v}^\mathrm{f}$ imply that the corresponding edge liftings $\mathcal{L}_{\boldsymbol{c}}^{F,E_i}(\widetilde{v}^\mathrm{f})$ defined as in (6.22) from within each of the two configurations coincide on E_i; cf. [20, Lemma 5.10]. If F is now an irregular face in the patch, then $[\![\widetilde{v}^\mathrm{c}]\!]_F$ is equal to $[\![\widetilde{v}^{\mathrm{f},F}]\!]_F$, where $\widetilde{v}^{\mathrm{f},F}$ is defined in (6.30) in terms of liftings $\mathcal{L}_{\boldsymbol{c}}^{F,E}(\widetilde{v}^\mathrm{f})$ and $\mathcal{L}_{\boldsymbol{c}}^{F}(\widetilde{v}^\mathrm{f})$ over the elements $\mathfrak{d}_{\boldsymbol{c}}^F$ associated with F. Lemma 6.8 yields conformity across F.

Corner–edge patches with refinement along one edge: Note that $\mathfrak{D}(\widetilde{\mathcal{M}}) = \emptyset$ in (6.36). We then use the representation (4.19)–(4.22) in Sect. 4.3.2. In each edge-patch block $\widetilde{\Psi}^{\ell',\boldsymbol{ce}}(\widetilde{\mathcal{M}}_\sigma^{\ell',\boldsymbol{e}})$, $2 \le \ell' \le \ell$, the definition (6.36) activates the edge-patch

liftings $\mathcal{L}_{\boldsymbol{e}}^{F,E}(\widetilde{v}^{\mathrm{f}})$ and $\mathcal{L}_{\boldsymbol{e}}^{F}(\widetilde{v}^{\mathrm{f}})$ as above; thereby ensuring conformity across irregular faces F within each of these blocks due to Lemma 6.5. In edge-perpendicular direction, the isotropic mesh $\widetilde{\mathfrak{S}}_{\sigma}^{\ell,\boldsymbol{ce},\perp} \dot{\cup} \widetilde{\mathcal{D}}_{\sigma}^{\ell,\boldsymbol{ce}}$ consists of two sequences of $\ell-1$ irregular and overlapping configurations as in Fig. 5, with the smallest configuration extending into the corner mesh $\widetilde{\mathfrak{T}}_{\sigma}^{\ell,\boldsymbol{c}}$; see Fig. 2. The approximation $\widetilde{v}^{\mathrm{c}}$ in (6.36) then invokes the corner-patch liftings $\mathcal{L}_{\boldsymbol{c}}^{F,E}(\widetilde{v}^{\mathrm{f}})$ and $\mathcal{L}_{\boldsymbol{c}}^{F}(\widetilde{v}^{\mathrm{f}})$, which, as in the corner patch case, enforce the continuity across irregular faces in $\widetilde{\mathfrak{S}}_{\sigma}^{\ell,\boldsymbol{ce},\perp} \dot{\cup} \widetilde{\mathcal{D}}_{\sigma}^{\boldsymbol{ce}}$ and from $\widetilde{\mathfrak{S}}_{\sigma}^{\ell,\boldsymbol{ce},\perp}$ into $\widetilde{\mathfrak{T}}_{\sigma}^{\ell,\boldsymbol{c}}$; cf. Lemma 6.8. The edge jump liftings $\mathcal{L}_{\boldsymbol{c}}^{F,E}(\widetilde{v}^{\mathrm{f}})$ and $\mathcal{L}_{\boldsymbol{e}}^{F,E}(\widetilde{v}^{\mathrm{f}})$ result in approximations which are conforming across edge-perpendicular faces of diagonal elements into the corresponding elements of $\widetilde{\mathcal{M}}_{\sigma}^{\ell,\boldsymbol{ce},\parallel}$ (for example, across the regular faces $f_{K_4',K_4''}$ and $f_{K_6',K_6''}$ in Fig. 2 (right)). Similarly, they yield continuous approximations from corner elements in $\widetilde{\mathfrak{T}}_{\sigma}^{\ell,\boldsymbol{c}}$ into elements in $\Psi^{2,\boldsymbol{ce}}(\widetilde{\mathcal{M}}_{\sigma}^{2,\boldsymbol{e}})$.

Corner–edge patches with refinement along two edges: We now have $\mathfrak{D}(\widetilde{\mathcal{M}}) \neq \emptyset$, as the refinements toward two edges introduce the geometric situation analyzed in Fig. 6 over the diagonal elements in $\widetilde{\mathcal{D}}_{\sigma}^{\ell,\boldsymbol{ce}_1} \cap \widetilde{\mathcal{D}}_{\sigma}^{\ell,\boldsymbol{ce}_2}$ (e.g., over K_6, K_6' in Fig. 3 (left)). We use the representation (4.24), (4.25) in Sect. 4.3.3. In the submeshes $\widetilde{\mathcal{M}}_{\sigma}^{\ell,\boldsymbol{ce}_1,\parallel}$ and $\widetilde{\mathcal{M}}_{\sigma}^{\ell,\boldsymbol{ce}_2,\parallel}$, the liftings $\mathcal{L}_{\boldsymbol{e}}^{F,E}(\widetilde{v}^{\mathrm{f}})$ and $\mathcal{L}_{\boldsymbol{e}}^{F}(\widetilde{v}^{\mathrm{f}})$ are again activated and ensure the continuity over edge-parallel anisotropic faces. Similarly, the liftings $\mathcal{L}_{\boldsymbol{c}}^{F,E}(\widetilde{v}^{\mathrm{f}})$ and $\mathcal{L}_{\boldsymbol{c}}^{F}(\widetilde{v}^{\mathrm{f}})$ yield continuity across the irregular faces in $\widetilde{\mathfrak{S}}_{\sigma}^{\ell,\boldsymbol{ce},\perp} \dot{\cup} (\widetilde{\mathcal{D}}_{\sigma}^{\ell,\boldsymbol{ce}_1} \cup \widetilde{\mathcal{D}}_{\sigma}^{\ell,\boldsymbol{ce}_2})$ in perpendicular direction and from $\widetilde{\mathfrak{S}}_{\sigma}^{\ell,\boldsymbol{ce},\perp}$ into the corner elements in $\widetilde{\mathfrak{T}}_{\sigma}^{\ell,\boldsymbol{c}}$. In addition to $\mathcal{L}_{\boldsymbol{e}}^{F,E}(\widetilde{v}^{\mathrm{f}})$, $\ell-1$ versions of the liftings $\mathcal{L}_{D}(\widetilde{v}^{\mathrm{f}})$ in (6.32) are invoked in (6.36) (e.g., from K_6 into $D=\{K_3', K_6'\}$ in Fig. 3 (left), where element K_3' (unlabelled in the figure) is situated underneath element K_6'). In the configuration closest to $\boldsymbol{c}$, these liftings extend into two corner elements of $\widetilde{\mathfrak{T}}_{\sigma}^{\ell,\boldsymbol{c}}$. With (6.35), this procedure ensures continuity over diagonal elements along the edges. In perpendicular direction, the edge jump liftings $\mathcal{L}_{\boldsymbol{c}}^{F,E}(\widetilde{v}^{\mathrm{f}})$ and $\mathcal{L}_{\boldsymbol{e}}^{F,E}(\widetilde{v}^{\mathrm{f}})$ give conforming approximations across faces of diagonal elements into the corresponding elements in the edge-patch blocks (e.g., across the regular faces $F_{K_1',K_1''}$ or $F_{K_4',K_4''}$ in Fig. 3 (left)), as well as from $\widetilde{\mathfrak{T}}_{\sigma}^{\ell,\boldsymbol{c}}$ into elements in $\Psi^{2,\boldsymbol{ce}_i}(\widetilde{\mathcal{M}}_{\sigma}^{2,\boldsymbol{e}_i})$ for $i=1,2$.

Corner–edge patches with refinement along three edges: Clearly, $\mathfrak{D}(\widetilde{\mathcal{M}}) \neq \emptyset$. With (4.27), the geometric situation in Fig. 6 now appears along three edges on the diagonal elements in $\widetilde{\mathcal{D}}_{\sigma}^{\ell,\boldsymbol{ce}_1} \cap \widetilde{\mathcal{D}}_{\sigma}^{\ell,\boldsymbol{ce}_2}$, $\widetilde{\mathcal{D}}_{\sigma}^{\ell,\boldsymbol{ce}_2} \cap \widetilde{\mathcal{D}}_{\sigma}^{\ell,\boldsymbol{ce}_3}$, and $\widetilde{\mathcal{D}}_{\sigma}^{\ell,\boldsymbol{ce}_1} \cap \widetilde{\mathcal{D}}_{\sigma}^{\ell,\boldsymbol{ce}_3}$ (e.g., over the element pairs $\{K_1, K_1'\}$, $\{K_4, K_4'\}$ and $\{K_6, K_6'\}$ in Fig. 3 (right)). Isotropic irregular faces as in Fig. 5 are not present in this case (i.e., $\mathfrak{F}_{\boldsymbol{c}}(\widetilde{\mathcal{M}}) = \emptyset$). Hence, in (6.36), only the liftings $\mathcal{L}_{\boldsymbol{e}}^{F,E}(\widetilde{v}^{\mathrm{f}})$, $\mathcal{L}_{\boldsymbol{e}}^{F}(\widetilde{v}^{\mathrm{f}})$ and $\mathcal{L}_{D}(\widetilde{v}^{\mathrm{f}})$ in (6.32) are active. The liftings $\mathcal{L}_{D}(\widetilde{v}^{\mathrm{f}})$ extend into the corner elements in $\widetilde{\mathfrak{T}}_{\sigma}^{\ell,\boldsymbol{c}}$. Property (6.35) then ensures the continuity over diagonal elements and into $\widetilde{\mathfrak{T}}_{\sigma}^{\ell,\boldsymbol{c}}$. □

We now complete the proof of Theorem 3.14 in Sect. 3.4.

Proof of Theorem 3.14 We set $\mathcal{L}_{\sigma,\mathfrak{s}}^{\ell}(v^{\mathrm{f}}) := v^{\mathrm{c}}$, with v^{c} defined above. By construction, $\mathcal{L}_{\sigma,\mathfrak{s}}^{\ell}$ is linear and reproduces functions in $V_{\sigma,\mathfrak{s}}^{\ell,1}$. Lemmas 6.11 and 6.10 imply

$v^{\mathrm{c}} \in V^{\ell,1}_{\sigma,\mathfrak{s}}$. From (6.36) and the properties of the liftings, we further find that

$$\Upsilon^{\perp}_{\widetilde{\mathcal{M}}}[\widetilde{v}^{\mathrm{f}} - \widetilde{v}^{\mathrm{c}}]^2 \lesssim \sum_{F\in\mathfrak{F}_{\boldsymbol{e}}(\widetilde{\mathcal{M}})} \big(\Upsilon^{\perp}_{\mathfrak{d}^F_{\boldsymbol{e}}}[\mathcal{L}^{F,E}_{\boldsymbol{e}}(\widetilde{v}^{\mathrm{f}})]^2 + \Upsilon^{\perp}_{\mathfrak{d}^F_{\boldsymbol{e}}}[\mathcal{L}^{F}_{\boldsymbol{e}}\widetilde{v}^{\mathrm{f}})]^2\big) + \sum_{F\in\mathfrak{F}_{\boldsymbol{c}}(\widetilde{\mathcal{M}})} \big(\Upsilon^{\perp}_{\mathfrak{d}^F_{\boldsymbol{c}}}[\mathcal{L}^{F,E}_{\boldsymbol{c}}(\widetilde{v}^{\mathrm{f}})]^2 + \Upsilon^{\perp}_{\mathfrak{d}^F_{\boldsymbol{c}}}[\mathcal{L}^{F}_{\boldsymbol{c}}(\widetilde{v}^{\mathrm{f}})]^2\big) + \sum_{D\in\mathfrak{D}(\widetilde{\mathcal{M}})} \Upsilon^{\perp}_{D}[\mathcal{L}_D(\widetilde{v}^{\mathrm{f}})]^2,$$

for any geometric reference mesh patch $\widetilde{\mathcal{M}}$. The stability estimates (6.7), (6.15) for $\mathcal{L}^{F,E}_{\boldsymbol{e}}(\widetilde{v}^{\mathrm{f}})$ and $\mathcal{L}^{F}_{\boldsymbol{e}}(\widetilde{v}^{\mathrm{f}})$, the estimates (6.24), (6.29) for $\mathcal{L}^{F,E}_{\boldsymbol{c}}(\widetilde{v}^{\mathrm{f}})$ and $\mathcal{L}^{F}_{\boldsymbol{c}}(\widetilde{v}^{\mathrm{f}})$, and the bound (6.33) for $\mathcal{L}_D(\widetilde{v}^{\mathrm{f}})$ finally yield

$$\Upsilon^{\perp}_{\widetilde{\mathcal{M}}}[\widetilde{v}^{\mathrm{f}} - \widetilde{v}^{\mathrm{c}}]^2 \lesssim |\boldsymbol{p}|^{10}\mathrm{jmp}_{\mathcal{F}^{\parallel}_{l}(\widetilde{\mathcal{M}})}[\widetilde{v}^{\mathrm{f}}]^2, \tag{6.37}$$

where $\mathcal{F}^{\parallel}_{l}(\widetilde{\mathcal{M}})$ denotes the interior faces on $\widetilde{\mathcal{M}}$ which satisfy (3.31), (3.32). After mapping to the physical patches and summing over all patches, this implies the bound (3.46). □

7 Conclusions

We established the H^1-norm exponential convergence rate $\exp(-b\sqrt[5]{N})$ of conforming hp-FEMs in axiparallel polyhedral domains $\Omega \subset \mathbb{R}^3$. The FE spaces are based on σ-geometric mesh families $\mathfrak{M}_\sigma$ of hexahedral elements containing, in general, irregular faces and edges. Geometric meshes $\mathcal{M} \in \mathfrak{M}_\sigma$ are obtained as finite unions of *four types* $\mathrm{t} \in \{\boldsymbol{c}, \boldsymbol{e}, \boldsymbol{ce}, \mathrm{int}\}$ *of* σ*-geometric reference geometric mesh patches* $\widetilde{\mathcal{M}}^{\ell,\mathrm{t}}_{\sigma}$. The hp-version FE spaces allow for anisotropic elemental polynomial degree distributions with $\mathfrak{s}$-linear growth in terms of the logarithmic element distance to the singularity set $\mathcal{S}$ of Ω. General subdivision ratios $0 < \sigma < 1$ and slope parameters $\mathfrak{s} > 0$ are admitted (the analysis extends in a straightforward fashion also to *directional slope parameters* $\mathfrak{s}^{\parallel}$ *and* $\mathfrak{s}^{\perp}$). Inter-patch mesh compatibility is ensured by a compatibility requirement on the patch maps, and inter-element continuity is ensured by a minimum degree rule on the local polynomial spaces.

Our principal technical contributions are the constructions of hp-version quasi-interpolation operators, which can be assembled from *four types of reference patch quasi-interpolants* $\widetilde{\Pi}^{\ell,1,\mathrm{t}}_{\sigma,\mathfrak{s}}$ which are well defined on $H^1(\widetilde{Q})$ and exponentially consistent in the H^1-norm for functions $\widetilde{u}$ belonging to an analytic reference class $B_{\mathrm{t}}(\widetilde{Q})$, with weighting toward corners and edges of $\widetilde{Q}$ according to the patch type $\mathrm{t} \in \{\boldsymbol{c}, \boldsymbol{e}, \boldsymbol{ce}, \mathrm{int}\}$. Analogous L^2-norm error bounds for L^2-projections for the approximation of solutions in $B_{-\boldsymbol{b}}(\Omega)$ are also obtained.

We considered the particular, second-order model elliptic problem (1.1)–(1.3) for which analytic regularity was established in [5]. The presently proved exponential convergence rate estimates are, however, independent of the particular PDE and apply to any elliptic problem which admits an analytic regularity shift in the analytic classes $B_{-1-\boldsymbol{b}}(\Omega)$ in Definition 2.1. The present results extend also to hp-FE spaces which enforce conformity by the maximum degree rule. They also imply exponential bounds

$d_N(\mathcal{K},\mathcal{X}) \lesssim \exp(-b\sqrt[5]{N})$ on the Kolmogorov N-widths $d_N(\mathcal{K},\mathcal{X})$ of the analytic classes $\mathcal{K} = B_{-1-\boldsymbol{b}}(\Omega) \cap H^{1+\theta}(\Omega)$ which are compact subsets of the Hilbert space $\mathcal{X} = H^1(\Omega)$. This bound is of interest in connection with reduced basis approximations generated by greedy algorithms in $\mathcal{X}$. We refer to [4] for theory, and to [17] for recent developments for elliptic problems.

8 Appendix: Proof of Theorem 4.3

We outline the major steps of the proof of Theorem 4.3.

8.1 Approximation Results

We first establish auxiliary approximation results.

8.1.1 Univariate Approximation Properties

The following consistency bound holds for the H^1-projector $\pi_{p,1}$ in (4.1) on $\widehat{I} = (-1, 1)$; see [26, Corollary 3.15].

Lemma 8.1 *Let $p \geq 1$, $\widehat{u} \in H^{s+1}(\widehat{I})$ and $0 \leq s \leq p$. Then there holds*

$$\|\widehat{u} - \widehat{\pi}_{p,1}\widehat{u}\|^2_{H^1(\widehat{I})} \lesssim \Psi_{p,s}\|\widehat{u}^{(s+1)}\|^2_{L^2(\widehat{I})}. \tag{8.1}$$

Here,

$$\Psi_{q,r} := \frac{\Gamma(q+1-r)}{\Gamma(q+1+r)}, \qquad 0 \leq r \leq q, \tag{8.2}$$

where Γ is the Gamma function satisfying $\Gamma(m+1) = m!$ for any $m \in \mathbb{N}_0$.

The subsequent H^1-norm error bound holds for the L^2-projection $\widehat{\pi}_{p,0}$ (see also [26, Theorem 3.11] for p-optimal bounds).

Lemma 8.2 *Let $p \geq 1$, $\widehat{u} \in H^{s+1}(\widehat{I})$ and $0 \leq s \leq p$. Then there holds*

$$\|\widehat{u} - \widehat{\pi}_{p,0}\widehat{u}\|^2_{H^1(\widehat{I})} \lesssim p^4\Psi_{p,s}\|\widehat{u}^{(s+1)}\|^2_{L^2(\widehat{I})}\,. \tag{8.3}$$

Proof We recall from [25, Lemma 5.1] that

$$\|(\widehat{\pi}_{p,0}\widehat{u})^{(s)}\|_{L^2(\widehat{I})} \lesssim \max\{1, p\}^{2s}\|\widehat{u}^{(s)}\|_{L^2(\widehat{I})}, \qquad p \geq 0,\ s \geq 0. \tag{8.4}$$

With (8.4) and for $p \geq 1$, we find that

$$\begin{aligned}\|\widehat{u} - \widehat{\pi}_{p,0}\widehat{u}\|_{H^1(\widehat{I})} &\leq \|\widehat{u} - \widehat{\pi}_{p,1}\widehat{u}\|_{H^1(\widehat{I})} + \|\widehat{\pi}_{p,0}(\widehat{u} - \widehat{\pi}_{p,1}\widehat{u})\|_{H^1(\widehat{I})} \\ &\lesssim p^2\|\widehat{u} - \widehat{\pi}_{p,1}\widehat{u}\|_{H^1(\widehat{I})}.\end{aligned}$$

Referring to (8.1) yields (8.3). □

8.1.2 Approximation Properties of $\widehat{\pi}_{\boldsymbol{p},r}$

We next derive approximation results for the tensor projectors in (4.3). On $\widehat{K} = \widehat{I}^3$, we introduce the tensor-product space

$$H^1_{\mathrm{mix}}(\widehat{K}) := H^1_{\mathrm{mix}}(\widehat{K}^\perp) \otimes H^1(\widehat{K}^\parallel) := H^1(\widehat{I}) \otimes H^1(\widehat{I}) \otimes H^1(\widehat{I}). \tag{8.5}$$

endowed with the standard (tensor-product) norm $\|\cdot\|_{H^1_{\mathrm{mix}}(\widehat{K})}$. Let $K = K^\perp \otimes K^\perp$ be an axiparallel element, $\boldsymbol{p}_K = (p_K^\perp, p_K^\parallel)$ an elemental degree vector and $r_K \in \{0, 1\}$ an elemental conformity index in edge-parallel direction. For $u : K \to \mathbb{R}$, we denote by $\widehat{u} := u \circ \Phi_K$ the pullback to the reference element $\widehat{K}$. In this setting, the tensor projection $\widehat{\pi}_{\boldsymbol{p}_K,r_K}\widehat{u} = \widehat{\pi}^\perp_{p_K^\perp,0} \otimes \widehat{\pi}^\parallel_{p_K^\parallel,r_K}\widehat{u}$ defined in (4.3) satisfies the subsequent bounds.

Proposition 8.3 *The error $\widehat{\eta}_0^\perp = \widehat{u} - \widehat{\pi}^\perp_{p_K^\perp,0}\widehat{u}$ in edge-perpendicular direction satisfies*

$$\|\widehat{\eta}_0^\perp\|^2_{H^1_{\mathrm{mix}}(\widehat{K})} \lesssim (p_K^\perp)^8 \Psi_{p_K^\perp,s_K^\perp} E^\perp_{s_K^\perp}(K;u), \tag{8.6}$$

for any $0 \le s_K^\perp \le p_K^\perp$, with

$$E^\perp_s(K;u) := \sum_{|\boldsymbol{\alpha}^\perp|=s+1}^{s+2} \sum_{\alpha^\parallel=0,1} (h_K^\perp)^{2|\boldsymbol{\alpha}^\perp|-2} (h_K^\parallel)^{2\alpha^\parallel-1} \|\mathsf{D}_\perp^{\boldsymbol{\alpha}^\perp} \mathsf{D}_\parallel^{\alpha^\parallel} u\|^2_{L^2(K)}. \tag{8.7}$$

The error $\widehat{\eta}^\parallel = \widehat{u} - \widehat{\pi}_{p_K^\parallel,r_K}\widehat{u}$ in edge-parallel direction satisfies

$$\|\widehat{\mathsf{D}}_\perp^{\boldsymbol{\alpha}^\perp} \widehat{\mathsf{D}}_\parallel^{\alpha^\parallel} \widehat{\eta}^\parallel\|^2_{L^2(\widehat{K})} \lesssim_p \Psi_{p_K^\parallel,s_K^\parallel} (h_K^\perp)^{2|\boldsymbol{\alpha}^\perp|-2} (h_K^\parallel)^{2s_K^\parallel+1} \|\mathsf{D}_\perp^{\boldsymbol{\alpha}^\perp} \mathsf{D}_\parallel^{s_K^\parallel+1} u\|^2_{L^2(K)}, \tag{8.8}$$

for any $r_K = 0, 1$, $|\boldsymbol{\alpha}^\perp| \ge 0$, $\alpha^\parallel = 0, 1$, and $0 \le s_K^\parallel \le p_K^\parallel$.

Proof We have

$$\widehat{\eta}_0^\perp = \widehat{u} - \widehat{\pi}^{(1)}_{p_K^\perp,0} \otimes \widehat{\pi}^{(2)}_{p_K^\perp,0}\widehat{u} = (\widehat{u} - \widehat{\pi}^{(1)}_{p_K^\perp,0}\widehat{u}) + \widehat{\pi}^{(1)}_{p_K^\perp,0}\left(\widehat{u} - \widehat{\pi}^{(2)}_{p_K^\perp,0}\widehat{u}\right).$$

Hence, by the triangle inequality and the stability property (8.4) of the univariate L^2-projector $\widehat{\pi}^{(1)}_{p_K^\perp,0}$, we find

$$\|\widehat{\eta}_0^\perp\|^2_{H^1_{\mathrm{mix}}(\widehat{K})} \lesssim (p_K^\perp)^4 \Big(\sum_{i=1}^{2} \|\widehat{u} - \widehat{\pi}^{(i)}_{p_K^\perp,0}\widehat{u}\|^2_{H^1_{\mathrm{mix}}(\widehat{K})} \Big).$$

The univariate approximation properties (8.3) in Lemma 8.2 now imply

$$\|\widehat{\eta}_0^{\perp}\|^2_{H^1_{\mathrm{mix}}(\widehat{K})} \lesssim (p_K^{\perp})^8 \Psi_{p_K^{\perp},s_K^{\perp}}\Big(\sum_{0\le\alpha_2^{\perp},\alpha^{\parallel}\le 1} \|\widehat{\mathsf{D}}^{(s_K^{\perp}+1,\alpha_2^{\perp},\alpha^{\parallel})}\widehat{u}\|^2_{L^2(\widehat{K})} + \sum_{0\le\alpha_1^{\perp},\alpha^{\parallel}\le 1} \|\widehat{\mathsf{D}}^{(\alpha_1^{\perp},s_K^{\perp}+1,\alpha^{\parallel})}\widehat{u}\|^2_{L^2(\widehat{K})}\Big),$$

for any $0 \le s_K^{\perp} \le p_K^{\perp}$ and where we write $\mathsf{D}^{\boldsymbol{\alpha}} = \mathsf{D}^{(\alpha_1,\alpha_2,\alpha_3)}$ for a multi-index $\boldsymbol{\alpha} = (\alpha_1, \alpha_2, \alpha_3)$. This bound and a scaling argument as in [24, Section 5.1.4] yield the desired bound (8.6) for $\widehat{\eta}_0^{\perp}$.

The bound for $\widehat{\eta}^{\parallel}$ is an immediate consequence of the consistency bounds (8.1) ($r_K = 1$) and (8.3) ($r_K = 0$) applied in edge-parallel direction, combined again with a scaling argument as in [24, Section 5.1.4]. □

8.1.3 Weighted Norm Estimates in Plane Domains

In plane domains perpendicular to edges, we shall use estimates in weighted spaces analogous to those in [13, Section 3]. To state them, let $\mathfrak{K}$ be an axiparallel and shape-regular rectangle of diameter $h_{\mathfrak{K}}$ which is affinely equivalent to the reference square $\widehat{\mathfrak{K}} = \widehat{I}^2$. Let $\boldsymbol{c}$ be a corner of $\mathfrak{K}$ and set $r(\boldsymbol{x}) = |\boldsymbol{x} - \boldsymbol{c}|$. For a weight exponent $\beta \in [0, 1)$, we denote by $L^2_\beta(\mathfrak{K})$ the weighted L^2-space endowed with the weighted norm $\|u\|_{L^2_\beta(\mathfrak{K})} := \|r^\beta u\|_{L^2(\mathfrak{K})}$. For $m = 1, 2$, the weighted Sobolev space $H^{m,m}_\beta(\mathfrak{K})$ is defined as the completion of all $C^\infty(\overline{\mathfrak{K}})$-functions with respect to the norm $\|u\|^2_{H^{m,m}_\beta(\mathfrak{K})} := \|u\|^2_{H^{m-1}(\mathfrak{K})} + |u|^2_{H^{m,m}_\beta(\mathfrak{K})}$, where $|u|^2_{H^{m,m}_\beta(\mathfrak{K})} := \sum_{|\boldsymbol{\alpha}|=m} \|r^\beta \mathsf{D}^{\boldsymbol{\alpha}} u\|^2_{L^2(\mathfrak{K})}$. We denote by $\pi^2_{p,0}$ the L^2-projection onto the tensor-product polynomial space $\mathbb{Q}_p(\mathfrak{K})$ obtained by mapping $\widehat{\pi}^2_{p,0}$ on $\widehat{\mathfrak{K}}$.

Lemma 8.4 *Let $\beta \in [0, 1)$ be a weight exponent. For $u \in H^{1,1}_\beta(\mathfrak{K})$ and $p \ge 0$, there holds*

$$\|u - \pi^2_{p,0}u\|^2_{L^2(\mathfrak{K})} \lesssim h_{\mathfrak{K}}^{2-2\beta} |u|^2_{H^{1,1}_\beta(\mathfrak{K})}. \tag{8.9}$$

Similarly, for $u \in H^{2,2}_\beta(\mathfrak{K})$ and $p \ge 1$, there holds

$$\|u - \pi^2_{p,0}u\|^2_{L^2(\mathfrak{K})} + h^2_{\mathfrak{K}} \|\nabla(u - \pi^2_{p,0}u)\|^2_{L^2(\mathfrak{K})} \lesssim p^4 h_{\mathfrak{K}}^{4-2\beta} |u|^2_{H^{2,2}_\beta(\mathfrak{K})}. \tag{8.10}$$

The implied constants depend on the aspect ratio of $\mathfrak{K}$.

Proof To prove (8.9), we apply the triangle inequality and the stability of the L^2-projection $\pi^2_{p,0}$ to obtain

$$\|u - \pi^2_{p,0}u\|_{L^2(\mathfrak{K})} \lesssim \|u - \pi^2_{0,0}u\|_{L^2(\mathfrak{K})} + \|\pi^2_{p,0}(u - \pi^2_{0,0}u)\|_{L^2(\mathfrak{K})} \lesssim \|u - \pi^2_{0,0}u\|_{L^2(\mathfrak{K})}.$$

The proof of (8.9) for $p = 0$ can then be found in [19, Proposition 27].

To show (8.10), upon scaling it is sufficient to consider the reference square $\widehat{\mathfrak{K}} = (-1, 1)^2$. We denote by $\widehat{\mathfrak{p}}^2_{1,0}$ the L^2-projection onto the polynomial space $\mathbb{P}_1(\widehat{\mathfrak{K}})$. With the stability bound (8.4), it follows that

$$\begin{aligned}\|\widehat{u} - \widehat{\pi}^2_{p,0}\widehat{u}\|^2_{H^1(\widehat{\mathfrak{K}})} &\lesssim \|\widehat{u} - \widehat{\mathfrak{p}}^2_{1,0}\|^2_{H^1(\widehat{\mathfrak{K}})} + \|\widehat{\pi}^2_{p,0}(\widehat{u} - \widehat{\mathfrak{p}}^2_{1,0}\widehat{u})\|^2_{H^1(\widehat{\mathfrak{K}})} \\ &\lesssim p^4\|\widehat{u} - \widehat{\mathfrak{p}}^2_{1,0}\widehat{u}\|^2_{H^1(\widehat{\mathfrak{K}})}.\end{aligned}$$

Hence, it suffices to prove (8.10) for $\widehat{\mathfrak{p}}^2_{1,0}$: We claim that there is a constant $\widehat{C} > 0$ independent of $\widehat{u}$ such that

$$\|\widehat{u}\|_{H^{2,2}_\beta(\widehat{\mathfrak{K}})} \le \widehat{C}\big(|\widehat{u}|_{H^{2,2}_\beta(\widehat{\mathfrak{K}})} + \|\widehat{\mathfrak{p}}^2_{1,0}\widehat{u}\|_{L^2(\widehat{\mathfrak{K}})}\big)\,. \tag{8.11}$$

The bound (8.11) follows with standard arguments from the Peetre–Tartar lemma (see [10, Lemma A.38]) and the fact that the embedding $H^{2,2}_\beta(\widehat{\mathfrak{K}}) \hookrightarrow H^1(\widehat{\mathfrak{K}})$ is compact (see [13, Lemma 3.4]). Invoking (8.11) for $\widehat{u} - \widehat{\mathfrak{p}}^2_{1,0}\widehat{u}$ and noting that $|\widehat{\mathfrak{p}}^2_{1,0}\widehat{u}|_{H^{2,2}_\beta(\widehat{\mathfrak{K}})} = 0$, $\widehat{\mathfrak{p}}^2_{1,0}(\widehat{u} - \widehat{\mathfrak{p}}^2_{1,0}\widehat{u}) = 0$, results in $\|\widehat{u} - \widehat{\mathfrak{p}}^2_{1,0}\widehat{u}\|_{H^{2,2}_\beta(\widehat{\mathfrak{K}})} \le \widehat{C}|\widehat{u}|_{H^{2,2}_\beta(\widehat{\mathfrak{K}})}$, which finishes the proof. □

8.1.4 Edge-Parallel Interpolation

We construct univariate *hp*-projectors and establish exponential convergence bounds for univariate geometric refinements on the interval $\omega = (0, 1)$ toward $x = 0$. These results will be used for the *hp*-approximations along edges $\boldsymbol{e} \in \mathcal{E}_{\boldsymbol{c}}$ toward corners $\boldsymbol{c} \in \mathcal{C}$.

In ω and for $\sigma \in (0, 1)$, we introduce geometric meshes $\mathcal{T}^\ell_\sigma = \{I_j\}_{j=1}^{\ell+1}$ with elements given by $I_1 = (0, \sigma^\ell)$ and $I_j = (\sigma^{\ell+2-j}, \sigma^{\ell+1-j})$ for $2 \le j \le \ell + 1$, respectively. We introduce the local mesh sizes $h_1 := \sigma^\ell$ and

$$h_j := \sigma^{\ell+1-j}(1 - \sigma), \qquad 2 \le j \le \ell + 1\,. \tag{8.12}$$

Then, there is a constant $\kappa > 0$ solely depending on $\sigma \in (0, 1)$ with

$$\kappa^{-1}h_j \le |x| \le \kappa h_j, \qquad x \in I_j,\ 2 \le j \le \ell + 1\,. \tag{8.13}$$

On the geometric mesh $\mathcal{T}^\ell_\sigma$, let $\boldsymbol{p}^\parallel = (p^\parallel_1, \dots, p^\parallel_{\ell+1}) \in \mathbb{N}^{\ell+1}$ be an (edge-parallel) polynomial degree vector with $p^\parallel_j = \max\{1, \lfloor \mathfrak{s} j \rfloor\}$, for $\mathfrak{s} > 0$ as in Sect. 3.2.1. We set $|\boldsymbol{p}^\parallel| = \max_{j=1}^{\ell+1} p^\parallel_j$ and introduce the space

$$V^0(\mathcal{T}^\ell_\sigma, \boldsymbol{p}^\parallel) := \left\{ v \in L^2(\omega) \,:\, v|_{I_j} \in \mathbb{P}_{p^\parallel_j}(I_j),\ j = 1, \dots, \ell + 1 \right\}. \tag{8.14}$$

For conformity indices $r_j \in \{0, 1\}$, we denote by π the projection onto $V^0(\mathcal{T}^\ell_\sigma, \boldsymbol{p}^\parallel)$, given on interval I_j as the (scaled) univariate projector $\pi_{p^\parallel_j, r_j} : H^{r_j}(I_j) \to \mathbb{P}_{p^\parallel_j}(I_j)$.

For $u \in H^1(\omega)$, we define the approximation errors $\eta := u - \pi u$, and set

$$T_j[\eta]^2 := h_j^{-2}\|\eta\|^2_{L^2(I_j)} + \|\eta'\|^2_{L^2(I_j)}. \tag{8.15}$$

Lemma 8.5 *For a weight exponent $\beta > 0$, let $u \in H^1(\omega)$ be such that*

$$\||x|^{-1-\beta+s}u^{(s)}\|_{L^2(\omega)} \le C_u^{s+1}\Gamma(s+1), \qquad s \ge 2. \tag{8.16}$$

Then, for any conformity indices $r_j \in \{0, 1\}$, there exist $b, C > 0$ independent of $\ell \ge 1$ such that $\sum_{j=2}^{\ell+1} T_j[\eta]^2 \le C\exp(-2b\ell)$.

Proof Fix $I_j \in \mathcal{T}_\sigma^\ell$ for $2 \le j \le \ell+1$. A straightforward scaling argument yields $T_j[\eta]^2 \simeq (h_j/2)^{-1}\|\widehat{\eta}\|^2_{H^1(\widehat{I})}$, where as usual we denote by $\widehat{v}$ the pullback operator from $v|_{I_j}$ to the reference interval $\widehat{I} = (-1, 1)$. The bounds in (8.1) and (8.3) yield

$$T_j[\eta]^2 \lesssim |\boldsymbol{p}^\parallel|^4\big(h_j/2\big)^{-1}\Psi_{p_j^\parallel,s_j^\parallel}\|\widehat{u}^{(s_j^\parallel+1)}\|^2_{L^2(\widehat{I})},$$

for any $1 \le s_j^\parallel \le p_j^\parallel$, where we exclude $s_j^\parallel = 0$ in (8.1), (8.3) to ensure that $s \ge 2$ in (8.16). Scaling the right-hand side above back to element I_j results in

$$T_j[\eta]^2 \lesssim |\boldsymbol{p}^\parallel|^4\,(h_j/2)^{2s_j^\parallel}\,\Psi_{p_j^\parallel,s_j^\parallel}\|u^{(s_j^\parallel+1)}\|^2_{L^2(I_j)}. \tag{8.17}$$

Moreover, by the equivalence (8.13),

$$\|u^{(s_j^\parallel+1)}\|^2_{L^2(I_j)} \simeq h_j^{2+2\beta-2(s_j^\parallel+1)}\||x|^{-1-\beta+(s_j^\parallel+1)}u^{(s_j^\parallel+1)}\|^2_{L^2(I_j)}. \tag{8.18}$$

By combining (8.17), (8.18) with the regularity assumption (8.16), we find that

$$\begin{aligned} T_j[\eta]^2 &\lesssim |\boldsymbol{p}^\parallel|^4 h_j^{2\beta}2^{-2s_j^\parallel}\Psi_{p_j^\parallel,s_j^\parallel}\||x|^{-1-\beta+(s_j^\parallel+1)}u^{(s_j^\parallel+1)}\|^2_{L^2(I_j)} \\ &\lesssim |\boldsymbol{p}^\parallel|^4 h_j^{2\beta}\,(C_u/2)^{2s_j^\parallel}\,\Psi_{p_j^\parallel,s_j^\parallel}\Gamma(s_j^\parallel+2)^2\,, \end{aligned} \tag{8.19}$$

for $1 \le s_j^\parallel \le p_j^\parallel$. An interpolation argument as in [24, Lemma 5.8] shows that the bound (8.19) holds for any real $s_j^\parallel \in [1, p_j^\parallel]$.

Next, we sum the bound (8.19) over all intervals $2 \le j \le \ell+1$. In view of (8.12), we obtain

$$\sum_{j=2}^{\ell+1} T_j[\eta]^2 \lesssim |\boldsymbol{p}^\parallel|^4\left(\sum_{j=2}^{\ell+1}\sigma^{2(\ell+1-j)\beta}\min_{s_j^\parallel\in[1,p_j^\parallel]}\left[C^{2s_j^\parallel}\Psi_{p_j^\parallel,s_j^\parallel}\Gamma(s_j+2)^2\right]\right).$$

By [24, Lemma 5.12], the bracket on the right-hand side above is exponentially small. Adjusting the constants to absorb $|\boldsymbol{p}^{\parallel}|^4$ finishes the proof. □

Similarly, we obtain the following result.

Lemma 8.6 *For a weight exponent $\beta > 0$, let $u \in L^2(\omega)$ be such that*

$$\| |x|^{-\beta+s} u^{(s)} \|_{L^2(\omega)} \le C_u^{s+2} \Gamma(s+2), \qquad s \ge 1\,. \tag{8.20}$$

For any conformity indices $r_j \in \{0,1\}$, there exist $b, C > 0$ independent of $\ell \ge 1$ such that $\sum_{j=2}^{\ell+1} \|\eta\|^2_{L^2(I_j)} \le C \exp(-2b\ell)$.

Proof This follows as in Lemma 8.5 or [25, Proposition 5.5]. □

8.2 Reference Corner–Edge Mesh

We consider the reference corner–edge mesh patch $\widetilde{\mathcal{M}}_\sigma^{\ell,\boldsymbol{ce}}$ on $\widetilde{Q}$ for $\boldsymbol{c} \in \mathcal{C}$ and $\boldsymbol{e} \in \mathcal{E}_{\boldsymbol{c}}$; cf. Fig. 1 (right). As in [25, Section 7], it is sufficient to focus on the elements in $\widetilde{\mathcal{M}}_\sigma^{\ell,\boldsymbol{ce}}$ near the corner–edge pair. To this end, we introduce the submesh $\widetilde{\mathcal{K}}_\sigma^{\ell,\boldsymbol{ce}} \subset \widetilde{\mathcal{M}}_\sigma^{\ell,\boldsymbol{ce}}$ given by

$$\widetilde{\mathcal{K}}_\sigma^{\ell,\boldsymbol{ce}} = \bigcup_{j=1}^{\ell+1} \bigcup_{i=1}^{j} \widetilde{\mathfrak{L}}_{\boldsymbol{ce}}^{ij}, \tag{8.21}$$

where the sets $\widetilde{\mathfrak{L}}_{\boldsymbol{ce}}^{ij}$ stand for layers of elements with identical scaling properties with respect to $\boldsymbol{c}$ and $\boldsymbol{e}$; cf. [24, Section 5.2.4]. The index j indicates the number of the geometric mesh layers in edge-parallel direction along the edge $\boldsymbol{e}$, whereas the index i indicates the number of mesh layers in direction perpendicular to $\boldsymbol{e}$. In agreement with [25, Section 7.1], we split $\widetilde{\mathcal{K}}_\sigma^{\ell,\boldsymbol{ce}}$ into interior elements away from $\boldsymbol{c}$ and $\boldsymbol{e}$, boundary layer elements along $\boldsymbol{e}$ (but away from $\boldsymbol{c}$), and corner elements abutting at $\boldsymbol{c}$. That is, we have $\widetilde{\mathcal{K}}_\sigma^{\ell,\boldsymbol{ce}} = \widetilde{\mathfrak{O}}_{\boldsymbol{ce}}^{\ell} \,\dot\cup\, \widetilde{\mathfrak{T}}_{\boldsymbol{e}}^{\ell} \,\dot\cup\, \widetilde{\mathfrak{T}}_{\boldsymbol{c}}^{\ell}$, with

$$\widetilde{\mathfrak{O}}_{\boldsymbol{ce}}^{\ell} := \bigcup_{j=2}^{\ell+1} \bigcup_{i=2}^{j} \widetilde{\mathfrak{L}}_{\boldsymbol{ce}}^{ij}, \qquad \widetilde{\mathfrak{T}}_{\boldsymbol{e}}^{\ell} := \bigcup_{j=2}^{\ell+1} \widetilde{\mathfrak{L}}_{\boldsymbol{ce}}^{1j}, \qquad \widetilde{\mathfrak{T}}_{\boldsymbol{c}}^{\ell} := \widetilde{\mathfrak{L}}_{\boldsymbol{ce}}^{11}. \tag{8.22}$$

Here, for $2 \le i, j \le \ell+1$, interior elements $K \in \widetilde{\mathfrak{L}}_{\boldsymbol{ce}}^{ij}$ satisfy

$$r_{\boldsymbol{e}}|_K \simeq h_K^{\perp} \simeq \sigma^{\ell+1-i}, \qquad r_{\boldsymbol{c}}|_K \simeq h_K^{\parallel} \simeq \sigma^{\ell+1-j}. \tag{8.23}$$

Similarly, boundary layer elements $K \in \widetilde{\mathfrak{L}}_{\boldsymbol{ce}}^{1j}$ satisfy

$$r_{\boldsymbol{e}}|_K \lesssim h_K^{\perp} \simeq \sigma^{\ell}, \qquad r_{\boldsymbol{c}}|_K \simeq h_K^{\parallel} \simeq \sigma^{\ell+1-j}, \qquad 2 \le j \le \ell+1. \tag{8.24}$$

Finally, a corner element in the layer $\widetilde{\mathfrak{T}}_{\boldsymbol{c}}^{\ell} = \widetilde{\mathfrak{L}}_{\boldsymbol{ce}}^{11}$ is isotropic with $r_{\boldsymbol{e}}|_K \lesssim h_K \simeq \sigma^{\ell}$, and $r_{\boldsymbol{c}}|_K \lesssim h_K \simeq \sigma^{\ell}$. The sets $\widetilde{\mathfrak{L}}_{\boldsymbol{ce}}^{1j}$ and $\widetilde{\mathfrak{L}}_{\boldsymbol{ce}}^{11}$ are in fact singletons, and without loss of

generality $K_j \in \widetilde{\mathfrak{L}}^{1j}_{\boldsymbol{ce}}$ can be written in the form

$$K_j = K^\perp \times K_j^\parallel, \qquad 2 \le j \le \ell + 1\,, \tag{8.25}$$

cf. (3.3), where $K^\perp = (0, \sigma^\ell)^2$, and the sequence $\{K_j^\parallel\}_{j=2}^{\ell+1}$ forms a one-dimensional geometric mesh $\mathcal{T}_\sigma^\ell$ along the edge $\boldsymbol{e}$ as in Sect. 8.1.4. The $\mathfrak{s}$-linearly increasing polynomial degree distributions on $\widetilde{\mathcal{K}}_\sigma^{\ell,\boldsymbol{ce}}$ in (8.21) are given by

$$\forall\, K \in \widetilde{\mathfrak{L}}^{ij}_{\boldsymbol{ce}}: \qquad \boldsymbol{p}_K = (p_i^\perp, p_j^\parallel) \simeq (\max\{1, \lfloor \mathfrak{s} i \rfloor\}, \max\{1, \lfloor \mathfrak{s} j \rfloor\}). \tag{8.26}$$

In the sequel, we introduce the domain $\widetilde{\Omega}^\ell_{\boldsymbol{ce}} := \big(\cup_{K \in \widetilde{\mathcal{K}}_\sigma^{\ell,\boldsymbol{ce}}} \overline{K}\big)^\circ$. Analogously to (2.6) and for exponents $\boldsymbol{\beta} = \{\beta_{\boldsymbol{c}}, \beta_{\boldsymbol{e}}\}$, we introduce the *non-homogeneous reference corner–edge semi-norm on* $\widetilde{\Omega}^\ell_{\boldsymbol{ce}}$:

$$|u|^2_{\widetilde{N}^k_{\boldsymbol{\beta}}(\widetilde{\Omega}^\ell_{\boldsymbol{ce}})} := \sum_{|\boldsymbol{\alpha}|=k} \Big\| r_{\boldsymbol{c}}^{\max\{\beta_{\boldsymbol{c}}+|\boldsymbol{\alpha}|,0\}}\, \rho_{\boldsymbol{ce}}^{\max\{\beta_{\boldsymbol{e}}+|\boldsymbol{\alpha}^\perp|,0\}} \mathsf{D}^{\boldsymbol{\alpha}} u \Big\|^2_{L^2(\widetilde{\Omega}^\ell_{\boldsymbol{ce}})}\,, \tag{8.27}$$

for any $k \ge 0$ and where $r_{\boldsymbol{c}}$ and $r_{\boldsymbol{e}}$ are the distances to $\boldsymbol{c}$ and $\boldsymbol{e}$, respectively, and $\rho_{\boldsymbol{ce}} = r_{\boldsymbol{e}}/r_{\boldsymbol{c}}$. For $m > k_{\boldsymbol{\beta}}$ as in (2.7), the weighted Sobolev spaces $\widetilde{N}^m_{\boldsymbol{\beta}}(\widetilde{\Omega}^\ell_{\boldsymbol{ce}})$ are defined as in Sect. 2.2 with respect to the norms $\|\cdot\|^2_{\widetilde{N}^m_{\boldsymbol{\beta}}(\widetilde{\Omega}^\ell_{\boldsymbol{ce}})} = \sum_{k=0}^m |\cdot|^2_{\widetilde{N}^k_{\boldsymbol{\beta}}(\widetilde{\Omega}^\ell_{\boldsymbol{ce}})}$. The corresponding analytic reference class $B_{\boldsymbol{\beta}}(\widetilde{\Omega}^\ell_{\boldsymbol{ce}})$ consists of all functions $u : \widetilde{\Omega}^\ell_{\boldsymbol{ce}} \to \mathbb{R}$ such that $u \in \widetilde{N}^k_{\boldsymbol{\beta}}(\widetilde{\Omega}^\ell_{\boldsymbol{ce}})$ for $k > k_{\boldsymbol{\beta}}$ and such that there is a constant $d_u > 0$ with

$$|u|_{\widetilde{N}^k_{\boldsymbol{\beta}}(\widetilde{\Omega}^\ell_{\boldsymbol{ce}})} \le d_u^{k+1} \Gamma(k+1) \qquad \forall\, k > k_{\boldsymbol{\beta}}. \tag{8.28}$$

In the following, we restrict ourselves to the classes $B_{-1-\boldsymbol{b}}(\widetilde{\Omega}^\ell_{\boldsymbol{ce}})$ and $B_{-\boldsymbol{b}}(\widetilde{\Omega}^\ell_{\boldsymbol{ce}})$ for exponents $\boldsymbol{b} = \{b_{\boldsymbol{c}}, b_{\boldsymbol{e}}\}$ in $(0, 1)$ as in Remark 2.3. In the first case, we have $k_{\boldsymbol{\beta}} \in (1, 2)$ and the norms on the right-hand in (8.27) are given by

$$\begin{cases} \|\mathsf{D}^{\boldsymbol{\alpha}} u\|^2_{L^2(\widetilde{\Omega}^\ell_{\boldsymbol{ce}})} & |\boldsymbol{\alpha}| = 0,\ 1,\ |\boldsymbol{\alpha}^\perp| = 0,\ 1, \\ \|r_{\boldsymbol{c}}^{-1-b_{\boldsymbol{c}}+|\boldsymbol{\alpha}|} \mathsf{D}^{\boldsymbol{\alpha}} u\|^2_{L^2(\widetilde{\Omega}^\ell_{\boldsymbol{ce}})} & |\boldsymbol{\alpha}| \ge 2,\ |\boldsymbol{\alpha}^\perp| = 0,\ 1, \\ \|r_{\boldsymbol{c}}^{b_{\boldsymbol{e}}-b_{\boldsymbol{c}}+\alpha^\parallel} r_{\boldsymbol{e}}^{-1-b_{\boldsymbol{e}}+|\boldsymbol{\alpha}^\perp|} \mathsf{D}^{\boldsymbol{\alpha}} u\|^2_{L^2(\widetilde{\Omega}^\ell_{\boldsymbol{ce}})} & |\boldsymbol{\alpha}| \ge 2,\ |\boldsymbol{\alpha}^\perp| \ge 2. \end{cases} \tag{8.29}$$

Similarly, for the second analytic class $B_{-\boldsymbol{b}}(\widetilde{\Omega}^\ell_{\boldsymbol{ce}})$, we have $k_{\boldsymbol{\beta}} \in (0, 1)$ and the norms on the right-hand side of (8.27) take the form

$$\begin{cases} \|u\|^2_{L^2(\widetilde{\Omega}^\ell_{\boldsymbol{ce}})} & |\boldsymbol{\alpha}| = 0,\ |\boldsymbol{\alpha}^\perp| = 0, \\ \|r_{\boldsymbol{c}}^{-b_{\boldsymbol{e}}+\alpha^\parallel} \mathsf{D}^{\boldsymbol{\alpha}} u\|^2_{L^2(\widetilde{\Omega}^\ell_{\boldsymbol{ce}})} & |\boldsymbol{\alpha}| = 1,\ |\boldsymbol{\alpha}^\perp| = 0, \\ \|r_{\boldsymbol{c}}^{b_{\boldsymbol{e}}-b_{\boldsymbol{c}}+\alpha^\parallel} r_{\boldsymbol{e}}^{-b_{\boldsymbol{e}}+|\boldsymbol{\alpha}^\perp|} \mathsf{D}^{\boldsymbol{\alpha}} u\|^2_{L^2(\widetilde{\Omega}^\ell_{\boldsymbol{ce}})} & |\boldsymbol{\alpha}| \ge 1,\ |\boldsymbol{\alpha}^\perp| \ge 1. \end{cases} \tag{8.30}$$

In the *axiparallel* setting considered in the present paper, when functions $u \in B_{-1-\boldsymbol{b}}(\Omega)$ and $u \in B_{-\boldsymbol{b}}(\Omega)$ as in Theorem 4.3 are localized and scaled to $\widetilde{\Omega}^{\ell}_{\boldsymbol{ce}}$, they belong to the reference classes $B_{-1-\boldsymbol{b}}(\widetilde{\Omega}^{\ell}_{\boldsymbol{ce}})$ and $B_{-\boldsymbol{b}}(\widetilde{\Omega}^{\ell}_{\boldsymbol{ce}})$, respectively; cf. [20, Section 3.4].

To prove Theorem 4.3 in the reference corner–edge framework, it is now enough to bound the error contributions as in (3.34), (3.33) over $\widetilde{\mathcal{K}}^{\ell,\boldsymbol{ce}}_{\sigma} = \widetilde{\mathfrak{O}}^{\ell}_{\boldsymbol{ce}} \dot\cup \widetilde{\mathfrak{T}}^{\ell}_{\boldsymbol{e}} \dot\cup \widetilde{\mathfrak{T}}^{\ell}_{\boldsymbol{c}}$.

Proposition 8.7 *For $b_{\boldsymbol{c}}, b_{\boldsymbol{e}} \in (0,1)$, let $u \in B_{-1-\boldsymbol{b}}(\widetilde{\Omega}^{\ell}_{\boldsymbol{ce}}) \cap H^{1+\theta}(\widetilde{\Omega}^{\ell}_{\boldsymbol{ce}})$ for some $\theta \in (0,1)$, and let $\pi u = \pi_0^{\perp} \otimes \pi^{\parallel} u$ be the base interpolant (4.4) over $\widetilde{\mathcal{K}}^{\ell,\boldsymbol{ce}}_{\sigma}$ for any conformity indices $r_K \in \{0,1\}$. For the errors η, $\eta_0^{\perp}$, $\eta^{\parallel}$ in (4.7), we have*

$$\Upsilon^{\perp}_{\widetilde{\mathfrak{O}}^{\ell}_{\boldsymbol{ce}}}[\eta_0^{\perp}]^2 + \Upsilon^{\parallel}_{\widetilde{\mathfrak{O}}^{\ell}_{\boldsymbol{ce}}}[\eta^{\parallel}]^2 + \Upsilon^{\perp}_{\widetilde{\mathfrak{T}}^{\ell}_{\boldsymbol{e}}}[\eta_0^{\perp}]^2 + \Upsilon^{\parallel}_{\widetilde{\mathfrak{T}}^{\ell}_{\boldsymbol{e}}}[\eta^{\parallel}]^2 + \Upsilon^{\parallel}_{\widetilde{\mathfrak{T}}^{\ell}_{\boldsymbol{c}}}[\eta]^2 \le C\exp(-2b\ell),$$

with $b, C > 0$ independent of ℓ.

Moreover, for $b_{\boldsymbol{c}}, b_{\boldsymbol{e}} \in (0,1)$, let $u \in B_{-\boldsymbol{b}}(\widetilde{\Omega}^{\ell}_{\boldsymbol{ce}}) \cap H^{\theta}(\widetilde{\Omega}^{\ell}_{\boldsymbol{ce}})$ for some $\theta \in (0,1)$, and let $\pi_0 u = \pi_0^{\perp} \otimes \pi_0^{\parallel} u$ be the L^2-projection over $\widetilde{\mathcal{K}}^{\ell,\boldsymbol{ce}}_{\sigma}$. For the errors η_0, $\eta_0^{\perp}$, $\eta_0^{\parallel}$ in (4.7), we have

$$\|\eta_0^{\perp}\|^2_{L^2(\widetilde{\mathfrak{O}}^{\ell}_{\boldsymbol{ce}})} + \|\eta_0^{\parallel}\|^2_{L^2(\widetilde{\mathfrak{O}}^{\ell}_{\boldsymbol{ce}})} + \|\eta_0^{\perp}\|^2_{L^2(\widetilde{\mathfrak{T}}^{\ell}_{\boldsymbol{e}})} + \|\eta_0^{\parallel}\|^2_{L^2(\widetilde{\mathfrak{T}}^{\ell}_{\boldsymbol{e}})} + \|\eta_0\|^2_{L^2(\widetilde{\mathfrak{T}}^{\ell}_{\boldsymbol{c}})} \le C\exp(-2b\ell),$$

with $b, C > 0$ independent of ℓ.

The remainder of this section is devoted to the proof of Proposition 8.7.

8.3 Proof of Proposition 8.7

We bound the errors in Proposition 8.7 separately for the set $\widetilde{\mathfrak{O}}^{\ell}_{\boldsymbol{ce}}$ (Propositions 8.9, 8.10), for $\widetilde{\mathfrak{T}}^{\ell}_{\boldsymbol{e}}$ (Propositions 8.11, 8.12), and for $\widetilde{\mathfrak{T}}^{\ell}_{\boldsymbol{c}}$ (Proposition 8.13).

8.3.1 Convergence on $\widetilde{\mathfrak{O}}^{\ell}_{\boldsymbol{ce}}$

We begin our analysis by recalling essential scaling properties; see [24, Section 5.1.4].

Lemma 8.8 *Let $K = (0, h_K^{\perp})^2 \times (0, h_K^{\parallel})$ be of the form (3.3). Let $v : K \to \mathbb{R}$, and $\widehat{v} = v \circ \Phi_K^{-1}$. Then:*

(i) $\|v\|^2_{L^2(K)} \lesssim (h_K^{\perp})^2 h_K^{\parallel} \|\widehat{v}\|^2_{L^2(\widehat{K})}$.

(ii) $(h_K^{\parallel})^{-2}\|v\|^2_{L^2(K)} + \|\mathsf{D}_{\parallel} v\|^2_{L^2(K)} \lesssim (h_K^{\perp})^2 (h_K^{\parallel})^{-1}\big(\|\widehat{v}\|^2_{L^2(\widehat{K})} + \|\widehat{\mathsf{D}}_{\parallel}\widehat{v}\|^2_{L^2(\widehat{K})}\big)$.

(iii) $(h_K^{\perp})^{-2}\|v\|^2_{L^2(K)} + \|\mathsf{D}_{\perp} v\|^2_{L^2(K)} \lesssim h_K^{\parallel}\big(\|\widehat{v}\|^2_{L^2(\widehat{K})} + \|\widehat{\mathsf{D}}_{\perp}\widehat{v}\|^2_{L^2(\widehat{K})}\big)$.

We bound $\eta_0^{\perp}$ over $\widetilde{\mathfrak{O}}^{\ell}_{\boldsymbol{ce}}$ as follows.

Proposition 8.9 *Let $u \in B_{-1-\boldsymbol{b}}(\widetilde{\Omega}^{\ell}_{\boldsymbol{ce}})$, respectively $u \in B_{-\boldsymbol{b}}(\widetilde{\Omega}^{\ell}_{\boldsymbol{ce}})$. Then there are constants $b, C > 0$ independent of ℓ such that $\Upsilon^{\perp}_{\widetilde{\mathfrak{O}}^{\ell}_{\boldsymbol{ce}}}[\eta_0^{\perp}]^2 \le C\exp(-2b\ell)$, respectively $\|\eta_0^{\perp}\|^2_{L^2(\widetilde{\mathfrak{O}}^{\ell}_{\boldsymbol{ce}})} \le C\exp(-2b\ell)$.*

Proof Let $u \in B_{-1-\boldsymbol{b}}(\widetilde{\Omega}^{\ell}_{\boldsymbol{ce}})$. We consider an element $K \in \widetilde{\mathfrak{L}}^{ij}_{\boldsymbol{ce}}$ with $2 \le j \le \ell+1$ and $2 \le i \le j$; see (8.22). With Lemma 8.8 (observing that $h^{\perp}_K \lesssim h^{\parallel}_K$), the approximation results for $\widehat{\eta}^{\perp}_0$ in Proposition 8.3 and (8.26), we conclude that

$$N^{\perp}_K[\eta^{\perp}_0]^2 \lesssim h^{\parallel}_K \|\widehat{\eta}^{\perp}_0\|^2_{H^1_{\mathrm{mix}}(\widehat{K})} \lesssim_p h^{\parallel}_K \Psi_{p^{\perp}_i,s^{\perp}_i} E^{\perp}_{s^{\perp}_i}(K;u),$$

for $1 \le s^{\perp}_i \le p^{\perp}_i$, where $E^{\perp}_{s^{\perp}_i}(K;u)$ is the expression in (8.7). Notice that here we exclude the choice $s^{\perp}_i = 0$ to ensure that $|\boldsymbol{\alpha}| \ge |\boldsymbol{\alpha}^{\perp}| \ge 2$ in $E^{\perp}_{s^{\perp}_i}(K;u)$. Thanks to the equivalences (8.24), we insert the appropriate weights as in (8.29) and obtain

$$\begin{aligned}\|\mathsf{D}^{\boldsymbol{\alpha}^{\perp}}_{\perp}\mathsf{D}^{\alpha^{\parallel}}_{\parallel}u\|^2_{L^2(K)} \simeq (h^{\parallel}_K)^{2b_{\boldsymbol{c}}-2b_{\boldsymbol{e}}-2\alpha^{\parallel}}(h^{\perp}_K)^{2+2b_{\boldsymbol{e}}-2|\boldsymbol{\alpha}^{\perp}|}\\ \times \|r^{b_{\boldsymbol{e}}-b_{\boldsymbol{c}}+\alpha^{\parallel}}_{\boldsymbol{c}} r^{-1-b_{\boldsymbol{e}}+|\boldsymbol{\alpha}^{\perp}|}_{\boldsymbol{e}}\mathsf{D}^{\boldsymbol{\alpha}^{\perp}}_{\perp}\mathsf{D}^{\alpha^{\parallel}}_{\parallel}u\|^2_{L^2(K)},\end{aligned}$$

for $2 \le s^{\perp}_i + 1 \le |\boldsymbol{\alpha}^{\perp}| \le s^{\perp}_i + 2$ and $\alpha^{\parallel} = 0, 1$. Hence, it follows that

$$N^{\perp}_K[\eta^{\perp}_0]^2 \lesssim_p \Psi_{p^{\perp}_i,s^{\perp}_i}(h^{\parallel}_K)^{2b_{\boldsymbol{c}}-2b_{\boldsymbol{e}}}(h^{\perp}_K)^{2b_{\boldsymbol{e}}} \sum_{k=s^{\perp}_i+1}^{s^{\perp}_i+3} |u|^2_{\widetilde{N}^k_{-1-\boldsymbol{b}}(K)}.$$

The analytic regularity (8.28) then implies the existence of $C > 0$ such that

$$N^{\perp}_K[\eta^{\perp}_0]^2 \lesssim_p \Psi_{p^{\perp}_i,s^{\perp}_i}(h^{\parallel}_K)^{2b_{\boldsymbol{c}}-2b_{\boldsymbol{e}}}(h^{\perp}_K)^{2b_{\boldsymbol{e}}} C^{2s^{\perp}_i}\Gamma(s^{\perp}_i+4)^2, \tag{8.31}$$

for all $1 \le s^{\perp}_i \le p^{\perp}_i$. Summing (8.31) over all layers in $\widetilde{\mathfrak{S}}^{\ell}_{\boldsymbol{ce}}$ in (8.22) in combination with (8.23) results in

$$\Upsilon^{\perp}_{\widetilde{\mathfrak{S}}^{\ell}_{\boldsymbol{ce}}}[\eta^{\perp}_0] \lesssim_p \sum_{j=2}^{\ell+1} \sigma^{2(b_{\boldsymbol{c}}-b_{\boldsymbol{e}})(\ell+1-j)}\Big(\sum_{i=2}^{j}\sigma^{2b_{\boldsymbol{e}}(\ell+1-i)}\Psi_{p^{\perp}_i,s^{\perp}_i}C^{2s^{\perp}_i}\Gamma(s^{\perp}_i+4)^2\Big).$$

By interpolating to real parameters $s^{\perp}_i \in [1, p^{\perp}_i]$ as in [24, Lemma 5.8], this sum is of the same form as $S^{\perp}$ in the proof of [24, Proposition 5.17], and the assertion now follows from the arguments there and after adjusting the constants to absorb the algebraic loss in $|\boldsymbol{p}|$.

For $u \in B_{-\boldsymbol{b}}(\widetilde{\Omega}^{\ell}_{\boldsymbol{ce}})$, we proceed similarly and note that

$$\|\eta^{\perp}_0\|^2_{L^2(K)} \lesssim (h^{\perp}_K)^2 h^{\parallel}_K \|\widehat{\eta}^{\perp}_0\|^2_{H^1_{\mathrm{mix}}(\widehat{K})} \lesssim_p (h^{\perp}_K)^2 h^{\parallel}_K \Psi_{p^{\perp}_i,s^{\perp}_i} E^{\perp}_{s^{\perp}_i}(K;u),$$

for $1 \le s_i^\perp \le p_i^\perp$. Hence, we obtain

$$\|\eta_0^\perp\|^2_{L^2(K)} \lesssim_p \Psi_{p_i^\perp, s_i^\perp}(h_K^\parallel)^{2b_c-2b_e}(h_K^\perp)^{2b_e} \sum_{k=s_i^\perp+1}^{s_i^\perp+3} |u|^2_{\widetilde{N}^k_{-\boldsymbol{b}}(K)}.$$

The second bound follows as before. □

Next, we establish the analog of Proposition 8.9 in edge-parallel direction.

Proposition 8.10 *Let $u \in B_{-1-\boldsymbol{b}}(\widetilde{\Omega}^\ell_{\boldsymbol{ce}})$, respectively $u \in B_{-\boldsymbol{b}}(\widetilde{\Omega}^\ell_{\boldsymbol{ce}})$. Then there are constants $b, C > 0$ independent of ℓ such that $\Upsilon^\parallel_{\widetilde{\mathfrak{S}}^\ell_{\boldsymbol{ce}}}[\eta^\parallel]^2 \le C\exp(-2b\ell)$, respectively $\|\eta_0^\parallel\|^2_{L^2(\widetilde{\mathfrak{S}}^\ell_{\boldsymbol{ce}})} \le C\exp(-2b\ell)$.*

Proof For $u \in B_{-1-\boldsymbol{b}}(\widetilde{\Omega}^\ell_{\boldsymbol{ce}})$, we claim that

$$N_K^\parallel[\eta^\parallel]^2 \lesssim_p \Psi_{p_K^\parallel, s_K^\parallel}(h_K^\parallel)^{2b_c}\|u\|^2_{\widetilde{N}^{s_K^\parallel+2}_{-1-\boldsymbol{b}}(K)}, \tag{8.32}$$

for any $K \in \widetilde{\mathfrak{S}}^\ell_{\boldsymbol{ce}}$ and $1 \le s_K^\parallel \le p_K^\parallel$. To prove (8.32), we start by employing Lemma 8.8 and the approximation property for $\widehat{\eta}^\parallel$ in Proposition 8.3:

$$\begin{aligned}(h_K^\parallel)^{-2}\|\eta^\parallel\|^2_{L^2(K)} + \|\mathsf{D}_\parallel\eta^\parallel\|^2_{L^2(K)} &\lesssim (h_K^\perp)^2(h_K^\parallel)^{-1}\sum_{\alpha^\parallel=0,1}\|\widehat{\mathsf{D}}_\parallel^{\alpha^\parallel}\widehat{\eta}^\parallel\|^2_{L^2(\widehat{K})}\\ &\lesssim_p \Psi_{p_K^\parallel, s_K^\parallel}(h_K^\parallel)^{2s_K^\parallel}\|\mathsf{D}_\parallel^{s_K^\parallel+1}u\|^2_{L^2(K)}\end{aligned}$$

for any $1 < s_K^\parallel \le p_K^\parallel$, where we again exclude the choice $s_K^\parallel = 0$ so that $|\boldsymbol{\alpha}| \ge 2$. We then insert suitable weights with the aid of (8.23), (8.29) to obtain

$$\|\mathsf{D}_\parallel^{s_K^\parallel+1}u\|^2_{L^2(K)} \simeq (h_K^\parallel)^{2b_c-2s_K^\parallel}\|r_{\boldsymbol{c}}^{-1-b_c+s_K^\parallel+1}\mathsf{D}_\parallel^{s_K^\parallel+1}u\|^2_{L^2(K)}.$$

Hence,

$$(h_K^\parallel)^{-2}\|\eta^\parallel\|^2_{L^2(K)} + \|\mathsf{D}_\parallel\eta^\parallel\|^2_{L^2(K)} \lesssim_p \Psi_{p_K^\parallel, s_K^\parallel}(h_K^\parallel)^{2b_c}|u|^2_{\widetilde{N}^{s_K^\parallel+1}_{-1-\boldsymbol{b}}(K)}.$$

By proceeding similarly, we find that, for $|\boldsymbol{\alpha}^\perp| = 1$,

$$\begin{aligned}\|\mathsf{D}_\perp^{\boldsymbol{\alpha}^\perp}\eta^\parallel\|^2_{L^2(K)} &\lesssim h_K^\parallel\sum_{\alpha^\parallel=0,1}\|\widehat{\mathsf{D}}_\perp^{\boldsymbol{\alpha}^\perp}\widehat{\mathsf{D}}_\parallel^{\alpha^\parallel}\widehat{\eta}^\parallel\|^2_{L^2(\widehat{K})}\\ &\lesssim_p \Psi_{p_K^\parallel, s_K^\parallel}(h_K^\parallel)^{2s_K^\parallel+2}\|\mathsf{D}_\perp^{\boldsymbol{\alpha}^\perp}\mathsf{D}_\parallel^{s_K^\parallel+1}u\|^2_{L^2(K)}\end{aligned}$$

$$\lesssim_p \Psi_{p_K^{\parallel},s_K^{\parallel}}(h_K^{\parallel})^{2b_c}\|r_{\boldsymbol{c}}^{-b_c+s_K^{\parallel}+1}\mathsf{D}_{\perp}^{\boldsymbol{\alpha}^{\perp}}\mathsf{D}_{\parallel}^{s_K^{\parallel}+1}u\|_{L^2(K)}^2$$
$$\lesssim_p \Psi_{p_K^{\parallel},s_K^{\parallel}}(h_K^{\parallel})^{2b_c}|u|^2_{\widetilde{N}^{s_K^{\parallel}+2}_{-1-\boldsymbol{b}}(K)}.$$

This establishes the bound (8.32).

For $u \in B_{-\boldsymbol{b}}(\widetilde{\Omega}^{\ell}_{\boldsymbol{ce}})$, we use analogous arguments based on Lemma 8.8, Proposition 8.3 and (8.30). This results in

$$\begin{aligned}\|\eta_0^{\parallel}\|^2_{L^2(K)} &\lesssim_p \Psi_{p_K^{\parallel},s_K^{\parallel}}(h_K^{\parallel})^{2s_K^{\parallel}+2}\|\mathsf{D}_{\parallel}^{s_K^{\parallel}+1}u\|^2_{L^2(K)}\\ &\lesssim_p \Psi_{p_K^{\parallel},s_K^{\parallel}}(h_K^{\parallel})^{2b_c}\|r_{\boldsymbol{c}}^{-b_c+s_K^{\parallel}+1}\mathsf{D}_{\parallel}^{s_K^{\parallel}+1}u\|^2_{L^2(K)}\\ &\lesssim_p (h_K^{\parallel})^{2b_c}|u|^2_{\widetilde{N}^{s_K^{\parallel}+1}_{-\boldsymbol{b}}(K)}.\end{aligned} \tag{8.33}$$

Next, we sum the bounds in (8.32), (8.33) over all layers of $\widetilde{\mathfrak{O}}^{\ell}_{\boldsymbol{ce}}$. By noticing (8.23), (8.26) and the analytic regularity (8.28), we conclude that

$$u \in B_{-1-\boldsymbol{b}}(\widetilde{\Omega}^{\ell}_{\boldsymbol{ce}}): \qquad \Upsilon^{\parallel}_{\widetilde{\mathfrak{O}}^{\ell}_{\boldsymbol{ce}}}[\eta^{\parallel}]^2 \lesssim_p \sum_{j=2}^{\ell+1}\sum_{i=2}^{j}\Psi_{p_j^{\parallel},s_j^{\parallel}}\sigma^{2(\ell+1-j)b_c}C^{2s_j^{\parallel}}\Gamma(s_j^{\parallel}+3)^2,$$

$$u \in B_{-\boldsymbol{b}}(\widetilde{\Omega}^{\ell}_{\boldsymbol{ce}}): \qquad \|\eta_0^{\parallel}\|^2_{L^2(\widetilde{\mathfrak{O}}^{\ell}_{\boldsymbol{ce}})} \lesssim_p \sum_{j=2}^{\ell+1}\sum_{i=2}^{j}\Psi_{p_j^{\parallel},s_j^{\parallel}}\sigma^{2(\ell+1-j)b_c}C^{2s_j^{\parallel}}\Gamma(s_j^{\parallel}+2)^2.$$

The terms in the sums above are independent of the inner index i. Interpolation to non-integer differentiation orders $s_j^{\parallel} \in [1, p_j^{\parallel}]$ as in [24, Lemma 5.8], applying [24, Lemma 5.12] and absorbing the algebraic loss in $|\boldsymbol{p}|$ complete the proof. □

8.3.2 Convergence on $\widetilde{\mathfrak{T}}^{\ell}_{\boldsymbol{e}}$

We first consider edge-perpendicular elements.

Proposition 8.11 *Let $u \in B_{-1-\boldsymbol{b}}(\widetilde{\Omega}^{\ell}_{\boldsymbol{ce}})$, respectively $u \in B_{-\boldsymbol{b}}(\widetilde{\Omega}^{\ell}_{\boldsymbol{ce}})$. Then there are constants $b, C > 0$ independent of ℓ such that $\Upsilon^{\perp}_{\widetilde{\mathfrak{T}}^{\ell}_{\boldsymbol{e}}}[\eta_0^{\perp}]^2 \le C\exp(-2b\ell)$, respectively $\|\eta_0^{\perp}\|^2_{L^2(\widetilde{\mathfrak{T}}^{\ell}_{\boldsymbol{e}})} \le C\exp(-2b\ell)$.*

Proof Let $K = K_j = K^{\perp} \times K_j^{\parallel}$ be an element of $\widetilde{\mathfrak{T}}^{\ell}_{\boldsymbol{e}}$ as in (8.25). We claim that

$$(h_K^{\perp})^{-2}\|\eta_0^{\perp}\|^2_{L^2(K)} + \|\mathsf{D}_{\perp}\eta_0^{\perp}\|^2_{L^2(K} \lesssim \sigma^{2\min\{b_c,b_e\}\ell}|u|^2_{\widetilde{N}^2_{-1-\boldsymbol{b}}(K)}, \tag{8.34}$$

$$\|\mathsf{D}_{\parallel}\eta_0^{\perp}\|^2_{L^2(K)} \lesssim \sigma^{2\min\{b_c,b_e\}\ell}|u|^2_{\widetilde{N}^3_{-1-\boldsymbol{b}}(K)}, \tag{8.35}$$

$$\|\eta_0^{\perp}\|^2_{L^2(K)} \lesssim \sigma^{2\min\{b_c,b_e\}\ell}|u|^2_{\widetilde{N}^1_{-\boldsymbol{b}}(K)}. \tag{8.36}$$

To show (8.34), let $s = |\boldsymbol{\alpha}^\perp| = 0, 1$. Applying the bound (8.10) with $\beta = 1 - b_{\boldsymbol{e}}$ (noting that $p_K^\perp = \max\{1, \mathfrak{s}\}$ by (8.26)) and from (8.24), (8.29), we see that

$$\begin{aligned}(h_K^\perp)^{2(s-1)} \|\mathsf{D}_\perp^{\boldsymbol{\alpha}^\perp} \eta_0^\perp\|_{L^2(K)}^2 &\lesssim (h_K^\perp)^{2b_{\boldsymbol{e}}} \|r_{\boldsymbol{e}}^{1-b_{\boldsymbol{e}}} \mathsf{D}_\perp^2 u\|_{L^2(K)}^2, \\ &\lesssim (h_K^\parallel)^{-2(b_{\boldsymbol{e}}-b_{\boldsymbol{c}})} (h_K^\perp)^{2b_{\boldsymbol{e}}} \|r_{\boldsymbol{c}}^{b_{\boldsymbol{e}}-b_{\boldsymbol{c}}} r_{\boldsymbol{e}}^{1-b_{\boldsymbol{e}}} \mathsf{D}_\perp^2 u\|_{L^2(K)}^2,\end{aligned}$$

where $|\mathsf{D}_\perp^2 v|^2 = \sum_{|\boldsymbol{\alpha}^\perp|=2} |\mathsf{D}_\perp^{\boldsymbol{\alpha}^\perp} v|^2$. Thus, combining these estimates and expressing the mesh sizes in terms of σ, see (8.24), we have

$$\begin{aligned}(h_K^\perp)^{2(s-1)} \|\mathsf{D}_\perp^{\boldsymbol{\alpha}^\perp} \eta_0^\perp\|_{L^2(K)}^2 &\lesssim \sigma^{2b_{\boldsymbol{c}}(\ell+1-j)+2b_{\boldsymbol{e}}(j-1)} |u|_{\widetilde{N}^2_{-1-\boldsymbol{b}}(K)}^2 \\ &\lesssim \sigma^{2\min\{b_{\boldsymbol{c}},b_{\boldsymbol{e}}\}\ell} |u|_{\widetilde{N}^2_{-1-\boldsymbol{b}}(K)}^2,\end{aligned}$$

which yields (8.34). To prove (8.35), we similarly conclude that

$$\begin{aligned}\|\mathsf{D}_\parallel \eta_0^\perp\|_{L^2(K)}^2 &\lesssim (h_K^\perp)^{2+2b_{\boldsymbol{e}}} \|r_{\boldsymbol{e}}^{1-b_{\boldsymbol{e}}} \mathsf{D}_\perp^2 \mathsf{D}_\parallel u\|_{L^2(K)}^2 \\ &\lesssim (h_K^\parallel)^{-2-2b_{\boldsymbol{e}}+2b_{\boldsymbol{c}}} (h_K^\perp)^{2+2b_{\boldsymbol{e}}} \|r_{\boldsymbol{c}}^{b_{\boldsymbol{e}}-b_{\boldsymbol{c}}+1} r_{\boldsymbol{e}}^{1-b_{\boldsymbol{e}}} \mathsf{D}_\perp^2 \mathsf{D}_\parallel u\|_{L^2(K)}^2 \\ &\lesssim \sigma^{2\min\{b_{\boldsymbol{c}},b_{\boldsymbol{e}}\}\ell} |u|_{\widetilde{N}^3_{-1-\boldsymbol{b}}(K)}^2 .\end{aligned}$$

For the bound (8.36), we employ an analogous argument based on (8.9) (with $\beta = 1 - b_{\boldsymbol{e}}$). Indeed, with (8.24) and (8.30), we conclude that

$$\begin{aligned}\|\eta_0^\perp\|_{L^2(K)}^2 &\lesssim (h_K^\perp)^{2b_{\boldsymbol{e}}} \|r_{\boldsymbol{e}}^{1-b_{\boldsymbol{e}}} \mathsf{D}_\perp u\|_{L^2(K)}^2 \\ &\lesssim (h_K^\parallel)^{2b_{\boldsymbol{c}}-2b_{\boldsymbol{e}}} (h_K^\perp)^{2b_{\boldsymbol{e}}} \|r_{\boldsymbol{c}}^{b_{\boldsymbol{e}}-b_{\boldsymbol{c}}} r_{\boldsymbol{e}}^{1-b_{\boldsymbol{e}}} \mathsf{D}_\perp u\|_{L^2(K)}^2 \\ &\lesssim \sigma^{2\min\{b_{\boldsymbol{c}},b_{\boldsymbol{e}}\}\ell} |u|_{\widetilde{N}^1_{-\boldsymbol{b}}(\widetilde{\Omega}_{\boldsymbol{ce}}^\ell)}^2,\end{aligned}$$

which is (8.36).

The assertions now follow by summing the estimates (8.34), (8.35) and (8.36) over all elements $K \in \widetilde{\mathfrak{T}}_{\boldsymbol{e}}^\ell$ (i.e., over $2 \le j \le \ell + 1$) and by suitably adjusting the constants. □

A similar estimate holds for the approximation errors in direction parallel to $\boldsymbol{e}$.

Proposition 8.12 *Let $u \in B_{-1-\boldsymbol{b}}(\widetilde{\Omega}_{\boldsymbol{ce}}^\ell)$, respectively $u \in B_{-\boldsymbol{b}}(\widetilde{\Omega}_{\boldsymbol{ce}}^\ell)$. Then there are constants $b, C > 0$ independent of ℓ such that $\Upsilon_{\widetilde{\mathfrak{T}}_{\boldsymbol{e}}^\ell}^\parallel [\eta^\parallel]^2 \le C \exp(-2b\ell)$, respectively $\|\eta_0^\parallel\|_{L^2(\widetilde{\mathfrak{T}}_{\boldsymbol{e}}^\ell)}^2 \le C \exp(-2b\ell)$.*

Proof For $u \in B_{-1-\boldsymbol{b}}(\widetilde{\Omega}_{\boldsymbol{ce}}^\ell)$ and $|\boldsymbol{\alpha}^\perp| = 1$, we have $u, \mathsf{D}_\parallel u, \mathsf{D}_\perp^{\boldsymbol{\alpha}^\perp} u \in L^2(\widetilde{\Omega}_{\boldsymbol{ce}}^\ell)$ due to (8.28), and there holds

$$\|r_{\boldsymbol{c}}^{-1-b_{\boldsymbol{c}}+\alpha^\parallel} \mathsf{D}_\parallel^{\alpha^\parallel} u\|_{L^2(\widetilde{\Omega}_{\boldsymbol{ce}}^\ell)} \le C^{\alpha^\parallel+1} \Gamma(\alpha^\parallel + 1), \qquad \alpha^\parallel \ge 2,$$

$$\|r_{\boldsymbol{c}}^{-b_{\boldsymbol{c}}+\alpha^{\|}}\mathsf{D}_{\|}^{\alpha^{\|}}\mathsf{D}_{\perp}u\|_{L^2(\widetilde{\Omega}_{\boldsymbol{ce}}^{\ell})} \leq C^{\alpha^{\|}+2}\Gamma(\alpha^{\|}+2), \qquad \alpha^{\|} \geq 1.$$

Similarly, for $u \in B_{-\boldsymbol{b}}(\widetilde{\Omega}_{\boldsymbol{ce}}^{\ell})$ it follows with (8.30) that $u \in L^2(\widetilde{\Omega}_{\boldsymbol{ce}}^{\ell})$ and

$$\|r_{\boldsymbol{c}}^{-b_{\boldsymbol{c}}+\alpha^{\|}}\mathsf{D}_{\|}^{\alpha^{\|}}u\|_{L^2(\widetilde{\Omega}_{\boldsymbol{ce}}^{\ell})} \leq C^{\alpha^{\|}+1}\Gamma(\alpha^{\|}+1), \qquad \alpha^{\|} \geq 1.$$

In view of (8.24), (8.25), these properties correspond to the one-dimensional analytic regularity assumptions considered in (8.16) and (8.20), respectively. Moreover, due to (8.26), the polynomial degrees $p_K^{\|}$ along the edge $\boldsymbol{e}$ are $\mathfrak{s}$-linearly increasing away from the corner $\boldsymbol{c}$. Hence, Lemma 8.5, respectively Lemma 8.6 along with the tensor-product structure of the elements yield the assertions. □

8.3.3 Convergence on $\widetilde{\mathfrak{T}}_{\boldsymbol{c}}^{\ell}$

It remains to show exponential convergence on $\widetilde{\mathfrak{T}}_{\boldsymbol{c}}^{\ell}$.

Proposition 8.13 *Let $u \in H^{1+\theta}(\widetilde{\Omega}_{\boldsymbol{ce}}^{\ell})$, respectively $u \in H^{\theta}(\widetilde{\Omega}_{\boldsymbol{ce}}^{\ell})$ for some $\theta \in (0,1)$. Then there exist constants $b, C > 0$ independent of ℓ such that $\Upsilon^{\|}_{\widetilde{\mathfrak{T}}_{\boldsymbol{c}}^{\ell}}[\eta]^2 \leq C\exp(-2b\ell)$, respectively $\|\eta_0\|^2_{L^2(\widetilde{\mathfrak{T}}_{\boldsymbol{c}}^{\ell})} \leq C\exp(-2b\ell)$.*

Proof The element $K \in \widetilde{\mathfrak{T}}_{\boldsymbol{c}}^{\ell}$ is isotropic with $h_K \simeq \sigma^{\ell}$; cf. (8.22). Standard h-version approximation properties then show that $N_K^{\|}[\eta]^2 \lesssim h_K^{2\theta}\|u\|^2_{H^{1+\theta}(K)}$, respectively $\|\eta_0\|^2_{L^2(K)} \lesssim h_K^{2\theta}\|u\|^2_{H^{\theta}(K)}$. □

References

1. I. Babuška and B. Q. Guo. The h-p version of the finite element method for domains with curved boundaries. *SIAM J. Numer. Anal.*, 25(4):837–861, 1988.
2. I. Babuška and B. Q. Guo. Regularity of the solution of elliptic problems with piecewise analytic data. Part I. Boundary value problems for linear elliptic equation of second order. *SIAM J. Math. Anal.*, 19(1):172–203, 1988.
3. I. Babuška and B. Q. Guo. Approximation properties of the h-p version of the finite element method. *Comput. Methods Appl. Mech. Engrg.*, 133(3-4):319–346, 1996.
4. P. Binev, A. Cohen, W. Dahmen, R. DeVore, G. Petrova, and P. Wojtaszczyk. Convergence rates for greedy algorithms in reduced basis methods. *SIAM J. Math. Anal.*, 43(3):1457–1472, 2011.
5. M. Costabel, M. Dauge, and S. Nicaise. Analytic regularity for linear elliptic systems in polygons and polyhedra.*Math. Models Methods Appl. Sci.*, 22(8), 2012. doi:10.1142/S0218202512500157.
6. W. Dahmen and K. Scherer. Best approximation by piecewise polynomials with variable knots and degrees. *J. Approx. Theory*, 26(1):1–13, 1979.
7. L. Demkowicz, J. Kurtz, D. Pardo, M. Paszynski, W. Rachowicz, and A. Zdunek. *Computing with hp-Adaptive Finite Elements. Volume 2, Frontiers: Three Dimensional Elliptic and Maxwell Problems with Applications*. Chapman & Hall/CRC Applied Mathematics and Nonlinear Science Series. Chapman & Hall/CRC, November 2007.
8. P. Dutt, Akhlaq Husain, A. S. Vasudeva Murthy, and C. S. Upadhyay. h-p spectral element methods for three dimensional elliptic problems on non-smooth domains, Part-I: Regularity estimates and stability theorem. *Proc. Indian Acad. Sci. Math. Sci.*, 125(2):239–270, 2015.
9. P. Dutt, Akhlaq Husain, A. S. Vasudeva Murthy, and C. S. Upadhyay. h-p spectral element methods for three dimensional elliptic problems on non-smooth domains, Part-II: Proof of stability theorem. *Proc. Indian Acad. Sci. Math. Sci.*, 125(3):413–447, 2015.

10. A. Ern and J.-L. Guermond. *Theory and Practice of Finite Elements*, volume 159 of *Applied Mathematical Sciences*. Springer, 2004.
11. W. Gui and I. Babuška. The h, p and h-p versions of the finite element method in one dimension. II. The error analysis of the h- and h-p versions. *Numer. Math.*, 49(6):613–657, 1986.
12. B. Q. Guo. The h-p version of the finite element method for solving boundary value problems in polyhedral domains. In *Boundary Value Problems and Integral Equations in Nonsmooth Domains*, volume 167 of *Lecture Notes in Pure and Appl. Math.*, pages 101–120. Dekker, New York, 1995.
13. B. Q. Guo and I. Babuška. The hp-version of the finite element method. Part I: The basic approximation results. *Comp. Mech.*, 1:21–41, 1986.
14. B. Q. Guo and I. Babuška. The hp-version of the finite element method. Part II: General results and applications. *Comp. Mech.*, 1:203–220, 1986.
15. B. Q. Guo and I. Babuška. Regularity of the solutions for elliptic problems on nonsmooth domains in $\mathbb{R}^3$. I. Countably normed spaces on polyhedral domains. *Proc. Roy. Soc. Edinburgh Sect. A*, 127(1):77–126, 1997.
16. B. Q. Guo and I. Babuška. Regularity of the solutions for elliptic problems on nonsmooth domains in $\mathbb{R}^3$. II. Regularity in neighbourhoods of edges. *Proc. Roy. Soc. Edinburgh Sect. A*, 127(3):517–545, 1997.
17. Y. Maday, O. Mula, A.T. Patera, and M. Yano. The generalized empirical interpolation method: Stability theory on Hilbert spaces with an application to the Stokes equation. *Comput. Methods Appl. Mech. Engrg.*, 287:310–334, 2015.
18. K. Scherer. On optimal global error bounds obtained by scaled local error estimates. *Numer. Math.*, 36:257–277, 1981.
19. D. Schötzau and Ch. Schwab. Exponential convergence in a Galerkin least squares hp-FEM for Stokes flow. *IMA J. Numer. Anal.*, 21(1):53–80, 2001.
20. D. Schötzau and Ch. Schwab. Exponential convergence for hp-version and spectral finite element methods for elliptic problems in polyhedra. *Math. Models Methods Appl. Sci.*, 25(9):1617–1661, 2015.
21. D. Schötzau, Ch. Schwab, and A. Toselli. Mixed hp-DGFEM for incompressible flows. *SIAM J. Numer. Anal.*, 40(6):2171–2194, 2003.
22. D. Schötzau, Ch. Schwab, and A. Toselli. Mixed hp-DGFEM for incompressible flows. II. Geometric edge meshes. *IMA J. Numer. Anal.*, 24(2):273–308, 2004.
23. D. Schötzau, Ch. Schwab, and T. P. Wihler. hp-DGFEM for second-order elliptic problems in polyhedra. I: Stability on geometric meshes. *SIAM J. Numer. Anal.*, 51(3):1610–1633, 2013.
24. D. Schötzau, Ch. Schwab, and T. P. Wihler. hp-DGFEM for second-order elliptic problems in polyhedra. II: Exponential convergence. *SIAM J. Numer. Anal.*, 51(4):2005–2035, 2013.
25. D. Schötzau, Ch. Schwab, and T. P. Wihler. hp-DGFEM for second-order mixed elliptic problems in polyhedra. *Math. Comp.*, 85(299):1051–1083, 2016.
26. Ch. Schwab. *p- and hp-FEM – Theory and Application to Solid and Fluid Mechanics*. Oxford University Press, Oxford, 1998.
27. T. P. Wihler and M. Wirz. Mixed hp-discontinuous Galerkin FEM for linear elasticity and Stokes flow in three dimensions. *Math. Models Methods Appl. Sci.*, 22(8), 2012. doi:10.1142/S0218202512500169.
28. L. Zhu, S. Giani, P. Houston, and D. Schötzau. Energy norm a posteriori error estimation for hp-adaptive discontinuous Galerkin methods for elliptic problems in three dimensions. *Math. Models Methods Appl. Sci.*, 21(2):267–306, 2011.